Benchmarking Study of TDOT D Mixtures for Balanced Mix Design

Research Final Report from University of Tennessee, Knoxville | Baoshan Huang, Jingyu Zhang, Kai Huang | April 30, 2026

Sponsored by Tennessee Department of Transportation
Strategic Planning, Research, & Innovation Division
Research Office & Federal Highway Administration

THE UNIVERSITY OF TENNESSEE KNOXVILLE

DISCLAIMER

This research was funded through the State Planning and Research (SPR) Program by the Tennessee Department of Transportation and the Federal Highway Administration under ***RES #: 2024-07 Research Project Title: Benchmarking Study of TDOT D Mixtures for Balanced Mix Design.***

This document is disseminated under the sponsorship of the Tennessee Department of Transportation and the United States Department of Transportation in the interest of information exchange. The State of Tennessee and the United States Government assume no liability of its contents or use thereof.

The contents of this report reflect the views of the author(s) who are solely responsible for the facts and accuracy of the material presented. The contents do not necessarily reflect the official views of the Tennessee Department of Transportation or the United States Department of Transportation.

Technical Report Documentation Page

1. Report No. RES2024-07	2. Government Accession No.	3. Recipient's Catalog No.
4. Title and Subtitle *Benchmarking Study of TDOT D Mixtures for Balanced Mix Design*		5. Report Date July 2026 6. Performing Organization Code
7. Author(s) Baoshan Huang, Jingyu Zhang, Kai Huang		8. Performing Organization Report No.
9. Performing Organization Name and Address Department of Civil and Environmental Engineering The University of Tennessee, Knoxville 851 Neyland Drive Knoxville, TN, 37996		10. Work Unit No. (TRAIS) 11. Contract or Grant No. RES2024-07
12. Sponsoring Agency Name and Address Tennessee Department of Transportation WRS – TN Tower, 12th Floor 312 Rosa L. Parks Ave. Nashville, TN 37243		13. Type of Report and Period Covered Final report, August 1,2023-July 31,2026 14. Sponsoring Agency Code
15. Supplementary Notes Conducted in cooperation with the U.S. Department of Transportation, Federal Highway Administration.		

16. Abstract

This study supported the Tennessee Department of Transportation's implementation of Balanced Mix Design (BMD) for TDOT 411-D dense-graded surface mixtures by developing local benchmarking data, evaluating aging procedures, comparing 6-inch Superpave gyratory-compacted and 4-inch Marshall-compacted specimens, and recommending preliminary performance thresholds. Twenty-four approved Tennessee mixtures were evaluated as plant-mixed, laboratory-compacted (PMLC) and laboratory-mixed, laboratory-compacted (LMLC) specimens using the IDEAL-CT, Tennessee Cracking Test (TN-CT), IDEAL-RT, high-temperature indirect tensile strength (HT-IDT), and Hamburg Wheel Tracking Test (HWTT). Five long-term aging protocols were assessed for aging severity and practical feasibility. Loose-mixture aging at 115°C for 20 hours was recommended because it successfully simulated long term aging effects while avoiding excessive conditioning time and overly high aging temperature and could be completed within a routine laboratory work schedule. An equivalent-aging-time framework was developed to integrate aging temperature and duration into a single aging severity parameter. Benchmarking results showed different performance distributions for PMLC and LMLC specimens, indicating that separate thresholds should be established for mixture design and production quality control. TN-CT correlated reasonably with IDEAL-CT, indicating that TN-CT can be used as a Marshall-compatible cracking evaluation test. In contrast, correlations among the results obtained using different rutting test protocols were relatively weak. Therefore, HT-IDT may serve as a Marshall-compatible rutting test but is not recommended as a replacement for HWTT at this stage. Preliminary thresholds were proposed for TDOT BMD implementation and

should be refined as BMD implementation progresses and additional field performance data become available for verification.			
17. Key Words **BALANCED MIX DESIGN, BENCHMARKING, PERFORMANCE TEST**		18. Distribution Statement No restriction. This document is available to the public from the sponsoring agency at the website http://www.tn.gov/.	
19. Security Classif. (of this report) Unclassified	20. Security Classif. (of this page) Unclassified	21. No. of Pages xxx	22. Price

Acknowledgement

The research team would like to sincerely thank the Tennessee Department of Transportation (TDOT) for funding this research project. We also appreciate the continued support and collaboration from TDOT regional engineers, personnel from the Materials and Tests Division, and local asphalt plant representatives throughout the project. Their assistance with mixture collection, technical coordination, and project implementation was essential to completing the research objectives. We would also like to thank the TDOT Research Office for its administrative support, guidance, and coordination in keeping the project on schedule.

Executive Summary

This study was conducted to support the Tennessee Department of Transportation's (TDOT) implementation of Balanced Mix Design (BMD) for TDOT 411-D dense-graded surface mixtures. The project developed a Tennessee-specific benchmarking database, evaluated practical short- and long-term aging procedures, compared 6-inch Superpave gyratory-compacted specimens with 4-inch Marshall-compacted specimens from both laboratory- and plant-produced mixtures, and proposed preliminary performance thresholds to support future BMD implementation. These efforts were intended to help TDOT transition from primarily volumetric specifications toward performance-informed asphalt mixture design and acceptance.

A total of twenty-four currently approved TDOT 411-D dense-graded surface mixtures were collected from all four regions across Tennessee. Both plant-mixed, laboratory-compacted (PMLC) and laboratory-mixed, laboratory-compacted (LMLC) specimens were collected and prepared using the Superpave gyratory compactor (SGC) and Marshall hammer. The adopted performance tests included the Indirect Tensile Asphalt Cracking Test (IDEAL-CT), Tennessee Cracking Test (TN-CT), IDEAL Rutting Test (IDEAL-RT), high-temperature indirect tensile strength (HT-IDT), and Hamburg Wheel Tracking Test (HWTT).

The study focused on three major objectives. First, five long-term aging (LTA) protocols were evaluated to identify a practical aging condition for cracking resistance evaluation. Second, performance results from 6-inch SGC specimens and 4-inch Marshall specimens were compared and correlated to evaluate the suitability of Marshall specimens and associated Marshall-based performance tests for BMD practice. Third, preliminary performance thresholds were developed based on the benchmarking database to support future TDOT BMD implementation. Together, the long-term aging evaluation, generalized aging method, benchmarking performance database, specimen-type comparison, test correlation analysis, and preliminary threshold recommendations provide a technical basis for TDOT's stepwise implementation of BMD for dense-graded surface mixtures.

Key Findings

- For the plant-mixed mixtures evaluated, the reheated PMLC specimens showed the highest CT index values, while long-term aged specimens showed substantial reductions in CT index. The aging severity generally followed the order: reheated condition < 85°C for 5 days compacted aging < 115°C for 20 hours loose aging < 95°C for 3 days loose aging < 135°C for 8 hours loose aging < 85°C for 5 days loose aging.
- Loose-mixture aging at 115°C for 20 hours was identified as the most practical LTA protocol for the current stage of TDOT BMD implementation. This protocol produced CT index results comparable to the 95°C for 3 days loose-aging protocol, which is considered a robust long-term aging condition, while requiring a shorter conditioning time and avoiding potential high-temperature concerns associated with 135°C aging. The 20-hour duration also provides a more laboratory-feasible conditioning schedule than multi-day aging protocols.
- A generalized aging method framework was developed to support the interpretation and comparison of cracking resistance under different long-term aging conditions. By

converting oven aging time to equivalent aging time, the framework integrates the effects of aging temperature and duration into a unified aging severity parameter and provides a potential bridge between laboratory aging protocols and field aging conditions once field-aged mixture data become available.

- The 4-inch Marshall-based TN-CT index showed a reasonably strong correlation to the 6-inch SGC-based IDEAL-CT index, with $R^2 \approx 0.86$ when PMLC and LMLC data were combined. Rutting-related relationships among IDEAL-RT, HT-IDT, and HWTT were weaker than the cracking-test relationship because these tests involve different loading modes, specimen configurations, and stress states. Therefore, HT-IDT may be considered as a Marshall-compatible rutting test but is not recommended to replace HWTT at this stage. Performance space diagrams showed similar overall distribution trends between 4-inch Marshall-based and 6-inch SGC-based tests, supporting the feasibility of Marshall-based performance testing for TDOT BMD implementation. The CT index and TN-CT index characterize post-peak cracking tolerance, whereas peak strength provides additional information on pre-peak tensile resistance. Interpreting these parameters together provides a more complete characterization of the cracking-test load–displacement response.
- The benchmarking results showed that PMLC and LMLC specimens had different performance distributions. For cracking-related tests, LMLC specimens subjected to 4 hours short-term aging generally showed lower CT index and TN-CT index values than reheated PMLC specimens. For rutting-related tests, LMLC specimens generally showed higher RT index and HT-IDT strength values than reheated PMLC specimens. These differences indicate that separate thresholds should be developed for LMLC specimens used in mix design and PMLC specimens used in QA/QC or production verification, respectively.

Key Recommendations

- Loose-mixture aging at 115°C for 20 hours is recommended as the primary LTA protocol for continued BMD research and preliminary implementation. This protocol provides a practical balance between aging severity and laboratory feasibility because it produces cracking results comparable to the 95°C for 3 days protocol while allowing a shorter, more practical conditioning schedule. Field validation would still be needed before formal specification adoption.
- Performance thresholds for PMLC and LMLC specimens should be developed separately because the two specimen preparation conditions produced different cracking and rutting performance distributions. LMLC thresholds are more appropriate for mix design evaluation, while PMLC thresholds are more appropriate for QA/QC or production verification.
- Performance thresholds for 6-inch SGC-based and 4-inch Marshall-based tests should also be developed separately because specimen size, compaction method, loading configuration, and test mechanics affect the measured performance indices. TN-CT can be used as a practical Marshall-compatible cracking test to support TDOT's transition toward BMD. HT-IDT can be used as a rutting test for Marshall specimens. Neither HT-IDT nor IDEAL-RT are considered as ideal replacements for HWTT. The peak strength of

cracking tests is recommended as a supplementary parameter to be interpreted together with the applicable CT index or TN-CT index.

- The 25th percentile and average minus one standard deviation are recommended as initial statistical approaches for preliminary BMD threshold development. These methods can identify lower-performing mixtures among currently approved TDOT mixtures without imposing overly restrictive requirements during the initial implementation stage. Preliminary recommended thresholds are summarized as follows: for reheated PMLC specimens, CT index = 75, RT index = 70, TN-CT index = 45, and HT-IDT strength = 210 kPa; for PMLC specimens after LTA at 115°C for 20 hours (LTA115), CT index = 25 and TN-CT index = 15; for LMLC specimens under STA conditions, CT index = 50 (STA for 4h at 135°C), RT index = 85 (STA for 2h at 135°C), TN-CT index = 30 (STA for 4h at 135°C), and HT-IDT strength = 230 kPa (STA for 2h at 135°C); and for LMLC specimens after LTA115, CT index = 15 and TN-CT index = 10. These values should be considered preliminary and refined using field performance data before formal specification adoption.
- Overall, this study provides TDOT with a local performance benchmarking database, a practical LTA recommendation, preliminary relationships between SGC-based and Marshall-based performance tests, and initial distribution-based threshold values. These outcomes can support TDOT's stepwise BMD implementation by identifying achievable performance ranges for currently approved 411-D mixtures, providing Marshall-compatible testing options, and establishing preliminary criteria that can be refined through future field performance validation.

Table of Contents

DISCLAIMER ii
Technical Report Documentation Page i
Acknowledgement iii
Executive Summary iv
Key Findings iv
Key Recommendations v
List of Tables x
List of Figures xi
Glossary of Key Terms and Acronyms xiii
Chapter 1 Introduction 1
1.1 Problem Description 1
1.2 Objectives of the Research 1
1.3 Scope of Work 1
Chapter 2 Literature Review 3
2.1 Introduction 3
2.2 Benchmarking Study for BMD 4
2.3 Performance Tests for BMD 5
2.4 Asphalt Mixture Aging Methods for BMD 7
2.5 Research gaps 8
Chapter 3 Methodology 9
3.1 Materials 9
3.2 Aging conditions 9
3.2.1 Reheated Conditioning for PMLC specimens 9
3.2.2 Short-term aging for LMLC specimens 9
3.2.3 Long-term aging conditioning 9
3.3 Specimen Preparation 10
3.3.1 Preparation of PMLC Specimens 10
3.3.2 Preparation of LMLC Specimens 11
3.3.3 Preparation of LTA Specimens 11
3.4 Performance Test 12
3.4.1 Indirect Tensile Cracking Test (IDEAL-CT) 13
3.4.2 Tennessee Cracking Test (TN-CT) 14

3.4.3 Rapid Shear Rutting Test (IDEAL-RT) 14
3.4.4 High-Temperature Indirect Tension Test (HT-IDT) 14
3.4.5 Hamburg Wheel-Tracking Test (HWTT) 14
Chapter 4 Results and Discussion 18
4.1 Long-term Aging Protocol Evaluation 18
4.1.1 CT index results under various long-term aging conditions 18
4.1.2 Long-term aging protocol recommendation 21
4.2 Development of a generalized aging method 22
4.2.1 Shifting aging time according to aging temperature 22
4.2.2 Determine the coefficient of equivalent aging time 24
4.2.3 Comparative analysis of the general aging method 26
4.2.4 Discussion of generalized aging method framework 28
4.3 Benchmark performance results 30
4.3.1 CT index of PMLC and LMLC 31
4.3.2 RT index of PMLC and LMLC 37
4.3.3 TN-CT Index of PMLC and LMLC 38
4.3.4 HT-IDT Strength of PMLC and LMLC 41
4.3.5 HWTT rut depth of PMLC and LMLC 42
4.3.6 Preliminary threshold recommendations 43
4.4 Correlation between performance tests 43
4.4.1 Correlation between CT_{index} and TN-CT_{index} 43
4.4.2 Correlation between RT_{index} and HT-IDT strength 44
4.4.3 Correlation Between RT Index and HWTT 45
4.4.4 Correlation Between HT-IDT strength and HWTT 47
4.5 Performance Space Diagram Analysis 48
4.5.1 Performance Space Diagram of PMLC 49
4.5.2 Performance Space Diagram of LMLC 50
4.5.3 Three-Dimensional Performance Space Considering Peak Strength 50
Chapter 5 Conclusion 51
References 53
Appendices 57

Appendix A: Mixture information 57
Appendix B: HWTT results and figures 59
Appendix C: Three-Dimensional Performance Spaces Incorporating Peak-Strength Thresholds 66

List of Tables

Table 2-1 BMD implementation information from NAPA website [5]. 4
Table 2-2 Commonly used performance tests for BMD implementation[5], [17], [18], [19] 6
Table 2-3 Summary of laboratory aging protocols 8
Table 3-1 Summary of Long-term aging protocols [33] 9
Table 3-2 Summary of Performance tests 13
Table 4-1 The corresponding equivalent aging time for different long-term aging protocols for loose mixture. 26
Table 4-2 Preliminary threshold 43
Table A-1 Summary of collected TDOT 411-D asphalt mixtures and JMF properties 57
Table A-2 HWTT results of PMLC and LMLC. 59

List of Figures

Figure 2-1 Graphical Illustration of BMD approaches [1] : (a) Approach A, (b) Approach B, (c) Approach C, and (d) Approach D. 4
Figure 3-1 breaking down and quartering the reheated plant-produced mixtures 11
Figure 3-2 Lab mixture preparation 11
Figure 3-3 Compacted and loose LTA conditioning 12
Figure 3-4 Performance tests 16
Figure 3-5 HWTT data processing template 17
Figure 4-1 CT index results of PMLC specimens under various aging conditions 19
Figure 4-2 Cumulative distribution curve of CT index under different aging conditions 20
Figure 4-3 CT index under different long-term aging conditions, (a) Box plot; (b) key statistics 21
Figure 4-4 Plots of CT index versus oven aging time (hours) and equivalent aging time for Mix C: (a) CT index versus oven aging time, (b) conceptual shifting from oven aging time to equivalent aging time, (c) CT index versus equivalent aging time, and (d) with two additional aging conditions: 100°C for 12 hours and 100°C for 132 hours. 23
Figure 4-5 Plots of CT index versus equivalent aging time for Mix C and E: (a) Linear and (b) semi-logarithmic. 24
Figure 4-6 Plots of CT index versus equivalent aging time for PMLC mixtures: (a) Linear scale and (b) semi-logarithmic scale. 26
Figure 4-7 Plots of CT index versus oven aging time (hours) and equivalent aging time using test results from Zhou et al., [28] (2022): (a) CT index versus oven aging time, (b) conceptual shifting from oven aging time to equivalent aging time, and (c) CT index versus equivalent aging time in semi logarithmic scale. 27
Figure 4-8 Plots of CT index versus oven aging time (hours) and equivalent aging time using test results from Elwardany et al.,) [42]: (a) CT index versus oven aging time, (b) conceptual shifting from oven aging time to equivalent aging time and (c) CT index versus equivalent aging time in semi-logarithmic scale. 28
Figure 4-9 Plots of (a) equivalent aging time versus oven aging time at different aging temperatures, (b) accumulated aging effect with various aging histories, and (c) CT index with accumulated aging effect with various aging histories. 30
Figure 4-10 PMLC VS LMLC (a) CT index; (b) CT index cumulative distribution;(c) CT index thresholds 31
Figure 4-11 PMLC VS LMLC 115℃ 20h loose aging (a) CT index; (b) cumulative distribution;(c) CT index thresholds 33
Figure 4-12 PMLC under reheated and LTA115℃ 20h (a)CT index; (b)Gf vs I75/m75 interaction diagram 34
Figure 4-13 CTindex components change rate after LTA115℃ 20h. 35
Figure 4-14 Load vs displacement curve of Mix K and Mix U. 36
Figure 4-15 Peak strength comparison and threshold analysis: (a) peak strength of reheated PMLC and STA4h LMLC specimens; (b) peak strength thresholds for reheated PMLC and STA4h LMLC specimens; (c) peak strength of PMLC and LMLC specimens after LTA115°C20h; and (d) peak strength thresholds after LTA115°C20h. 37
Figure 4-16 PMLC vs LMLC (a) RT index; (b) RT index cumulative distribution;(c) RT index thresholds 38

Figure 4-17 PMLC VS LMLC (a)TN CT index; (b) TN CT index cumulative distribution;(c) TNCT index thresholds 39
Figure 4-18 PMLC VS LMLC under LTA115℃ 20h (a) TN CT index; (b) cumulative distribution;(c) TNCT index thresholds 40
Figure 4-19 Peak strength comparison and threshold analysis: (a) peak strength thresholds for reheated PMLC and STA4h LMLC specimens; (b) peak strength thresholds after LTA115°C20h. 41
Figure 4-20 PMLC VS LMLC(a) HT-IDT strength; (b) cumulative distribution; (c)HT-IDT thresholds 42
Figure 4-21 Corrected rut depth at 20k pass of PMLC and LMLC 42
Figure 4-22 Correlation between CT $_{index}$ and TNCT $_{index}$ 44
Figure 4-23 Correlation between RT $_{index}$ and HT-IDT strength 45
Figure 4-24 Correlation between RT $_{index}$ and HWTT results: (a) RT $_{index}$ vs CRD20k; (b) RT $_{index}$ vs RRI 46
Figure 4-25 Correlation between HT-IDT strength and HWTT results: (a) HT-IDT strength vs CRD20k;(b) HT-IDT strength vs RRI 48
Figure 4-26 Performance Space Diagram of PMLC: (a) SGC specimens;(b) Marshall specimens 49
Figure 4-27 Performance Space Diagram of LMLC: (a) SGC specimens;(b) Marshall specimens 50
Figure A-1 HWTT results of PMLC 62
Figure A-2 HWTT results of LMLC 65
Figure A-3 Three-dimensional performance space for reheated PMLC SGC specimens based on CT index, RT index, and IDEAL-CT peak strength 69
Figure A-4 Three-dimensional performance space for reheated PMLC Marshall specimens based on TN-CT index, HT-IDT strength, and TN-CT peak strength. 73
Figure A-5 Three-dimensional performance space for STA-conditioned LMLC SGC specimens based on CT index, RT index, and IDEAL-CT peak strength. 77
Figure A-6 Three-dimensional performance space for STA-conditioned LMLC Marshall specimens based on TN-CT index, HT-IDT strength, and TN-CT peak strength. 81

Glossary of Key Terms and Acronyms

ANOVA: Analysis of variance

BMD: Balanced Mix Design

CDF/CFD: Cumulative distribution function / cumulative frequency distribution

CRD20k: Corrected rut depth at 20,000 passes

CT index: Cracking tolerance index from IDEAL-CT

HT-IDT: High-temperature indirect tensile strength test

HWTT: Hamburg Wheel Tracking Test

IDEAL-CT: Indirect Tensile Asphalt Cracking Test

IDEAL-RT: IDEAL Rutting Test

JMF: Job Mix Formula

LMLC: Laboratory-mixed, laboratory-compacted

LTA: Long-term aging

NMAS: Nominal maximum aggregate size

PMLC: Plant-mixed, laboratory-compacted

QA/QC: Quality assurance / quality control

RAP: Reclaimed asphalt pavement

RRI: Rutting Resistance Index

SGC: Superpave Gyratory Compactor

STA: Short-term aging

TN-CT: Tennessee Cracking Test

Chapter 1 Introduction

1.1 Problem Description

Like many state agencies, the Tennessee Department of Transportation (TDOT) seeks to enhance asphalt mixture durability to support a more sustainable, longer-lasting, and cost-effective roadway network. BMD addresses this need by incorporating performance criteria into asphalt mixture design and acceptance. TDOT's transition from primarily prescriptive volumetric specifications to performance-informed specifications requires reliable local data that reflect Tennessee materials, mixture designs, and production practices.

Thousands of asphalt mixtures are approved under existing specifications. TDOT, producers, and contractors therefore need to understand how currently approved TDOT 411-D mixtures perform relative to potential BMD criteria. Benchmarking current mixtures provides a practical basis for defining achievable performance ranges and identifying how much improvement may be required for future specification implementation.

TDOT has historically used Marshall hammer compaction for asphalt mix design, whereas many nationally developed BMD performance tests were developed around 6-inch SGC specimens. This creates an implementation need to evaluate whether 4-inch Marshall-based tests can provide performance information that is compatible with SGC-based BMD testing.

In addition, no national consensus has been established for the short-term and long-term aging procedures that should accompany BMD performance testing. A practical aging protocol is needed so that cracking resistance can be evaluated in a manner that is meaningful, repeatable, and feasible for implementation.

1.2 Objectives of the Research

The objectives of this research are to:

- Benchmark currently produced D mixes in Tennessee against the IDEAL-CT, TN-CT, Hamburg Wheel Tracking Test (HWTT), and Hot Indirect Tensile Strength.
- Develop a practical method for asphalt mixture short and long-term aging.
- Correlate the performance results of the samples compacted with Marshall Compactor and Superpave Gyratory Compactor (SGC).
- Recommend specification limits for different performance tests.

1.3 Scope of Work

The scope of the research work includes the following:

- Selecting materials and developing the testing plan.
- Collecting asphalt plant mixtures and component materials.
- Conducting performance tests of plant-produced and laboratory-produced mixtures.
- Comparing different asphalt mixture aging methods.
- Correlating performance results obtained from 4" Marshall compacted specimens and 6" SGC specimens.
- Making recommendations to TDOT specifications regarding Balanced Mix Design.

The scope of this study was limited to TDOT 411-D dense-graded surface mixtures, laboratory-compacted specimens prepared from plant-produced or laboratory-produced mixtures, and the performance tests included in the approved test plan. The preliminary thresholds recommended in this report were based on the benchmarking database and should be refined using field performance data before formal specification adoption.

The remainder of this report is organized as follows. Chapter 2 reviews BMD benchmarking, performance testing, and aging methods. Chapter 3 describes the materials, specimen preparation, aging procedures, performance tests, and data analysis methods. Chapter 4 presents the aging evaluation, benchmarking results, correlation analysis, and threshold recommendations. Chapter 5 summarizes the conclusions and implementation recommendations.

Chapter 2 Literature Review

2.1 Introduction

Traditional volumetric mixture design methods, including Hveem, Marshall, and Superpave, primarily control mixture proportions through volumetric properties such as air voids, voids in the mineral aggregate, voids filled with asphalt, and effective binder content. These volumetric parameters remain important for constructability and quality control; however, they do not directly quantify how mixtures resist cracking, rutting, moisture damage, or the effects of recycled and modified materials [1]. Consequently, mixtures that satisfy volumetric requirements may still exhibit premature distress under field traffic and environmental conditions.

BMD was developed to address this limitation by incorporating mechanical performance tests on appropriately conditioned specimens. Current BMD practice considers multiple distress modes, mixture aging, traffic, climate, and pavement-layer location[2], [3]. There are four BMD approaches described in Standard Practice for Balanced Design of Asphalt Mixtures (AASHTO R132-25)[4]. Approach A uses performance testing only to verify a conventional volumetric design at the selected optimum binder content. Approach B expands this process by testing multiple binder contents and selecting the binder content that best satisfies performance criteria. Approach C allows performance test results to modify the conventional volumetric design, including changes in binder content or mixture proportions. Approach D relies primarily on performance testing for mixture design, with limited or no mandatory volumetric requirements. Figure 2-1 illustrates the flow chart of the four BMD approaches.

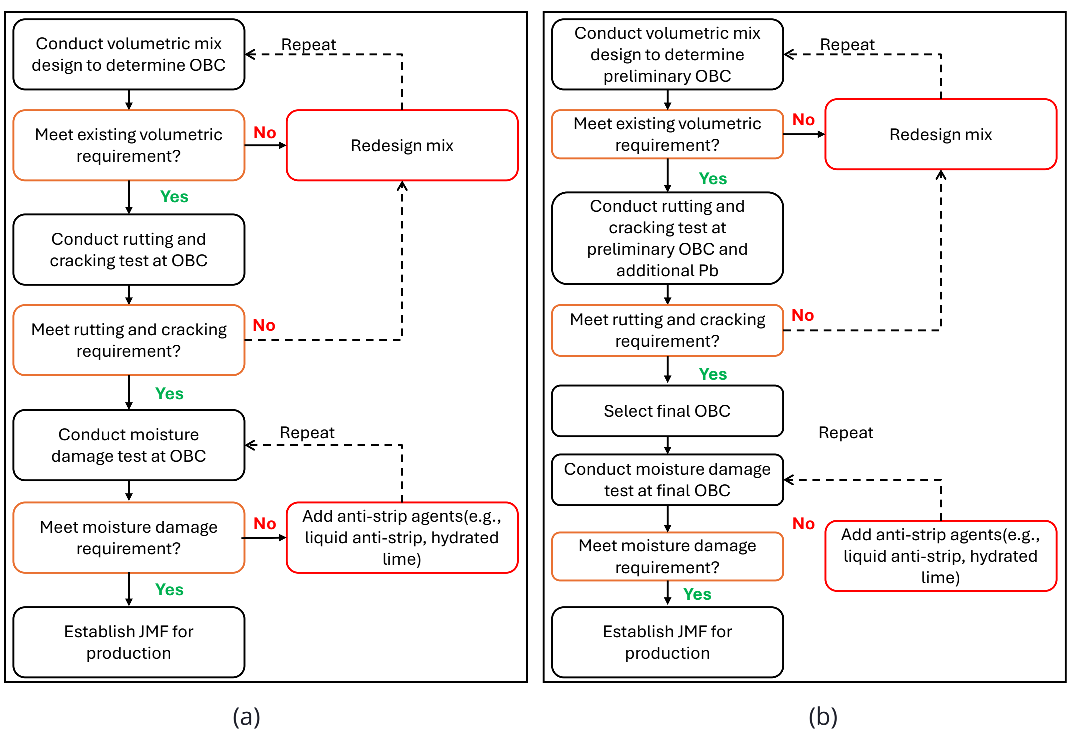

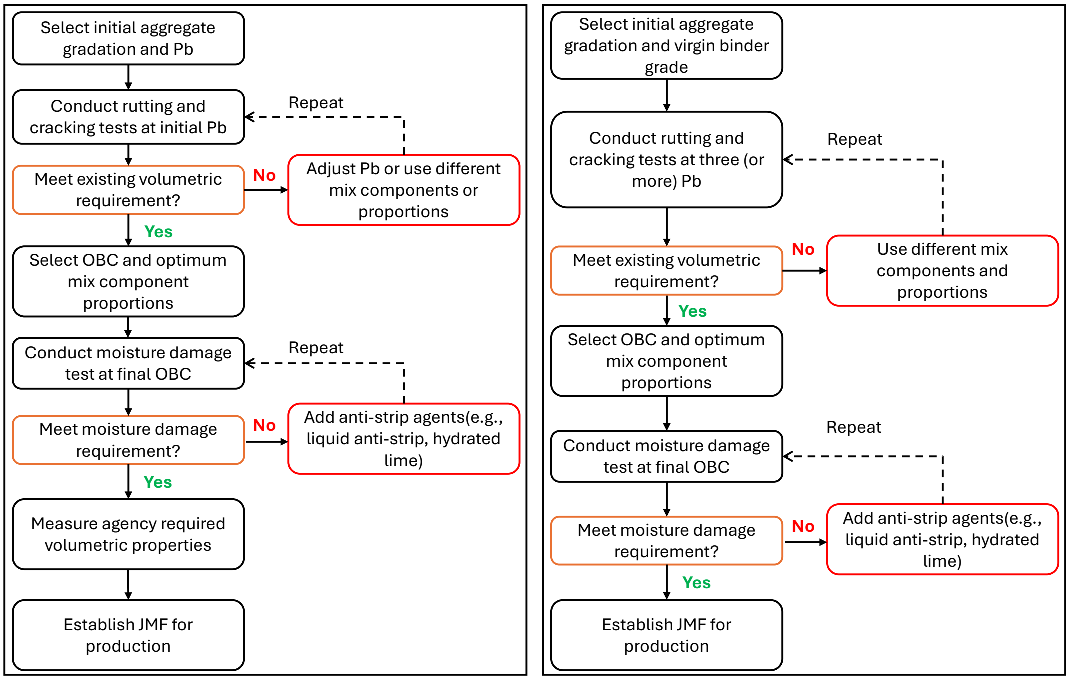

(c) (d)

Figure 2-1 Graphical Illustration of BMD approaches [1] : (a) Approach A, (b) Approach B, (c) Approach C, and (d) Approach D.

Table 2-1 provides status of BMD implementation in United States [5]. Although six states have adopted Approach A, four have implemented Approach B, and two are utilizing Approach C, many states (24) have currently remained in the pre-implementation phase, indicating the need for local benchmarking before performance criteria are adopted.

Table 2-1 BMD implementation information from NAPA website [5].

BMD Approach	State
Approach A	Texas, Louisiana, Wisconsin, Illinois, New York, Vermont
Approach B	Virginia, Oklahoma, Missouri, Kentucky
Approach A&B	New Jersey
Approach C	Alabama, California
Approach D	NA
Pre-implementation	Arkansas, Mississippi, Tennessee, North Carolina, South Carolina, Georgia, Washington, Oregon, Idaho, Montana, North Dakota, South Dakota, Utah, Colorado, New Mexico, Iowa, Ohio, Kansas, Pennsylvania, Maine, Massachusetts, Maryland

2.2 Benchmarking Study for BMD

Establishing performance-test criteria is one of the most important steps in BMD implementation. Criteria that are too strict can increase contractor risk and production cost, while criteria that are too lenient may allow mixtures with inadequate long-term performance.

Therefore, many state highway agencies use benchmarking as an intermediate step before implementing formal BMD specifications.

Benchmarking is the performance testing of a representative set of currently approved asphalt mixtures used within a state to understand the variability and distribution of test results under local materials, production practices, and environmental conditions [6]. The primary objective of a benchmarking experiment is to evaluate existing mix designs using selected performance tests so that the agency can establish realistic preliminary criteria for future specification implementation. Benchmarking datasets commonly include laboratory-mixed, laboratory-compacted (LMLC) specimens for mix design and plant-mixed, laboratory-compacted (PMLC) specimens for production verification. Comparing LMLC and PMLC results helps agencies understand how laboratory design performance translates to plant-produced mixture performance.

Previous benchmarking efforts have used different performance tests and statistical approaches depending on agency needs. Virginia [7], [8], Alabama [1], Georgia [9], Louisiana [10], [11], Oregon [12], [13], Nebraska [14], [15], Wisconsin [16], and other agencies have evaluated existing mixtures to select appropriate cracking and rutting tests, quantify variability, and establish preliminary thresholds. Common threshold approaches include minimum or maximum values, averages, average plus or minus one standard deviation, and percentile-based values. Performance thresholds are often region-specific and may vary with mixture type, traffic level, and material characteristics. Benchmarking datasets are also frequently used to establish relationships among different performance tests, enabling the development of surrogate tests for quality control and acceptance. For example, Zhou et al. established the relevance between the IDEAL-CT and Overlay Test (OT). The results show the CT index correlates well with the OT cracking parameters. Based on the OT results, the CT index criteria were established [17].

For TDOT, benchmarking is especially important because current practice relies on Marshall-compacted specimens, whereas many nationally used BMD performance tests were developed for 6-inch SGC specimens. A TDOT-specific benchmarking database is therefore needed to define achievable performance levels for 411-D mixtures and to relate Marshall-based tests to SGC-based tests.

2.3 Performance Tests for BMD

BMD relies on performance tests to evaluate asphalt mixture resistance to major distress mechanisms, particularly cracking, rutting, and moisture damage. Test selection directly affects the reliability, cost, turnaround time, and practicality of BMD implementation in both mix design and quality assurance/quality control (QA/QC).

A wide range of laboratory performance tests have been used for BMD. Common cracking tests include Disk-shaped Compact Tension (DCT), Semi-Circular Bend (SCB), Illinois Flexibility Index Test (I-FIT), Overlay Test (OT), and Indirect Tensile Asphalt Cracking Test (IDEAL-CT). For rutting resistance, the Hamburg Wheel Tracking Test (HWTT), Asphalt Pavement Analyzer (APA), Flow Number (FN), and the Rapid Shear Rutting Test (IDEAL-RT) are widely used. Moisture susceptibility is commonly evaluated using Tensile Strength Ratio (TSR) and HWTT-based stripping indicators.

As summarized in A key gap for TDOT is that most standardized performance tests were developed for 6-inch SGC specimens. Limited research has validated equivalent or correlated procedures for 4-inch Marshall-compacted specimens, even though Marshall compaction remains important for TDOT mix design practice

Table 2-2, these tests differ substantially in equipment cost, testing time, complexity, and suitability for routine implementation. Advanced mechanistic tests such as Beam Fatigue and cyclic fatigue tests require 3–5 days of conditioning and testing time and involve high-cost equipment (>$85,000–$100,000). In contrast, simplified tests such as IDEAL-CT, IDEAL-RT, and HT-IDT can typically be completed within one day using relatively low-cost equipment (<$10,000), making them more suitable for routine laboratory use and QA/QC applications.

From a practical implementation perspective, test selection must balance accuracy and feasibility. While mechanistic tests provide detailed material characterization, their long testing duration and high cost limit their applicability in production environments. On the other hand, simpler monotonic tests, such as IDEAL-CT and IDEAL-RT, have gained increasing attention due to their rapid turnaround, ease of operation, and acceptable repeatability, which align better with construction schedules and QA/QC requirements.

A key gap for TDOT is that most standardized performance tests were developed for 6-inch SGC specimens. Limited research has validated equivalent or correlated procedures for 4-inch Marshall-compacted specimens, even though Marshall compaction remains important for TDOT mix design practice

Table 2-2 Commonly used performance tests for BMD implementation[5], [17], [18], [19]

Tests	*Approximated total conditioning and test time*	*Evaluation metrics*	*Equipment cost*
Cracking tests			
Disk-shaped Compact Tension (DCT) *ASTM D7313*	4-5 days	Fracture energy	$50,000
Beam fatigue test *AASHTO T321*	days to weeks depending on strain level	Number of cycles (fatigue life)	>$100,000
Cyclic fatigue test *AASHTO TP 107*	4-5 days	Fatigue damage parameters	$85,000
Indirect Tensile Asphalt Cracking Test (IDEAL-CT) *ASTM D8225*	1 day	Crack tolerance index (CT Index)	<$10,000
IDT-University of Florida *AASHTO T322*	4-5 days	Energy ratio	>$100,000
Illinois flexibility index test (I-FIT) *AASHTO TP124*	2-3 days (including sample drying)	Flexibility index	<$10,000
Overlay test (OT) *Tex-248-F*	3-4 days	Crack resistance index	$50,000
Semi-Circular Bend (SCB) *AASHTO TP105*	3-4 days	Fracture energy	$100,000
SCB-Jc *ASTM D8044*	7-8 days (including 5 days aging @ 85°C)	Jc-critical strain energy release rate	$10,000
Rutting Tests			

Asphalt Pavement Analyzer (APA) *AASHTO T340*	2 days	Rutting depth (mm) after a set number of wheel passes (typically 8,000 cycles).	>$100,000
Hamburg Wheel Tracking Test (HWTT) *AASHTO T324*	2 days	Rut depth after 20,000 cycles or at failure, Stripping inflection point (SIP)	$50,000
Rapid Shear Rutting Test (IDEAL-RT) *ASTM D8360*	1 day	RT Index	<$10,000
High Temperature Indirect Tensile Strength Test (HT-IDT) *Agency-specific*	1 day	IDT strength at high temperature	<$10,000
Flow Number Test (FN) *AASHTO T378*	4 days	Flow number (FN), Creep slope	$85,000
Hveem Stability Test *AASHTO T246*	-	Hveem stability value	-
Repeated Load Triaxial Test (RLT) *AASHTO T307-99*	-	Permanent deformation (strain) vs. Cycles, Elastic modulus	-
Marshall Stability Test *AASHTO T245 / ASTM D6927*	1 day	Marshall stability, Flow value	<$10,000
Moisture Damage Tests			
Tensile Strength Ratio (TSR) *AASHTO T283*	3-4 days	Tensile Strength Ratio (TSR)	<$10,000
Hamburg Wheel Tracking Test (HWTT) *AASHTO T324*	2 days	Rutting depth, Stripping inflection point	$50,000
Cantabro Test *ASTM D7064 or AASHTO TP 108 (for OGFC)*	-	Mass loss (%) after 300 revolutions (or other specified cycles)	$10,000
Modified Lottman Test *AASHTO T283 (Modified)*	3-4 days	Tensile Strength Ratio	<$10,000

2.4 Asphalt Mixture Aging Methods for BMD

Aging strongly affects asphalt mixture performance because oxidation increases binder stiffness, reduces ductility, and increases cracking susceptibility. Asphalt mixtures experience short-term aging (STA) during production, transportation, placement, and compaction [20], followed by long-term aging (LTA) during service life [21]. For BMD applications, STA is generally sufficient for rutting-related tests, while cracking evaluation often requires consideration of both STA and LTA.

The subject of long-term aging protocol has been widely investigated. Several protocols have been developed but no single method has been universally accepted. AASHTO R30 specifies aging compacted asphalt specimens for 5 days at 85 °C [22],but compacted aging may create radial and vertical oxidation gradients within the specimen[23].Loose-mixture aging protocols were therefore developed to improve aging uniformity, including 85°C for 5 days, 95°C for variable durations, 115°C for 20 hours, and 135°C for shorter durations [23], [24], [25], [26], [27], [28].

Table 2-3 summarized commonly used laboratory aging protocols. The diversity of aging protocols limits direct comparison among agencies and studies. For TDOT BMD implementation, the aging procedure must be severe enough to represent long-term cracking susceptibility but practical enough for laboratory workflow. Accordingly, this study evaluated multiple LTA protocols to compare aging severity, testing practicality, and suitability for future TDOT specifications.

Table 2-3 Summary of laboratory aging protocols

Aging type	*Duration*	*Temperature*	*Mixture status*	*Reference*
Short-term aging	2 hours	135℃ for HMA 116℃ for WMA	Loose	AASHTO R30 - 22[22];Newcomb et al.[20];Epps-Martin et al.[29]
	4 hours	135℃	Loose	AASHTO R30 - 02[30]
	2 hours	Compaction Temperature	Loose	Verginia DOT[31]
	4 hours	Compaction temperature	Loose	Verginia DOT[32]
Long-term aging	120 hours	85℃	Compacted	AASHTO R 121-24 (Method A) [33]
	120 hours	85°C	Loose	AASHTO R 121-24 (Method B) [33]
	Based on Climate Aging Index	95°C	Loose	AASHTO R 121-24[33] (Method C) [33]
	20 hours	100-125°C	Loose	AASHTO R 121-24 (Method D) [33]
	6 or 8 hours	135°C	Loose	AASHTO R 121-24 (Method E) [33]

2.5 Research gaps

Although significant progress has been made in BMD research, several gaps remain for TDOT implementation:

- A TDOT-specific benchmarking database is needed for currently approved 411-D mixtures to define achievable performance levels and variability under local materials, mix designs, and production practices.
- A wide range of short-term and long-term aging protocols has been proposed; however, no consistent and practical method has been established for BMD implementation. In particular, long-term aging procedures are often time-consuming and difficult to integrate into laboratory workflows and QA/QC processes, creating a gap between laboratory evaluation and field application.
- Most BMD performance tests are developed based on 6-inch SGC specimens, while limited research has been conducted on 4-inch Marshall-compacted specimens. The lack of well-defined relationships between these two specimen types restricts the applicability of BMD in agencies that continue to rely on Marshall mix design methods.

Chapter 3 Methodology

3.1 Materials

A total of twenty-four (24) TDOT 411-D dense-graded surface mixtures were collected from different regions across Tennessee and labeled from Mix A to Mix X according to the order in which the materials were received. The collected mixtures covered a broad range of binder grades, coarse aggregate types, NMAS, optimum asphalt contents, RAP contents, volumetric properties, and Marshall design properties. The JMF information, including Gmm, VMA, VFA, effective aggregate specific gravity, Marshall stability, and flow, is summarized in Table A-1. These materials were used to establish a representative performance database for currently approved TDOT 411-D mixtures and to support the development of preliminary BMD performance thresholds.

3.2 Aging conditions

The aging conditions used in this study included reheated PMLC mixtures, two short-term aging protocols for LMLC mixtures, and five different long-term aging protocols for evaluating the aging sensitivity of asphalt mixtures.

3.2.1 Reheated Conditioning for PMLC specimens

For PMLC specimens, plant-produced loose mixtures were reheated to the laboratory compaction temperature specified in the JMF. No additional short-term aging was applied to PMLC mixtures before compaction, except for the reheating required to make the plant mixture workable for quartering, weighing, and compaction.

3.2.2 Short-term aging for LMLC specimens

For laboratory-produced mixtures, short-term aging was selected based on the testing purpose: 2 hours at 135°C for rutting-related tests and 4 hours at 135°C for cracking-related tests. Additional no-STA and 2-hour STA cracking conditions were investigated for selected mixtures to compare LMLC performance with reheated PMLC specimens.

3.2.3 Long-term aging conditioning

To evaluate the cracking resistance of asphalt mixtures under different LTA conditions, five aging protocols specified in AASHTO R121-24 were examined, including 85°C for 5 days compacted aging, 85°C for 5 days loose aging, 95°C for 3 days loose aging, 115°C for 20 hours loose aging, and 135°C for 8 hours loose aging. Table 3-1 summarized all the different LTA protocols used in this study.

Table 3-1 Summary of Long-term aging protocols [33]

Method	*Aging Type*	*Temp (°C)*	*Duration*	*CDD Simulated*	*Field Aging Simulated*
A	Compacted Specimens	85	5 days	23,000	1-2 yrs (warm region) 2-3 yrs (cold region)
B	Loose Mixture	85	5 days	134,000	7-10 yrs (warm region), 12-14 yrs (cold region)

C	Loose Mixture	95	3 days	Based on CAI, ~8 yrs @ 30 mm depth	8 yrs @ 30 mm depth
D	Loose Mixture	115	20 hours	Simulates ~12 yrs at 50 mm depth	12 yrs @ 50 mm depth
E	Loose Mixture	135	8 hours	70,000	4.6 yrs (Tennessee)

Note: CDD = cumulative degree-days; CAI = Climate Aging Index. The CDD values and estimated field aging periods were obtained from AASHTO R121-24 and the original studies referenced therein.

3.3 Specimen Preparation

Two specimen compaction methods were used in this study: Superpave Gyratory Compactor (SGC) compaction and Marshall hammer compaction. The SGC specimens were used for the 6-inch performance tests, including IDEAL-CT, IDEAL-RT, and HWTT. The Marshall specimens were used for the 4-inch performance tests, including TN-CT and HT-IDT. Both plant-mixed laboratory-compacted (PMLC) and laboratory-mixed laboratory-compacted (LMLC) specimens were prepared to evaluate the difference between plant-produced mixtures and laboratory-produced mixtures.

3.3.1 Preparation of PMLC Specimens

For PMLC specimens, the plant-produced mixtures were reheated to ensure that mixtures were sufficiently soft to be separated manually. After the mixtures became workable, the loosened mixtures were then quartered and weighed into individual containers for each specimen, as shown in Figure 3-1. The weighed mixtures were reheated to the laboratory compaction temperature specified in the corresponding JMF. Once the mixtures reached a stable target compaction temperature, they were compacted using either the SGC or Marshall hammer, depending on the specimen type. Trial specimens were prepared for each mixture to determine the required mass needed to achieve the target air void content. After the target mass was established, batch specimen production was conducted.

For 6-inch SGC specimens, the mixtures were compacted using the Superpave Gyratory Compactor in height-control mode to the height of 62 ± 1 mm. The target air void content was 7 ± 0.5%. The bulk specific gravity of each compacted specimen was measured according to ASTM D2726, and the air void content was then calculated.

4-inch Marshall specimens were quartered, weighed, and compacted using a Marshall hammer. The specimen air voids were controlled by adjusting the number of Marshall blows and the mass placed in the Marshall mold. Trial specimens were prepared for each mixture to determine the specific mass and compaction effort required to produce specimens with a height of 63.5 ± 2.5 mm and an air void content of 7 ± 0.5%.

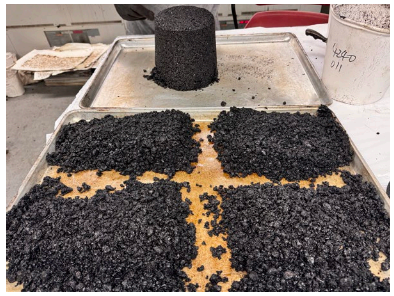

Figure 3-1 breaking down and quartering the reheated plant-produced mixtures

3.3.2 Preparation of LMLC Specimens

For LMLC specimens, the component materials were prepared according to the approved JMF. Aggregates were oven-dried at approximately 110°C to remove moisture. The required mass of each aggregate stockpile was determined based on the JMF proportions. Each batch of laboratory-produced mixture was designed to produce either three SGC specimens or six Marshall specimens. Aggregates and asphalt binder were preheated to the target mixing temperature specified in the JMF. Approximately 30 minutes before mixing, RAP was added to the preheated aggregates to allow the recycled material to reach the target mixing temperature. Once temperature was reached, the aggregates, RAP, and asphalt binder were mixed using an asphalt bucket mixer. After thoroughly mixing, the loose mixture was transferred to a pan and spread to a uniform thickness of approximately 25 to 50 mm for STA, as shown in Figure 3-2. During STA, the mixture was stirred every 60 minutes to promote uniform conditioning.

After aging in short-term, the laboratory-produced mixtures were quartered and weighed into individual containers for each specimen. Then mixtures were reheated to the compaction temperature and compacted by SGC to 62 ± 1 mm with 7 ± 0.5% air voids and Marshall specimens were compacted to 63.5 ± 2.5 mm in height with 7 ± 0.5% air voids.

(a) mixing the aggregates and asphalt binder

(b) lab-produced mixture for short-term aging

Figure 3-2 Lab mixture preparation

3.3.3 Preparation of LTA Specimens

LTA specimens were prepared to evaluate the influence of laboratory aging conditions on asphalt mixture cracking resistance and to support the selection of a practical aging protocol. In the earlier phase of the study, five LTA protocols listed in Table 3-1 were applied to Mix A to L. These LTA protocols were applied to both PMLC and LMLC 6-in SGC specimens.

3.3.3.1 Compacted Specimen Aging

For the plant-produced mixtures, the PMLC specimens were prepared as described above for the reheated condition. For LMLC mixtures, the laboratory-produced loose mixtures were first subjected to 4 hours of STA at 135°C and then mixtures were compacted using the SGC to a target height of 62 ± 1 mm and an air void content of 7 ± 0.5%. Only specimens meeting the target air void range of 7 ± 0.5% were selected for compacted LTA. The selected specimens were placed on steel plates to ensure that they did not touch each other and were then placed in a forced-draft oven at 85°C for 5 days (120 hours). During the aging period, the oven door was kept closed to maintain a stable aging environment. After 5 days of aging, the oven was turned off, the door was opened, and the specimens were allowed to cool to room temperature before being removed and prepared for performance testing.

3.3.3.2 Loose Mixture Aging

For PMLC specimens, the plant-produced mixtures were reheated until workable and broken apart. The loose mixture was spread in pans following the requirements of the corresponding aging protocol in AASHTO R121-24. Methods B and D specified a layer thickness of approximately 25 to 50 mm, whereas Methods C and E required the loose mixture layer thickness to NMAS±2mm. For LMLC specimens, the laboratory-produced loose mixtures were first subjected to 4 hours of short-term aging at 135°C. After STA was completed, the loose mixtures were allowed to cool to room temperature then were placed in a forced-draft oven at the target LTA temperature. After the target aging duration was completed, the loose mixtures were allowed to cool to room temperature and then were reheated. Once a stable compaction temperature was reached, the mixtures were compacted. For SGC specimens, the target height was 62 ± 1 mm with an air void content of 7 ± 0.5%. For Marshall specimens, the same loose mixture aging procedure was used. It should be noted that only the 115°C for 20 hours loose mixture aging condition was applied to Marshall specimens for both PMLC and LMLC specimens.

Figure 3-3 Compacted and loose LTA conditioning

3.4 Performance Test

Table 3-2 summarized the performance tests used in this study.

Table 3-2 Summary of Performance tests

Tests	*Test standard*	*Test Temp.*	*Sample size*	*Sample amount*	*Compact method*	*Target air voids*	*Test parameter*	*Aging methods*
IDEAL-CT	ASTM D 8225	25°C	D = 150 mm h = 62 mm	5 samples per mix	SGC	7±0.5%	Failure energy, l_{75}/$\|m_{75}\|$ CT index	PMLC: Reheated; LTAs (A, B, C, D, E) LMLC: STA 4h; LTAs (A, B, C, D, E)
TN-CT	ASTM D 8225	25°C	D = 100mm h = 63.5mm	5 samples per mix	Marshall	7±0.5%	Failure energy, l_{75}/$\|m_{75}\|$ TNCT index	PMLC: Reheated; LTA(D) LMLC: STA 4h; LTA (D)
IDEAL-RT	ASTM D 8360	50°C	D = 150 mm h = 62 mm	3 samples per mix	SGC	7±0.5%	RT index	PMLC: Reheated LMLC: STA 2h
HT-IDT	ASTM D 6931	50°C	D = 100mm h = 63.5mm	3 samples per mix	Marshall	7±0.5%	IDT strength	PMLC: Reheated LMLC: STA 2h
HWTT	AASHTO T 324	50°C (submerged)	D = 150 mm h = 62 mm	4 samples per mix	SGC	7±0.5%	TRD20k, RRI, SIP, CRD20k, etc.	PMLC: Reheated LMLC: STA 2h

3.4.1 Indirect Tensile Cracking Test (IDEAL-CT)

The Indirect Tensile Cracking Test (IDEAL-CT) was used to evaluate the intermediate temperature cracking susceptibility of 6-inch SGC specimens, as shown in Figure 3-4 (a). For each mixture and aging condition, three or five replicate specimens with a diameter of 150 mm, height of approximately 62 mm, and air void content of 7 ± 0.5% were prepared. Before testing, specimens were conditioned in a water bath at 25°C for 2 hours ± 10 minutes. The specimens were then tested at 25°C using a monotonic loading rate of 50 mm/min following ASTM D8225. The test was completed within 4 minutes after specimen removal from the water bath to maintain uniform specimen temperature.

The CT index was used as the primary cracking performance parameter. In general, a higher CT index indicates better cracking resistance. The fracture energy, Gf, was calculated from the work of failure and the cross-sectional area of the specimen, using Equation (3-1). The CT index was calculated based on specimen thickness, diameter, fracture energy, post-peak slope, and displacement at 75% of the post-peak load, using Equation (3-2) .

$$G_f = \frac{W_f}{D \times t} \times 10^6 \tag{3-1}$$

$$CT_{index} = \frac{t}{62} \times \frac{l_{75}}{D} \times \frac{G_f}{|m_{75}|} \tag{3-2}$$

where W_f is work of failure (Joules); CT_{index} is cracking tolerance index; G_f is failure energy (Joules/m^2); $|m_{75}|$ is absolute value of the post-peak slope m_{75} (N/m); l_{75} is displacement at 75% of the peak load after the peak (mm), t is thickness of specimen (mm), and D is specimen diameter (mm).

3.4.2 Tennessee Cracking Test (TN-CT)

The Tennessee Cracking Test (TN-CT), a modified IDEAL-CT test, was used to evaluate the cracking resistance of 4-inch Marshall specimens, as shown in Figure 3-4 (b). This test followed the same general conditioning and loading procedure as the IDEAL-CT test. Each Marshall specimen was conditioned in a water bath at 25°C for 2 hours ± 10 minutes and tested at a loading rate of 50 mm/min at 25°C. The fracture energy and TN-CT index were calculated using Equation (3-1) and Equation (3-2), the same conceptual framework as the IDEAL-CT index with, specimen geometry adjusted for the 4-inch Marshall specimen. The TN-CT test was included to determine whether cracking resistance measured using 4-inch Marshall specimens could be correlated with the IDEAL-CT results obtained from 6-inch SGC specimens.

3.4.3 Rapid Shear Rutting Test (IDEAL-RT)

The IDEAL Rutting Test (IDEAL-RT) was used to evaluate the rutting resistance of 6-inch SGC specimens, as shown in Figure 3-4 (c). For each mixture, three replicate specimens with a diameter of 150 mm, height of 62 mm, and air void content of 7 ± 0.5% were prepared. Specimens were conditioned in a water bath at 50°C for 45 ± 5 minutes, and a monotonic load was applied at a loading rate of 50 mm/min, following ASTM D8360. The test was completed within 2 minutes after specimen removal from the water bath. The loading conditions created two shear planes in the specimen, and the resulting peak load was used to calculate the shear strength(τ_f) and rutting tolerance index, RT_{index}, using Equation (3-3) and Equation (3-4), respectively. In general, a higher shear strength or higher RT_{index} indicates better rutting resistance.

$$\tau_f = 0.356 \times \frac{P_{max}}{t \times w} \tag{3-3}$$

$$RT_{index} = 6.618 \times 10^{-5} \times \frac{\tau_f}{1Pa} \tag{3-4}$$

where τ_f is the shear strength (Pa); RT_{index} is the rutting tolerance index; P_{max} is the maximum load(N); t is the specimen thickness (m); and w is the width of the upper loading trip (0.0191m).

3.4.4 High-Temperature Indirect Tension Test (HT-IDT)

The High-temperature Indirect Tensile Strength test (HT-IDT) was used to evaluate the rutting-related strength of 4-inch Marshall specimens. Each specimen was conditioned in a water bath at 50°C for 45 ± 5 minutes and then tested by applying an indirect tensile load at a loading rate of 50 mm/min. The test was completed within 2 minutes after removing the specimen from the water bath. The HT-IDT strength was calculated from the maximum load, specimen thickness, and specimen diameter, using Equation (3-5).

$$S_t = \frac{2000P_{max}}{\pi D t} \tag{3-5}$$

Where P_{max} is the maximum load (N); t is the specimen thickness (mm); D is the diameter of specimens (mm)

3.4.5 Hamburg Wheel-Tracking Test (HWTT)

The Hamburg Wheel Tracking Test (HWTT) was used to evaluate the rutting resistance and moisture susceptibility by applying cycles of loaded steel wheels passing across test specimens, as shown in Figure 3-4 (d). For each mixture, four SGC specimens with a diameter of 150 mm, height of approximately 62 mm, and air void content of 7 ± 0.5% were prepared and trimmed to fit the Hamburg test molds. Testing was conducted using the Asphalt Pavement Analyzer according to AASHTO T324-19. Before testing, the equipment was calibrated for temperature, vertical displacement, and load. Specimens were mounted in the test mold and submerged in water at 50°C for 45 ± 5 minutes. The test was conducted under a wheel load of 158 ± 1 lb for up to 20,000-wheel passes while the specimens remained submerged at 50°C. Rut depths (RD) along the specimens are recorded during each wheel pass. The specimens are commonly loaded for a maximum of 20,000 passes or until the RD reaches the preset failure point. Analysis of the plots of RD versus passes are used to assess rutting susceptibility and/or moisture damage susceptibility of the mixture.

HWTT results are typically evaluated using the total rut depth at 20,000 passes (TRD20k) and the number of passes required to reach 12.5 mm rut depth (N12.5). However, relying solely on rut depth measurements may not always provide an accurate assessment of mixture rutting resistance. This is primarily due to the confounding effects of permanent deformation and moisture-induced damage (i.e., stripping), especially for asphalt mixtures that are susceptible to moisture damage. To address these limitations, several alternative HWTT parameters have been proposed by researchers and practitioners. These include rutting resistance index (RRI) and corrected rut depth (CRD) for evaluating rutting resistance, as well as stripping-to-creep slope ratio (SS/CS ratio) and stripping number (SN) for assessing moisture susceptibility [34].

Rutting Resistance Index (RRI) was developed to address the difficulty of comparing the rutting resistance determined by the rut depth at 20,000 cycles or number of cycles at specified maximum rut dept like 12.5mm. As expressed in Equation (3-6), RRI considers both rut depth and the number of wheel passes at completion of the test.

$$RRI = N \times (25.4 - RD) \tag{3-6}$$

where *N* is the number of wheel passes at completion of test; *RD* is the rut depth in mm.

According to the studies from NCAT, the RT index exhibits a strong correlation with CRD20k as a representative pure rutting parameter [35]. This relationship has been found to be applicable across mixtures with varying material compositions, test temperatures, and performance characteristics, including those with significantly different rutting and moisture resistance. Based on these findings, a similar framework was adopted in this study to process and analyze the HWTT data.

A HWTT data processing template was developed using Excel, as shown in Figure 3-5, to streamline the analysis of rut depth data, particularly for mixtures exhibiting a SIP. The raw rut depth data were directly copied into the template. The SIP location was visually identified by inspecting the rut depth versus load cycle curve. Based on this observation, the corresponding pass number was manually input as the *Working SIP*. In addition, a *Fit Start Pass* was specified to define the starting point of the fitting range.

The rutting behavior prior to stripping was modeled using a power function of the form in Equation (3-7).

$$y = y_0 + A \cdot N^P \qquad (3\text{-}7)$$

where y is the rut depth, N is the number of load cycles, and y_0, A, and P are fitting parameters. The fitting is performed using only the data between the *Fit Start Pass* and the *Working SIP*, thereby capturing the pre-stripping rutting trend. Once the model is established, the fitted curve is extrapolated from the *Working SIP* to 20,000 passes. The extrapolated rut depth at 20,000 passes is taken as the corrected rut depth (CRD20k), which represents the rutting component without the influence of stripping.

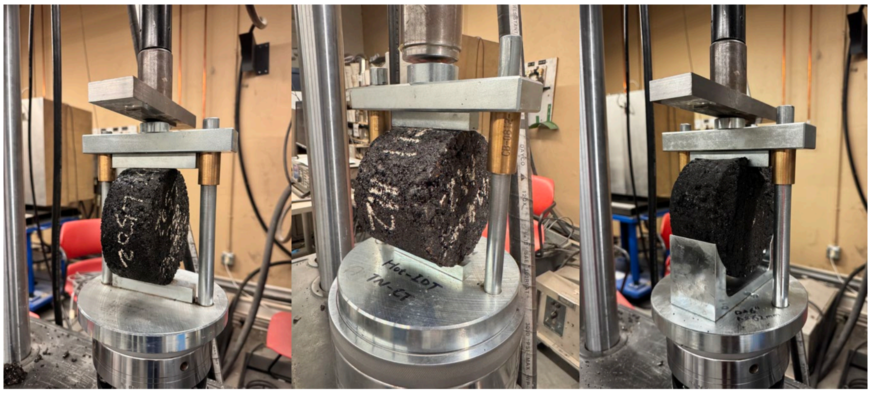

(a) IDEAL-CT (b) TN-CT&HT-IDT (c) IDEAL-RT

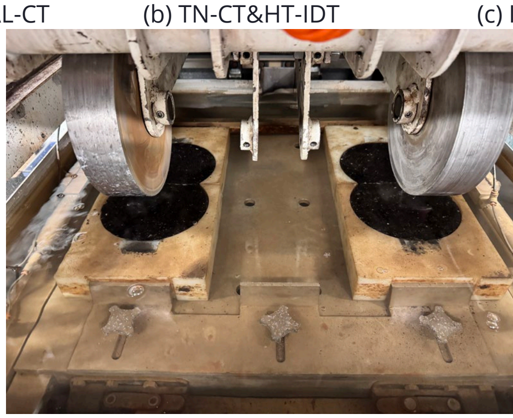

(d) HWTT

Figure 3-4 Performance tests

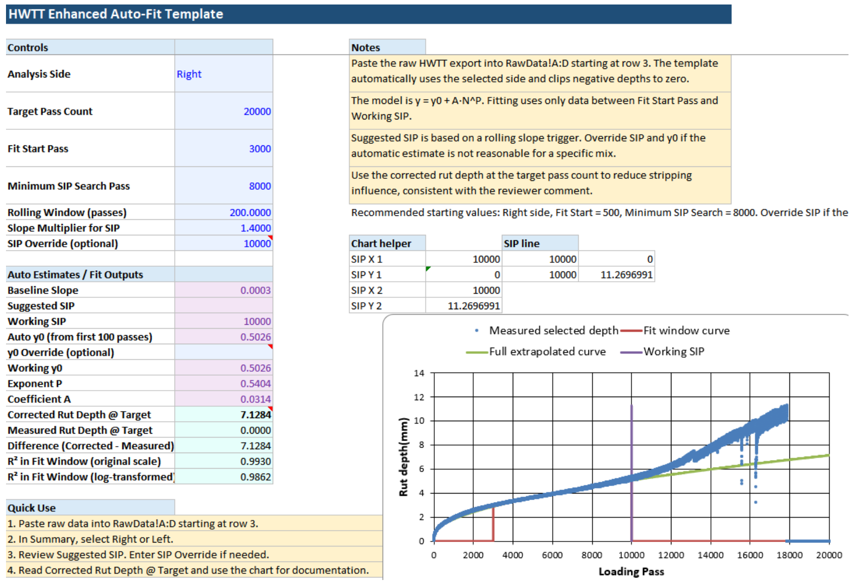

HWTT Enhanced Auto-Fit Template

Controls	
Analysis Side	Right
Target Pass Count	20000
Fit Start Pass	3000
Minimum SIP Search Pass	8000
Rolling Window (passes)	200.0000
Slope Multiplier for SIP	1.4000
SIP Override (optional)	10000

Auto Estimates / Fit Outputs	
Baseline Slope	0.0003
Suggested SIP	
Working SIP	10000
Auto y0 (from first 100 passes)	0.5026
y0 Override (optional)	
Working y0	0.5026
Exponent P	0.5404
Coefficient A	0.0314
Corrected Rut Depth @ Target	7.1284
Measured Rut Depth @ Target	0.0000
Difference (Corrected - Measured)	7.1284
R² in Fit Window (original scale)	0.9930
R² in Fit Window (log-transformed)	0.9862

Quick Use
1. Paste raw data into RawData!A:D starting at row 3.
2. In Summary, select Right or Left.
3. Review Suggested SIP. Enter SIP Override if needed.
4. Read Corrected Rut Depth @ Target and use the chart for documentation.

Notes
Paste the raw HWTT export into RawData!A:D starting at row 3. The template automatically uses the selected side and clips negative depths to zero.
The model is y = y0 + A·N^P. Fitting uses only data between Fit Start Pass and Working SIP.
Suggested SIP is based on a rolling slope trigger. Override SIP and y0 if the automatic estimate is not reasonable for a specific mix.
Use the corrected rut depth at the target pass count to reduce stripping influence, consistent with the reviewer comment.

Recommended starting values: Right side, Fit Start = 500, Minimum SIP Search = 8000. Override SIP if the

Chart helper		SIP line	
SIP X 1	10000	10000	0
SIP Y 1	0	10000	11.2696991
SIP X 2	10000		
SIP Y 2	11.2696991		

Figure 3-5 HWTT data processing template

Chapter 4 Results and Discussion

4.1 Long-term Aging Protocol Evaluation

A major objective of this study was to identify a practical LTA protocol for evaluating the cracking resistance of TDOT 411-D surface mixtures within a BMD framework. Cracking resistance is strongly affected by oxidative aging. Therefore, a mixture that performs well under an unaged or short-term aged condition may not necessarily maintain adequate cracking resistance after long-term field aging. However, current LTA protocols vary considerably in aging temperature, aging duration, and whether the mixture is aged in the loose or compacted state. This creates uncertainty for BMD implementation because different aging protocols can produce different cracking performance results and, consequently, different conclusions regarding mixture acceptability.

To address this issue, the research team evaluated several LTA protocols using PMLC specimens and the IDEAL-CT test. The aging protocols included: compacted specimen aging at 85°C for 5 days, loose mixture aging at 85°C for 5 days, loose mixture aging at 95°C for 3 days, loose mixture aging at 115°C for 20 hours, and loose mixture aging at 135°C for 8 hours. A reheated condition without additional LTA was used as the control condition.

4.1.1 CT index results under various long-term aging conditions

Figure 4-1 presents the CT index results of twelve evaluated PMLC specimens (Mix A to L) under six different aging conditions. The column and error bars represent average value, average value plus or minus one standard deviation, respectively. It is worth noting that the CT index value of Mix I is significantly higher compared to the other mixtures, which could mislead the overall distribution of CT index values. Therefore, the results of Mix I were removed from the database.

As shown in Figure 4-1, there is significant variation in CT index across different mixtures, with reheated specimens showing a range from 62 to 230, and specimens subjected to different LTA methods showing a range from 11 to 123, which reflects the difference in cracking resistance of various mixtures. In general, the reheated specimens exhibited the highest CT_{index} values, while those subjected to LTA conditions, whether compacted aging or loose aging, showed a significant reduction in CT_{index}. This indicates that LTA conditions diminish the cracking resistance of asphalt mixtures. This observation is consistent with the expected effect of oxidative aging, where asphalt binder becomes stiffer and more brittle, leading to lower cracking tolerance. In addition, these observations also confirmed that the CT index, as an indicator of asphalt mixture cracking resistance, is highly sensitive to different aging conditions, which aligns with the findings of other researchers [36], [37].

The reduction in CT index following the 5-day aging at 85 °C in compacted specimens is less pronounced compared to that observed in loose aging protocols. This suggests that compacted aging is less severe than loose aging, even with a longer duration. This may be because the aging of the compacted specimens mainly affects the outer layer of the specimens, while the aging degree of the inner part of specimens is lower. Notably, Mix K is the only exception, exhibiting a slightly higher CT index after aging at 85 °C for 5 days in compacted specimens compared to its reheated condition. This anomaly may be related to the issues inherent in the compacted aging method. Previous studies have stated that compacted aging method may lead to softening or slumping of specimens during the aging process, which potentially alter air voids and specimens geometry [38]. Additionally, compacted specimen aging could induce radial and vertical aging gradients within the asphalt mixture, resulting in non-uniform aging degree throughout the specimen. This variability could be a cause for concern when compacted specimens are used for performance testing, as it may compromise the accuracy and representativeness of the test results [25].

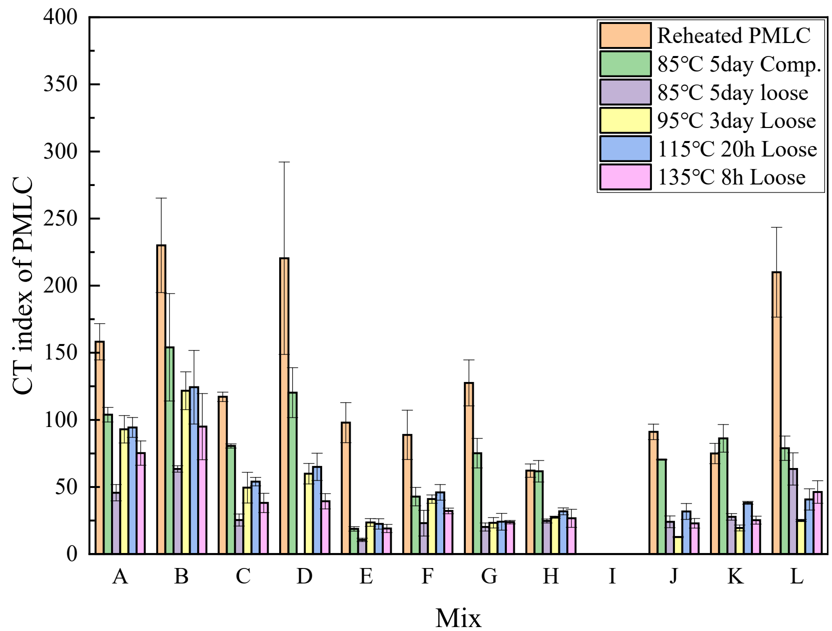

Figure 4-1 CT index results of PMLC specimens under various aging conditions

To further evaluate the effects of different long-term aging protocols on the cracking resistance of plant-produced mixtures, Figure 4-2 presents the cumulative distribution curves of CT index values under different aging conditions. The reheated PMLC condition, which did not receive additional long-term aging, showed the highest CT index values. Its cumulative distribution curve shifted farthest to the right and covered the widest range, indicating that the mixtures retained the greatest cracking resistance under this condition.

In contrast, the 85°C for 5 days loose-mixture aging condition showed the most severe aging effect. Its cumulative distribution curve shifted farthest to the left and exhibited a relatively narrow range of low CT index values, indicating a substantial reduction in cracking resistance. The 85°C for 5 days compacted-specimen aging condition resulted in higher CT index values than the 85°C for 5 days loose-mixture aging condition. This indicates that compacted-specimen aging produced a less severe apparent aging effect than loose-mixture aging at the same temperature and duration. This difference is likely related to nonuniform oxidation within compacted specimens. During compacted aging, the outer portion of the specimen is directly exposed to heat and oxygen, while the inner portion is less exposed and therefore experiences a lower degree of aging. In contrast, loose-mixture aging provides greater exposure of the asphalt-coated aggregates to oxygen, resulting in more uniform and more severe aging.

The other loose-mixture aging conditions, including 95°C for 3 days, 115°C for 20 hours, and 135°C for 8 hours, produced intermediate levels of aging severity. Their cumulative distribution curves were located between the reheated PMLC condition and the 85°C for 5 days loose-aging condition. The CT index values of specimens aged at 135 °C for 8 hours, 115 °C for 20 hours, and 95 °C for 3 days are comparable overall, suggesting that these LTA protocols produce similar levels of cracking degradation. Among them, the results from 115 °C for 20 hours and 95 °C for 3 days appear particularly close, indicating a more consistent aging response between these protocols.

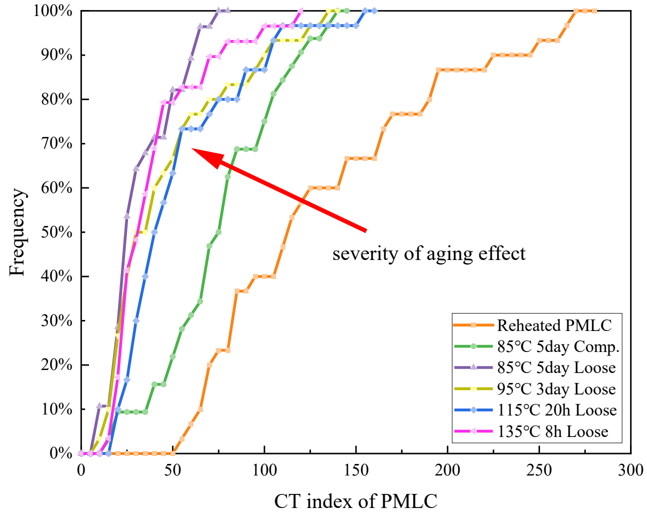

Figure 4-2 Cumulative distribution curve of CT index under different aging conditions

Sensitive analysis of CT index results under various aging protocols was conducted. The one-way analysis of variance (ANOVA) results yielded a p-value of 6.28×10^{-8}, indicating that the differences in CT index values under various long-term aging protocols are statistically highly significant. This confirms that the LTA method has a pronounced effect on the cracking performance of asphalt mixtures as measured by the CT index. Tukey's Honest Significant Difference (HSD) test was employed to identify statistically significant differences among individual aging protocols, and the results are presented in Figure 4-3 (a) using the Compact Letter Display (CLD). Groups with the same letters mean that the difference between their means is not statistically significant at the chosen significance level. Conversely, if groups do not share the same letter, it indicates there is a significant difference between them.

The box plot in Figure 4-3 (a) shows the distribution of CT index values under the different LTA protocols, with superimposed letters indicating Tukey HSD post-hoc groupings. The reheated condition exhibits the highest median CT index, along with a wider interquartile range (IQR) and overall spread than the aged samples. This group is uniquely labeled "*a*," indicating that the reheated condition yields a statistically higher CT index than all LTA conditions, confirming the pronounced detrimental effect of aging on cracking resistance. The 85 °C 5-day Compacted protocol, labeled "*b*," has a CT index significantly lower than reheated condition but significantly higher than the 85 °C 5-day Loose condition, labeled "*c*." The 95 °C 3-day Loose, 115 °C 20-hour Loose, and 135 °C 8-hour Loose protocols share the grouping letters "*bc*," indicating no statistically significant differences in CT index among them. This is consistent with the similar CT index cumulative distribution curves observed in Figure 4-2.

Figure 4-3 (b) presents the key statistics derived from the box plot and key distribution metrics, including median, interquartile, and percentile value. Based on the cumulative distribution curves, boxplot and key statistics, the aging severity generally followed this order: Reheated condition < 85°C for 5 days compacted aging < 115°C for 20 hours loose aging < 95°C for 3 days loose aging < 135°C for 8 hours loose aging < 85°C for 5 days loose aging.

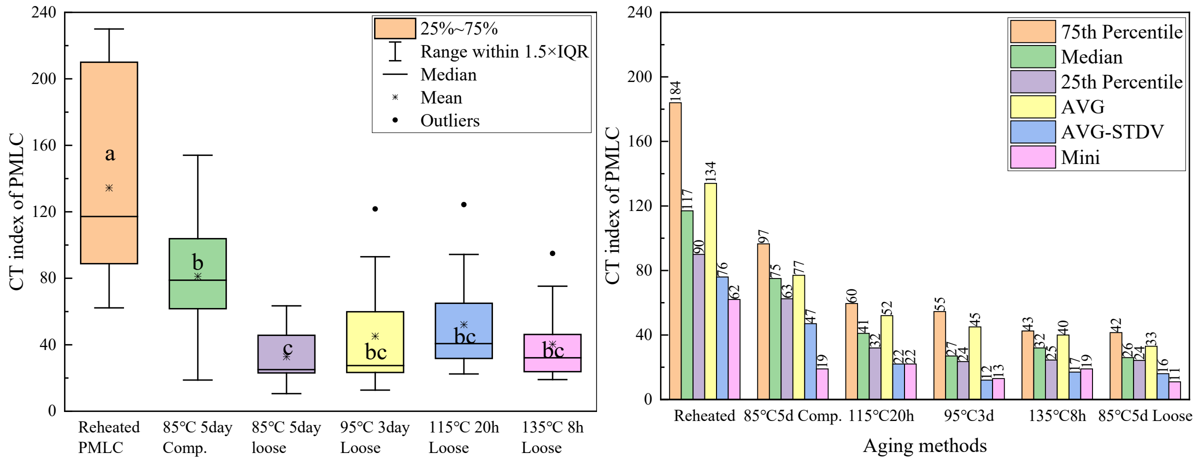

(a) (b)

Figure 4-3 CT index under different long-term aging conditions, (a) Box plot; (b) key statistics

4.1.2 Long-term aging protocol recommendation

Although the 85°C for 5 days compacted-specimen aging protocol, specified in AASHTO R30, has been widely used by state highway agencies, several concerns have been reported regarding the use of compacted specimens for long-term aging, as discussed previously. Specifically, compacted-specimen aging may cause changes in specimen air voids and geometry due to specimen softening and slumping [39] and may also produce radial and vertical aging gradients within the asphalt mixture, which is a concern for the use of compacted specimens in performance testing because properties differ throughout a specimen [25].

The cumulative distribution curves and box plot showed that the CT index distributions for the 95°C for 3 days and 115°C for 20 hours loose-mixture aging conditions were close to each other, indicating that these two protocols produced similar aging effects. The 95°C for 3 days loose protocol is generally considered one of the most robust because it was developed and validated with more than 35 sets of lab-to-field aging data from 10 field projects across the US [40]. However, this method requires a 3-day aging period, followed by additional time for reheating, compaction, cooling, specimen preparation, conditioning, and testing. Therefore, it is not practical for routine BMD implementation, particularly for QA/QC applications where timely results are required [21].

The 115°C for 20 hours and 135°C for 8 hours loose-mixture aging methods offer improved efficiency because accelerated aging at elevated temperatures allows test results to be obtained within approximately two days. This is beneficial for state highway agencies and asphalt contractors. However, the 135°C for 8 hours protocol may not be appropriate for all

HMA mixtures because very high aging temperatures could cause potential thermal degradation of SBS-modified binders [40]. In addition, aging loose mixtures at elevated temperatures may lead to asphalt mastic drain-down because of the reduced viscosity of asphalt binder at high temperatures [25].

Based on the cumulative distribution curves and the recommendations from previous studies [40], the aging effect of loose-mixture aging at 115°C for 20 hours is comparable to that of loose-mixture aging at 95°C for 3 days, which is one of the most robust loose aging methods. Compared with the 135°C for 8 hours protocol, the 115°C for 20 hours condition uses a lower aging temperature, which may reduce the risk of excessive high-temperature effects while still providing practical laboratory efficiency. In addition, the 20-hour duration is more compatible with routine laboratory scheduling because the aging process can be conducted overnight and followed by compaction and testing on the next workday. It fits the 8-hour work schedule better. Therefore, loose-mixture aging at 115°C for 20 hours is recommended as a reasonable long-term aging protocol for the current stage of TDOT BMD implementation. However, additional field validation is still required before this protocol is adopted as a formal specification requirement.

4.2 Development of a generalized aging method

In the current BMD framework, the variables in the aging protocols primarily focus on three factors: aging temperature, duration, and the state of the mixture (loose or compacted). To identify the optimal aging protocol, it is necessary to understand the influence of these three factors on the aging effect. Because compacted aging introduces additional complexity related to nonuniform oxidation [25], the generalized aging analysis focused on the loose-mixture aging protocols.

Laboratory aging of asphalt mixtures is primarily influenced by oven temperature and oven aging duration, both of which critically affect the rate and severity of oxidative aging. Higher temperatures accelerate oxidation, enabling simulation of long-term field aging within a shorter timeframe, while longer durations increase the overall aging effect.

4.2.1 Shifting aging time according to aging temperature

Figure 4-4 (a) presents scatter plots of the CT index versus oven aging time for Mix C, illustrating the relationship between CT index, aging temperature, and aging duration. CT index generally decreased with aging time. However, specimens aged at a higher temperature of 135°C for 8 hours exhibited significantly lower CT index, highlighting the pronounced effect of elevated temperature. The CT index for specimens aged at 95°C for 72 hours and 115°C for 20 hours were comparable, as mentioned in the previous section, despite the aging duration for the 95°C condition being more than three times longer. The phenomenon indicates that oven aging time or temperature alone cannot fully represent the severity of aging.

To further explore this observation, an integrated parameter, referred to as the dimensionless coefficient of “equivalent aging time”, is introduced to account for the combined effects of aging temperature and duration. This parameter reflects the cumulative aging effect by shifting the oven aging time based on temperature, where higher temperatures correspond to longer equivalent aging times. The shifting is visualized in Figure 4-4 (b). The plot of the CT index and the equivalent aging time is shown in Figure 4-4 (c), therefore, the CT index follows a more consistent descending exponential pattern with equivalent aging time fitted well using an exponential function, with $R^2 = 0.9407$. To further validate the rationality of the fitted curve, two additional aging methods (100°C for 12 hours and 100°C for 132 hours) were conducted on the asphalt mixture, and the corresponding CT index values were measured under these conditions. These two aging conditions are to check whether CT index measurement follows the exponential curve specified in Figure 4-4 (c): (i) between unaged and 115°C 20 hours and (ii) beyond 85°C for 120 hours, respectively. After applying the same shifting process to the results, it was found that the CT index values from the two additional aging protocols aligned well with the fitted curve, as shown in Figure 4-4 (d).

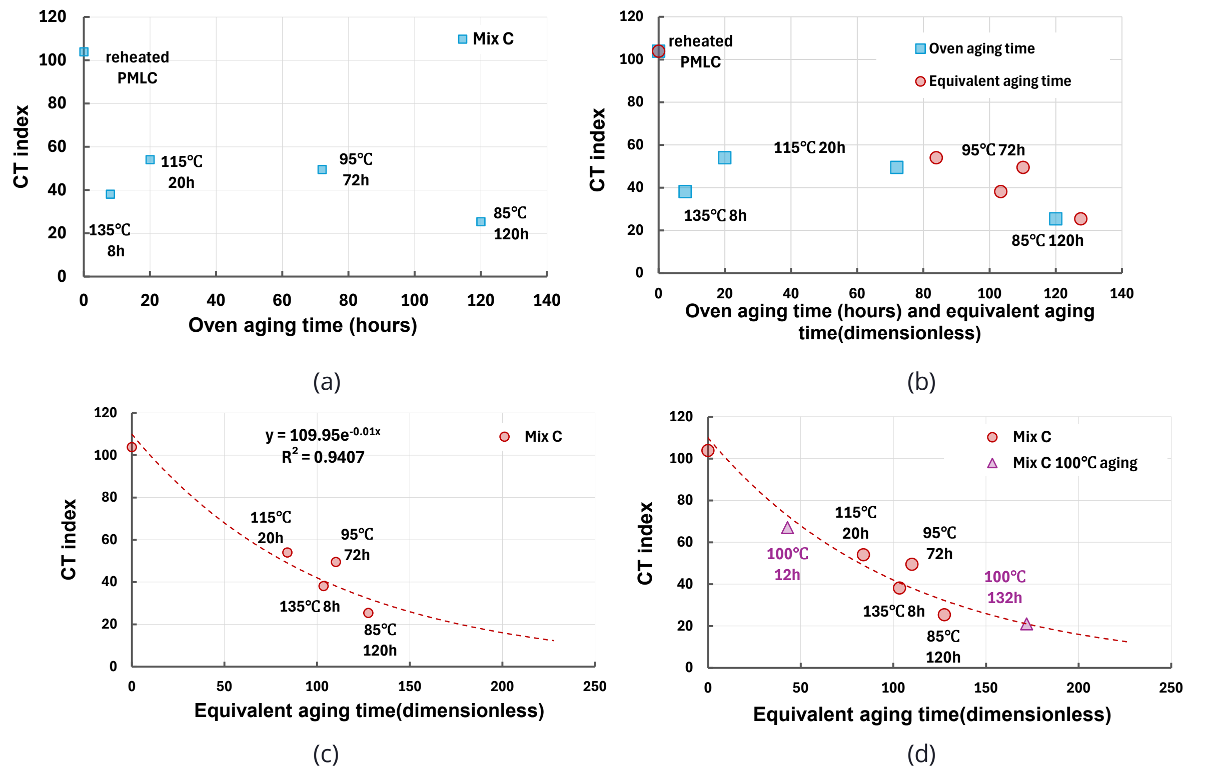

Figure 4-4 Plots of CT index versus oven aging time (hours) and equivalent aging time for Mix C: (a) CT index versus oven aging time, (b) conceptual shifting from oven aging time to equivalent aging time, (c) CT index versus equivalent aging time, and (d) with two additional aging conditions: 100°C for 12 hours and 100°C for 132 hours.

The same experiments were further conducted on another plant mixture, Mix E, with generally a lower level of CT index, including two additional aging conditions and corresponding data processing. The results, as shown in Figure 4-5 (a), indicate that the shifted data also exhibit a similar exponential relationship, and the additional two random aging conditions produced results that closely align with the fitted curve. This consistency further demonstrates the robustness and applicability of the proposed aging curves across different asphalt mixtures. Additionally, it can be observed from Figure 4-5 that the fitted curve for Mix C lies above that of Mix E, indicating that Mix C has generally better cracking resistance than Mix E under various aging conditions. As shown in Figure 4-5 (b), a semi-logarithmic graph exhibited different slopes for the two mixtures. The slope represents the severity of the mixture's response to the aging effect, or in other words, the sensitivity of the mixture to aging effects. This provides a more nuanced understanding of how each mixture is influenced by long-term aging.

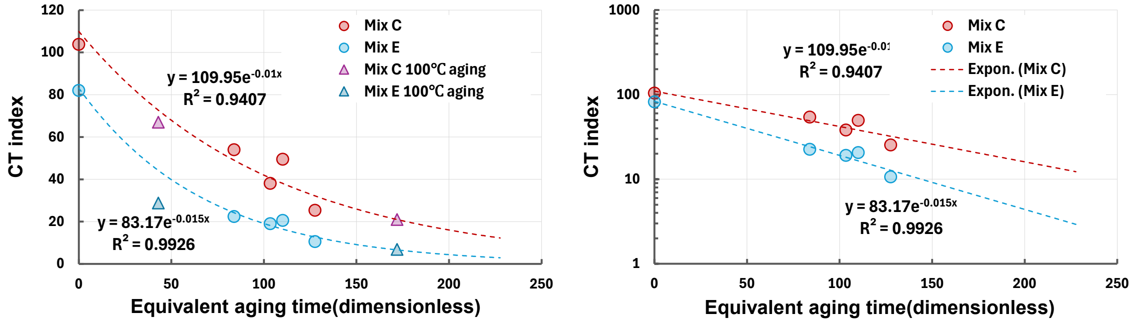

(a) (b)

Figure 4-5 Plots of CT index versus equivalent aging time for Mix C and E: (a) Linear and (b) semi-logarithmic.

4.2.2 Determine the coefficient of equivalent aging time

The equivalent aging time follows the mathematical structure of the Time–Temperature Superposition Principle (TTSP), commonly used in constructing dynamic modulus master curves. In master curve development, time (or frequency) is shifted through a temperature-dependent shift factor a_T, allowing responses at different temperatures to be represented on a single reference curve. The reduced time can be expressed using Equation (4-1) [41]

$$t_r = \frac{t}{a_T(T)} \tag{4-1}$$

where t_r is the reduced time, t is the real time, $a_T(T)$ represents a temperature-dependent shift factor. The shift factor follows the Williams-Landel-Ferry (WLF) equation, as shown in Equation (4-2)

$$\log(a_T) = \frac{-C_1\left(T - T_{ref}\right)}{C_2 + \left(T - T_{ref}\right)} \tag{4-2}$$

where C_1 and C_2 are the constants, T and T_{ref} are the temperature and reference temperature, respectively.

By substituting the shift factor back into the reduced time in Equation (4-1).

$$t_r = \frac{t}{a_T(T)} = \frac{t}{10^{\frac{-C_1(T-T_{ref})}{C_2+(T-T_{ref})}}} = t \cdot 10^{\frac{C_1(T-T_{ref})}{C_2+(T-T_{ref})}} = 10^{\log(t)+\frac{C_1(T-T_{ref})}{C_2+(T-T_{ref})}} \tag{4-3}$$

In this study, the shift factor was inspired by the WLF functional form to allow sufficient flexibility in capturing the nonlinear acceleration observed at elevated temperatures. The "equivalent aging time" can be expressed using the aging temperature and oven aging time through Equation (4-4)

$$t_{eq} = k_1 10^{k_2 \log(t) + k_3\left(\log(T-T_{ref})\right)^{k_4}} \tag{4-4}$$

where t_{eq} is the equivalent aging time; t is the oven aging time (hour); T is the aging temperature (°C); T_{ref} is the reference temperature that is set to be room temperature, 25°C; k_i are constants, where i = (1,2,3,4). k_1 = 6.5, k_2 = 0.578792271, k_3 = 1.92495×10^{-5}, and k_4 = 14.6726882. The parameters ki are calibrated using the least root mean squared error (RMSE) on the CT index results and the proposed equivalent aging time for all the tested mixtures in this work. The parameter k_1 serves as a global scaling factor controlling the magnitude of equivalent aging time. Parameter k_2 governs the sensitivity to oven aging duration, while k_3 represents the temperature acceleration effect. The exponent k_4 introduces curvature to capture nonlinear aging acceleration at elevated temperatures.

This method was applied to the CT index results of other tested plant-produced mixtures, as shown in Figure 4-6. It can be observed that all the curves fit well, with R^2 ranging from 0.8744 to 0.9845. From the semi-logarithmic plot, the curve slopes range approximately from -0.008 to −0.014, indicating the mixtures' sensitivity to aging effects. For the five aging protocols adopted in this work, the corresponding equivalent aging times are listed in Table 4-1, which are considered as an aging effect severity metric in the framework of the generalized aging method.

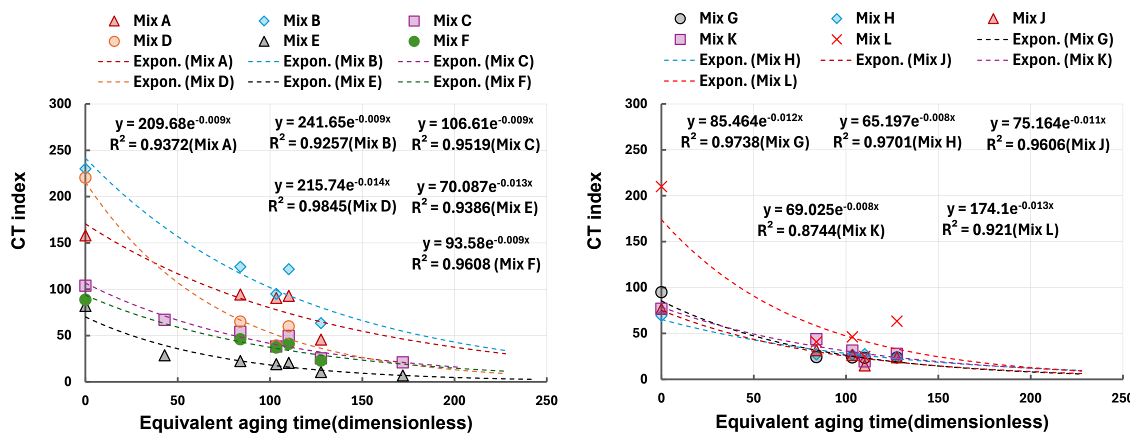

(a)

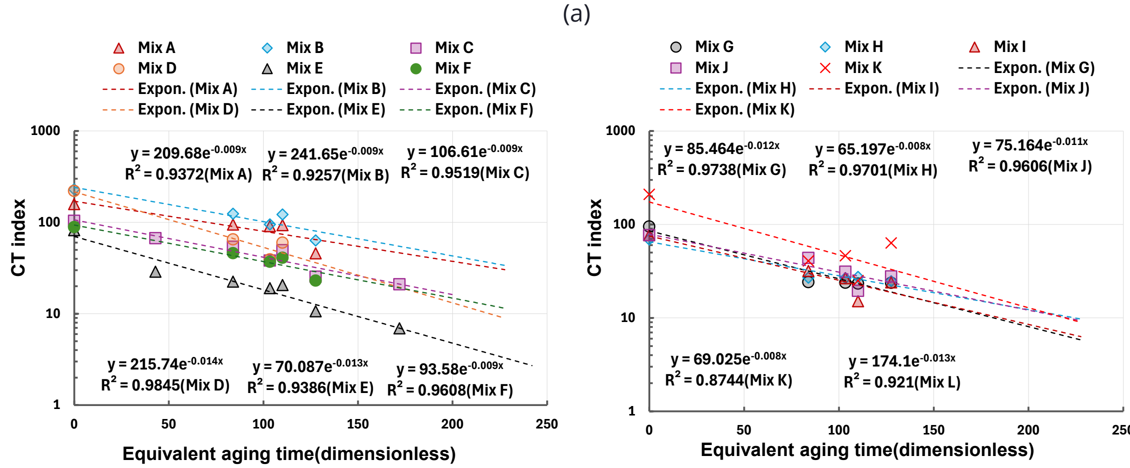

(b)

Figure 4-6 Plots of CT index versus equivalent aging time for PMLC mixtures: (a) Linear scale and (b) semi-logarithmic scale.

Table 4-1 The corresponding equivalent aging time for different long-term aging protocols for loose mixture.

Method	*Temp.(°C)*	*Duration*	*Field Aging Simulated*	*Equivalent aging time*
B	85	5 days	7-10 yrs (warm region), 12-14 yrs (cold region)	129.39
C	95	3 days	8 yrs @ 30 mm depth	107.25
D	115	20 hours	12 yrs @ 50 mm depth	82.14
E	135	8 hours	4.6 yrs (Tennessee)	102.98
Reheated	-	-	None	Zero

4.2.3 Comparative analysis of the general aging method

To further evaluate the robustness of the equivalent aging time method for capturing the pattern of CT index with aging in dense-graded asphalt mixtures in other states, a comparative study was conducted using CT index results reported by Zhou et al. [28] and Elwardany et al. [42].

In the study by Zhou et al. [28], seven dense-graded laboratory-produced asphalt mixtures with a nominal maximum aggregate size (NMAS) of 9.5 mm were evaluated, with six originating from the state of Texas and one from the state of Massachusetts. Five aging protocols were examined, including 3-day and 6-day loose mix aging at 95°C, and 20-hour aging at 110°C, 115°C, and 120°C.

Figure 4-7 (a) presents the CT index results under these five conditions plotted against oven aging time, emphasizing two distinct effects: (1) the impact of increasing temperature (from 100°C to 125°C) at a constant aging duration of 20 hours, and (2) the effect of extended aging duration (from 72 to 144 hours) at a constant temperature of 95°C. The equivalent aging times for Mix 3 and Mix 5, reported in Zhou et al. [28], were calculated using (4-4) and are presented in Figure 4-7 (b). After applying the equivalent aging time transformation, the CT index for both mixtures exhibits a more consistent exponentially decreasing trend. Figure 4-7 (c) plots the CT_{index} versus equivalent aging time in semi logarithmic scale. It can be observed that all the curves fit reasonably well, but with lower R^2 ranging from 0.55 to 0.69 compared with the results presented in the previous section. Besides, the semi-logarithmic curve slopes range approximately from -0.005 to −0.009 that descend relatively more slowly than Tennessee's results. The CT index of Tennessee Mix C is also plotted in red dots in Figure 4-7 (c) and is observed in a similar range to all other curves and exhibits a similar slope in semi-logarithm scale.

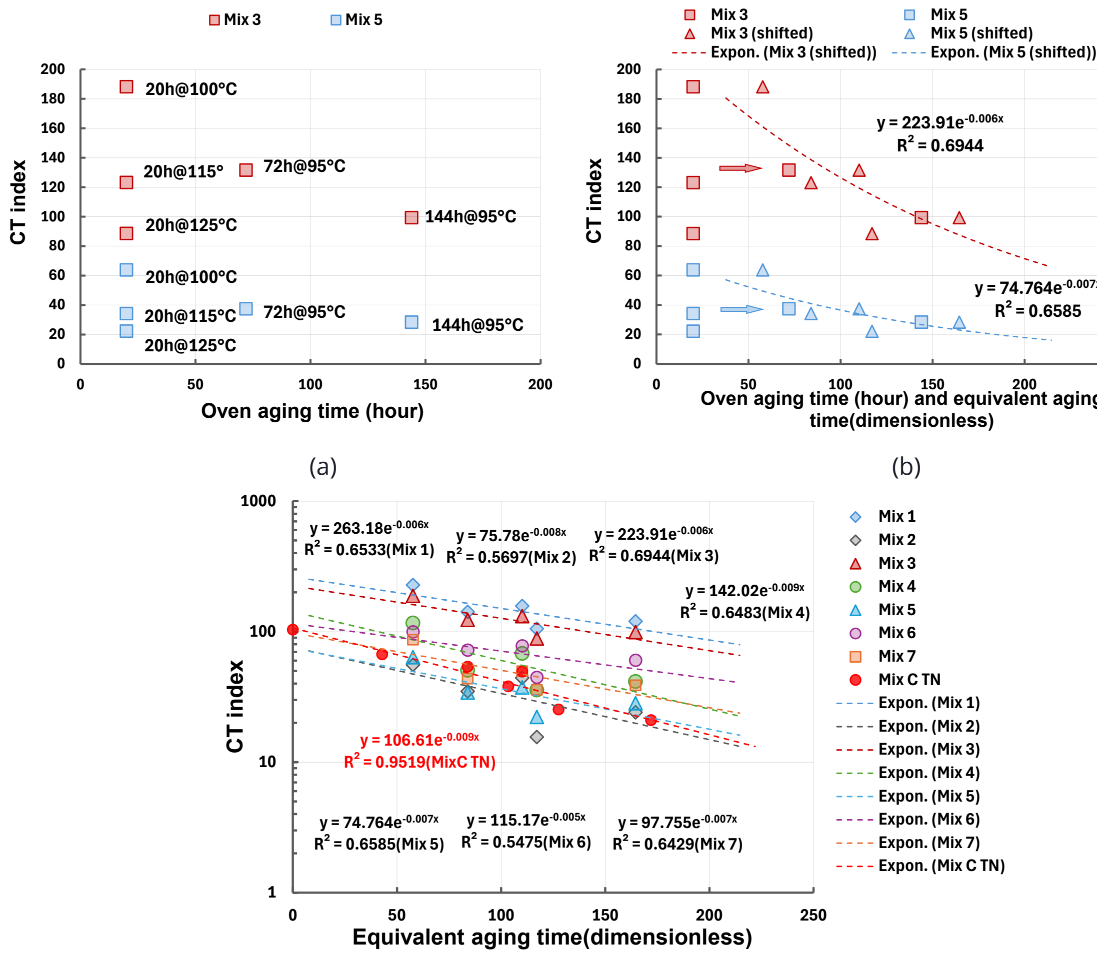

(c)

Figure 4-7 Plots of CT index versus oven aging time (hours) and equivalent aging time using test results from Zhou et al., [28] (2022): (a) CT index versus oven aging time, (b) conceptual shifting from oven aging time to equivalent aging time, and (c) CT index versus equivalent aging time in semi logarithmic scale.

In the study by Elwardany et al. [42], the tested mixtures were plant-produced and laboratory-compacted specimens from Florida, Montana, Ohio, and Vermont, featuring varying nominal maximum aggregate sizes (NMAS) and reclaimed asphalt pavement (RAP) contents. Based on the aging duration map developed by Elwardany et al., which estimates the oven aging time at 95°C equivalent to 8 years of field aging at 20 mm depth, the following durations were selected: 7 days for Florida (FL) mixtures, 4 days for Ohio (OH) mixtures, and 3 days for Montana (MT) and Vermont (VT) mixtures. Figure 4-8 (a) shows the CT_{index} results for Ohio and Montana mixtures under these aging conditions plotted against oven aging time. Figure 4-8 (b) presents the CT_{index} versus with the equivalent aging time after applying the aging duration shifting. Figure 4-8 (c) displays the CT index on a semi-logarithmic scale with respect to equivalent aging time. It can be observed that all the data points fit well with exponential curves, with R^2 values ranging from 0.86 to nearly 1.0. The slopes of most curves fall between −0.006 and −0.01 on the semi-logarithmic scale. Notably, Tennessee Mix C also demonstrates a similar trend, both in CT index range and slope, indicating consistent aging behavior across different mixtures from different sources.

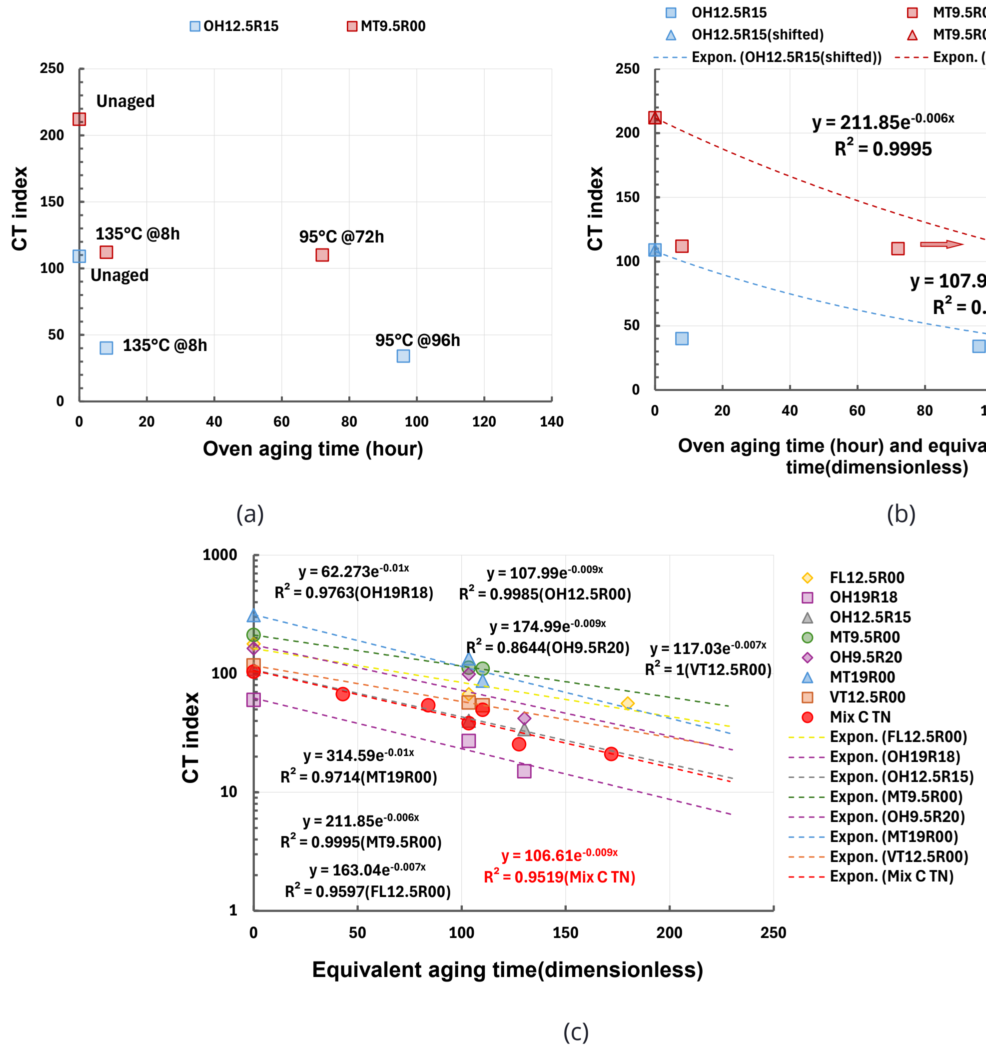

Figure 4-8Plots of CT index versus oven aging time (hours) and equivalent aging time using test results from Elwardany et al.,) [42]: (a) CT index versus oven aging time, (b) conceptual shifting from oven aging time to equivalent aging time and (c) CT index versus equivalent aging time in semi-logarithmic scale.

4.2.4 Discussion of generalized aging method framework

The dimensionless coefficient of equivalent aging time is derived solely from IDEAL-CT test results of dense-graded mixtures under various aging temperatures and durations. While other cracking resistance tests and other mix types within the BMD framework may exhibit similar trends when analyzed using the concept of equivalent aging time, this study provides no empirical evidence to support the generalization of this approach across all cracking tests. Additionally, the evaluated aging temperatures ranged from 85°C to 135°C, with long-term aging durations between 8 hours and 132 hours. Therefore, the applicability of the resulting CT index trend beyond these temperature and time ranges remains uncertain to some extent.

After shifting the oven aging time to the equivalent aging time, the CT index exhibits a consistent exponentially descending pattern, which can be described using an exponential function. Thus, an aging curve relating the CT index to equivalent aging time could be established using only two or more IDEAL-CT results, based on at least one from the unaged condition and one from a long-term aging condition.

The comprehensive aging curve provides a means to evaluate the cumulative aging effect and the corresponding CT index value. As shown in Figure 4-9 (a), equivalent aging time curves at various constant temperatures (ranging from 85°C to 135°C) are plotted based on (4-4). These curves depict the nonlinear relationship between oven aging time and equivalent aging time, with higher temperatures resulting in substantially greater aging severity for the same oven duration. This exponential trend highlights the amplified impact of temperature on the aging process. Figure 4-9 (b) conceptually demonstrates how cumulative aging can be quantified by summing the equivalent aging times from multiple aging stages. Once the total equivalent aging time is determined, the corresponding CT index can be estimated using the aging curve presented in Figure 4-9 (c), if such a curve is available.

This method could be valuable in the implementation of BMD, as it reveals the relationship between the aging effects of different aging protocols and the cracking resistance of asphalt mixtures, represented by the CT index. It could be used to evaluate the cracking resistance of mixtures. For instance, a higher position of the fitted curve suggests better cracking resistance of the mixture. Moreover, it illustrates the sensitivity of the cracking resistance of asphalt mixtures to aging. In the semi-logarithmic plot, a steeper slope indicates greater sensitivity to aging effects. In other words, the mixture is more prone to being affected by aging.

In addition, this method allows the prediction of the cracking resistance of mixtures under different aging conditions if field validation is available. Since the relationship between equivalent aging time and cracking resistance takes the form of an exponential function, its expression can be determined using only two data points. For example, the results from unaged samples and the ones aged at 115°C can be used to derive the aging curve for the mixture, which in turn can predict the CT index value for samples aged at 85°C. This could provide valuable guidance for state agencies, particularly as various states currently adopt different long-term aging protocols during the implementation of BMD. Such variability makes it challenging to compare the performance of similar asphalt mixtures across different regions, due to inconsistencies in aging conditions applied prior to performance testing.

Additionally, this method serves as an effective bridging tool for linking field aging with laboratory aging protocols. For instance, once the CT index values of field cores from in-service pavements are determined, the proposed generalized aging method can be applied to design realistic laboratory aging protocols. This method utilizes the established relationship between CT index and equivalent aging time, in conjunction with the correlation between equivalent aging time and oven-aging conditions, to simulate field-aged conditions with better accuracy.

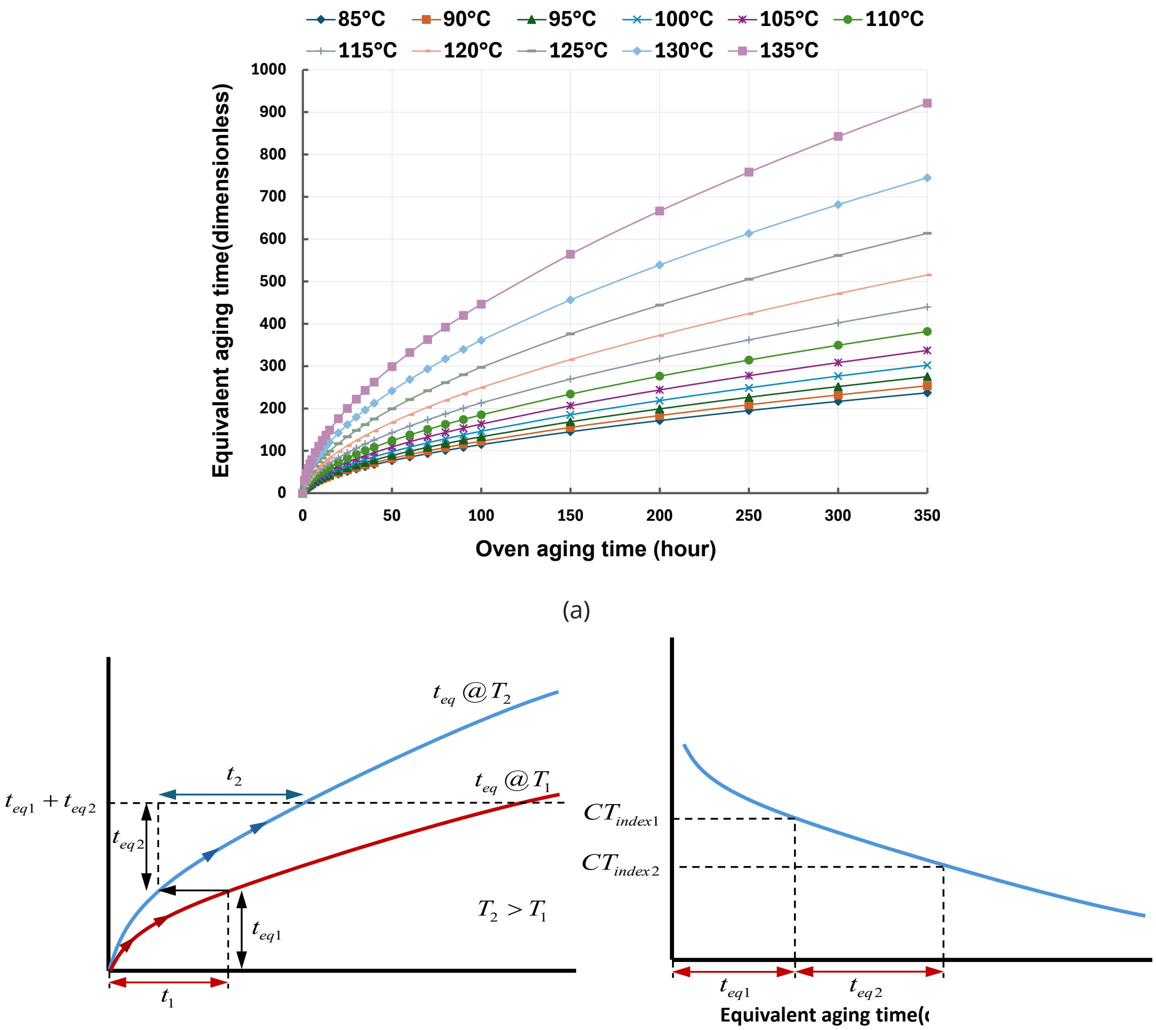

(b) (c)

Figure 4-9 Plots of (a) equivalent aging time versus oven aging time at different aging temperatures, (b) accumulated aging effect with various aging histories, and (c) CT index with accumulated aging effect with various aging histories.

4.3 Benchmark performance results

This section summarizes the benchmarking performance results of TDOT 411-D mixtures using both plant-mixed, laboratory-compacted (PMLC) and laboratory-mixed, laboratory-compacted (LMLC) specimens. The results provide a basis for developing preliminary threshold values for TDOT BMD implementation.

For the cracking evaluation, the comparison focused on the IDEAL-CT index obtained from 6-inch SGC specimens and the TN-CT index obtained from 4-inch Marshall specimens. Based on the LTA protocol evaluation presented in the previous section, only the 115°C for 20 hours loose-mixture aging protocol, referred to as LTA115, was used for the subsequent cracking resistance evaluation. For PMLC mixtures, cracking-related tests were conducted under both the reheated condition and the LTA115 condition. For LMLC mixtures, cracking-related tests were conducted under the 4-hour short-term aging condition and the LTA115 condition. For rutting evaluation, the comparison included the IDEAL-RT index from 6-inch SGC specimens, HT-IDT strength from 4-inch Marshall specimens, and Hamburg Wheel Tracking Test (HWTT) results from 6-inch SGC specimens. For LMLC mixtures, the 2-hour short-term aging condition was used for rutting-related tests.

4.3.1 CT index of PMLC and LMLC

4.3.1.1 CT index of reheated PMLC and STA4h LMLC

Figure 4-10 (a) presents the IDEAL-CT index results of reheated PMLC specimens and LMLC specimens subjected to 4 hours of short-term aging at 135°C. The column and error bars represent the average value and the average value plus or minus one standard deviation, respectively. Overall, the CT index values of the LMLC specimens were noticeably lower than those of the corresponding reheated PMLC specimens. The average CT index of the LMLC specimens ranged from approximately 30 to 171 across the evaluated mixtures, whereas the reheated PMLC specimens showed a much wider and higher range, from 62 to 449. This result indicates that the laboratory-produced mixtures after 4 hours of STA generally exhibited lower cracking resistance than the reheated plant-produced mixtures.

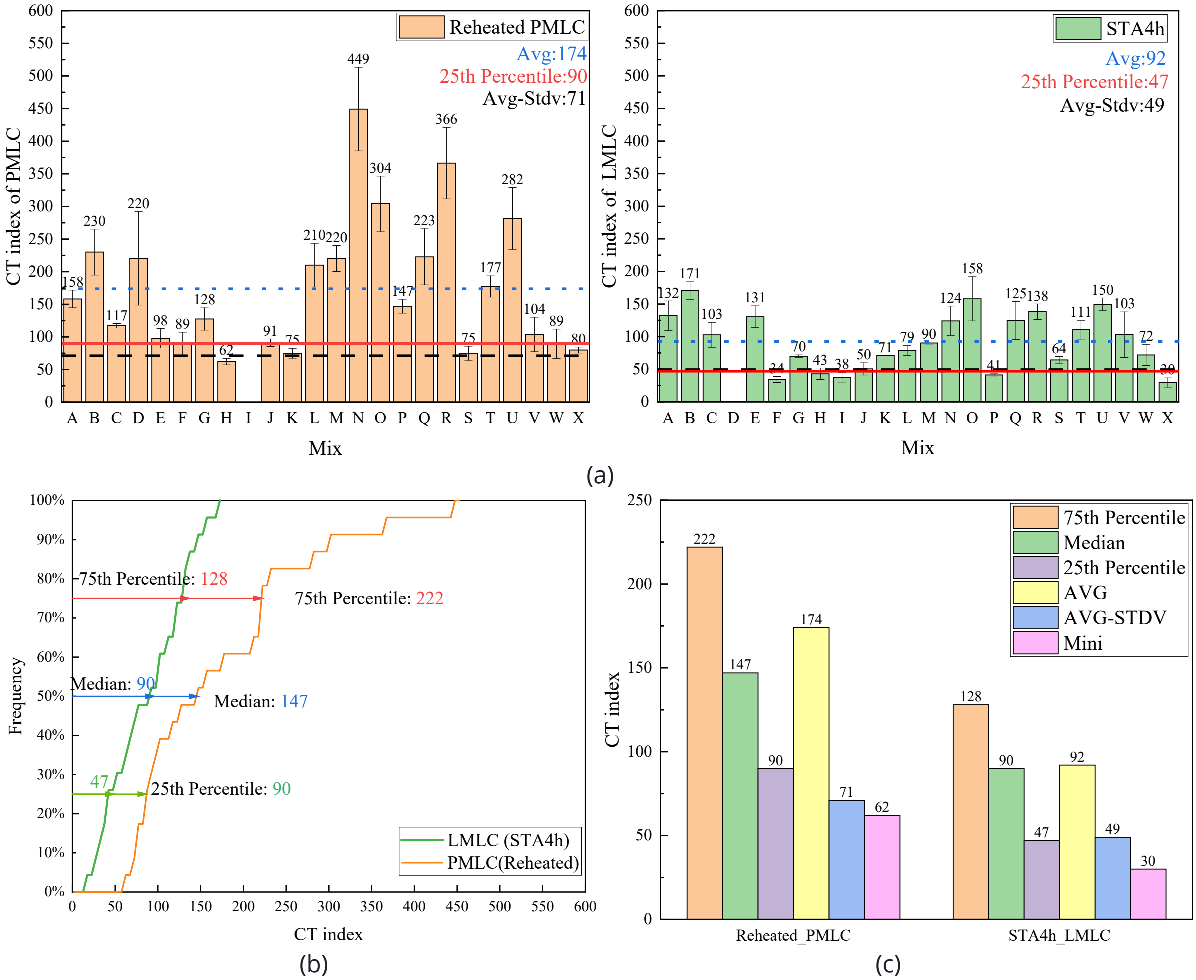

Figure 4-10 PMLC VS LMLC (a) CT index; (b) CT index cumulative distribution;(c) CT index thresholds

The cumulative frequency distribution curves further confirmed this trend, as shown in Figure 4-10 (b). It is worth noting that the CFD curves were constructed based on the average CT index values of 3 to 5 replicate specimens for each mixture. The LMLC distribution shifted toward lower CT index values compared with the PMLC distribution. For the LMLC specimens, the 25th, 50th, and 75th percentiles were approximately 47, 90, and 128, respectively. In contrast, the reheated PMLC specimens showed higher percentile values, with the 25th, 50th, and 75th percentiles approximately equal to 90, 147, and 222, respectively. This difference suggests that the 4-hour STA protocol applied to LMLC mixtures may create a higher aging level than that experienced by reheated PMLC mixtures.

From a threshold development perspective, four statistical metrics were considered: minimum value, mean value, mean minus one standard deviation, and selected percentile values. The percentile-based thresholds provide insight into the overall distribution of cracking performance. For example, adopting the 25th percentile as the threshold implies that 25% of the unaged mixtures would fall below this value. If this value is selected as the minimum acceptable CT index, approximately 25% of the currently approved mixtures would not satisfy the cracking resistance requirement. In contrast, adopting the 50th percentile as the threshold would result in approximately half of the tested mixtures being rejected. Using the mean or the 75th percentile as thresholds would be overly stringent, as the majority of mixtures would fail to meet the requirement.

It is important to note that the mixtures evaluated in this study were all surface mixtures previously approved by TDOT based on current volumetric design specifications. Therefore, both the 25th percentile and the mean minus one standard deviation are reasonable initial candidates. For example, assuming the CT index threshold is set at the 25th percentile, the corresponding values are 90 for PMLC specimens and 47 for LMLC specimens. As shown in Figure 4-10 (a), Mix F, H, K, S, and X did not meet the PMLC threshold of 90, while Mix F, H, I, K, P, and X failed to meet the LMLC threshold of 47. Notably, Mix F, H, K, and X were consistently identified as failing to meet the threshold in both PMLC and LMLC conditions, indicating relatively poor cracking resistance. These thresholds can filter out asphalt mixtures with relatively poor cracking resistance, thereby enhancing the overall durability of pavements in Tennessee, without imposing unrealistically high-performance requirements that may be difficult for local contractors to achieve under current mix design practices.

4.3.1.2 CT index of PMLC and LMLC under LTA115 ℃ for 20h

The CT index of PMLC and LMLC specimens after loose aging at 115℃ for 20 hours are shown in Figure 4-11. After LTA, both PMLC and LMLC specimens exhibited substantial reductions in CT index, confirming that long-term aging significantly reduced cracking resistance. The LMLC specimens generally remained lower than the PMLC specimens after the same LTA protocol. This is consistent with the short-term condition, where the LMLC specimens already showed lower initial cracking resistance before LTA. Therefore, when both specimen types were subjected to the same 115°C for 20 hours LTA protocol, the LMLC mixtures continued to show lower cracking tolerance.

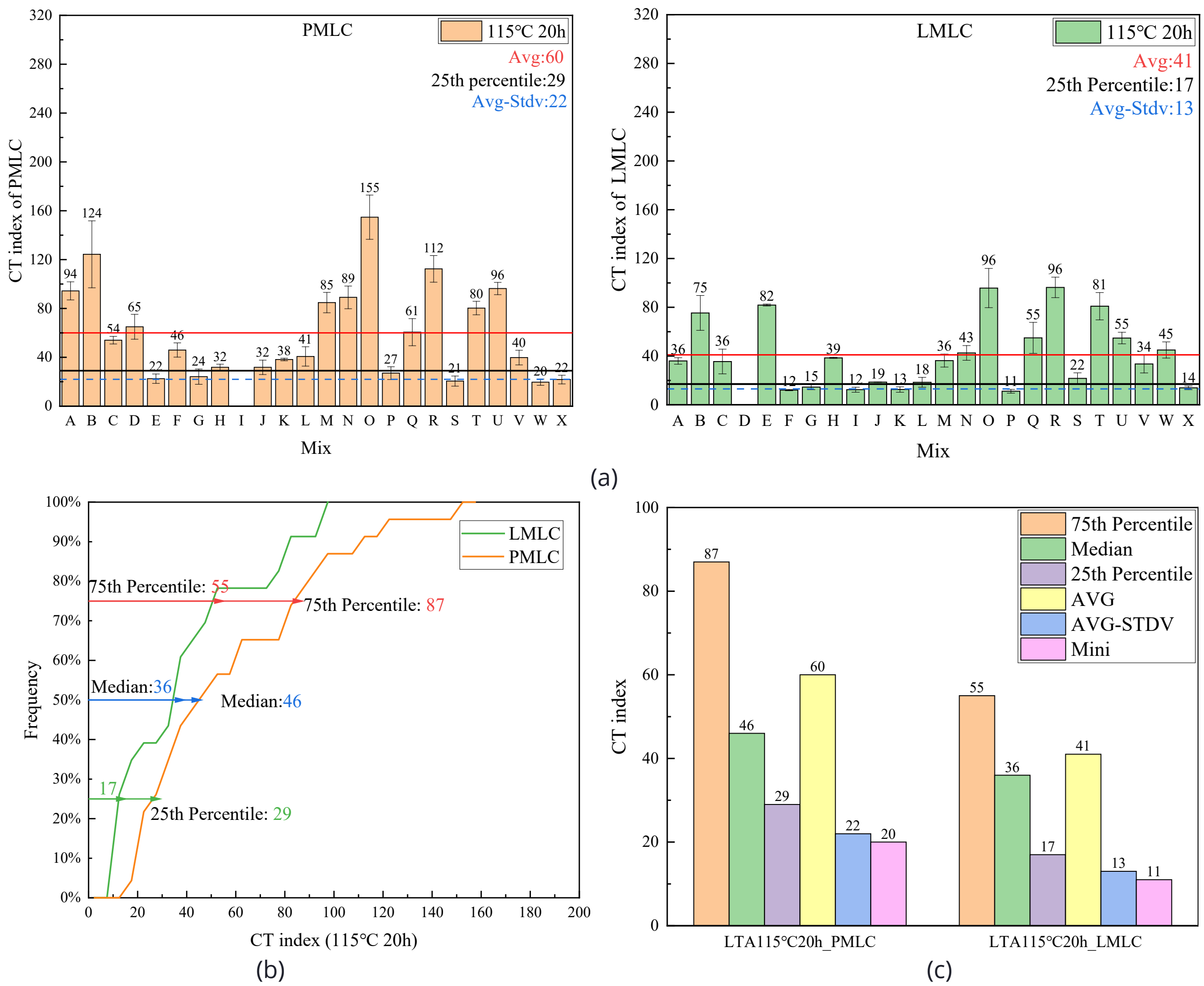

Figure 4-11 PMLC VS LMLC 115℃ 20h loose aging (a) CT index; (b) cumulative distribution;(c) CT index thresholds

Under the LTA115 condition, the 25th percentile and mean minus one standard deviation values were relatively close, indicating that either metric could be considered as an initial threshold candidate. Assuming the 25th percentile is adopted as the threshold, Mix E, G, P, S, W, and X did not meet the PMLC threshold of 29, while mixtures F, G, I, K, P, and X failed to meet the corresponding LMLC requirement. Among these, Mix P and X consistently failed under both LMLC and PMLC conditions, whereas the other mixtures showed different pass/fail outcomes between the two specimen preparation methods. This inconsistency indicates that the ranking and screening outcomes of mixtures can be affected by the aging effect and specimen preparation. Specifically, some mixtures that were rejected under short-term aging conditions may satisfy the threshold after long-term aging, while others that passed under short-term aging conditions may fail under long-term aging conditions.

Overall, the CT index results showed that LMLC specimens with 4-hour STA generally produced lower cracking indices than reheated PMLC specimens. This difference should be considered when developing a performance threshold. Directly applying a PMLC-based threshold to LMLC specimens may be overly stringent, while applying an LMLC-based threshold to PMLC specimens may be too lenient. Therefore, the threshold framework should clearly specify the specimen preparation condition and aging condition associated with each criterion.

4.3.1.3 Effect of LTA115 on CT Index and Cracking Components of PMLC Specimens

Figure 4-12 (a) compares the CT index of PMLC Specimens under reheated conditions and LTA115°C for 20 h. For all evaluated mixtures, the CT Index values decreased markedly after LTA, indicating a consistent degradation in cracking resistance due to aging. To better interpret the mechanisms responsible for the CT index reduction, Figure 4-12 (b) presents the interaction diagram between fracture energy, Gf, and asphalt flexibility ratio, l75/|m75|. The interaction diagram includes a series of CT index contour curves and provides a more mechanistic interpretation of cracking performance than relying on CT index alone. Based on the CT index equation, higher values of Gf and l75/|m75| generally produce higher CT index values. Therefore, mixtures with higher cracking tolerance are located closer to the upper-right portion of the interaction diagram.

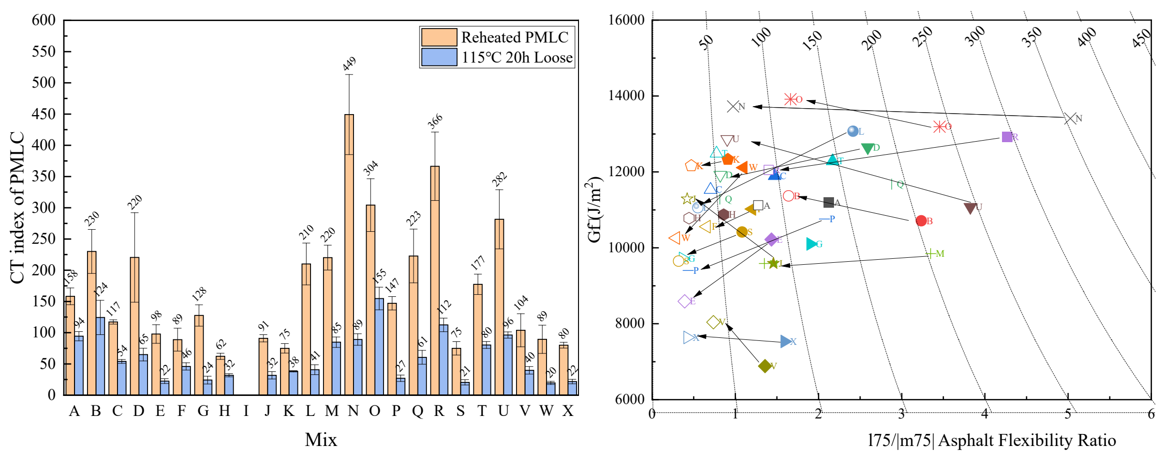

(a) (b)

Figure 4-12 PMLC under reheated and LTA115℃ 20h (a)CT index; (b)Gf vs l75/m75 interaction diagram.

As shown in Figure 4-12 (b), the solid markers represent the reheated PMLC condition, while the hollow markers represent the LTA115 condition. After LTA115, most data points shifted predominantly leftward along the asphalt flexibility ratio axis, indicating a substantial reduction in asphalt flexibility. In contrast, the vertical displacement along the fracture energy axis was comparatively small. This suggests that the reduction in CT index after long-term aging was governed primarily by the decrease in asphalt flexibility ratio rather than by a large reduction in fracture energy.

Further analysis of the CT index components showed that the percentage change in l75/|m75| was consistently larger than the percentage change in Gf for nearly all mixtures, as shown in Figure 4-13. Specifically, the reduction in l75/|m75| ranged from approximately 40% to more than 80%, whereas the change in Gf was generally smaller and more variable. For some mixtures, Gf even increased after aging (such as Mix B, J, U, and V). This increase can be attributed to the increase in peak strength caused by binder hardening after aging. Since fracture energy is calculated from the area under the load–displacement curve, an increase in peak strength may lead to a modest increase in Gf for certain mixtures. These results indicate that I75/|m75| is more sensitive to long-term aging than Gf and is a key parameter controlling the aging-induced reduction in CT index [43].

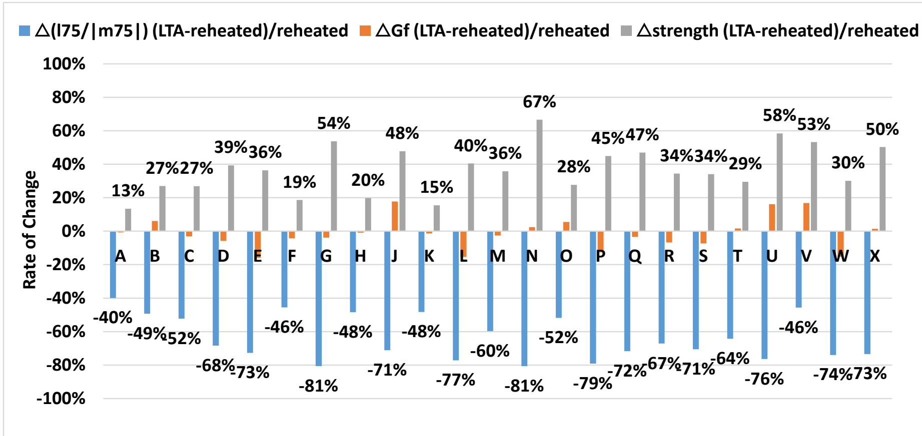

Figure 4-13 CTindex components change rate after LTA115℃ 20h.

4.3.1.4 Peak strength in IDEAL-CT test results

Although the CT index is the primary parameter used in the IDEAL-CT test to evaluate the cracking resistance of asphalt mixtures, relying on this index alone may not fully characterize the cracking behavior of a mixture. The CT index is strongly influenced by the post-peak portion of the curve, particularly the post-peak slope, | m_{75} |, and the displacement corresponding to 75% of the peak load. Consequently, a mixture with a steep post-peak slope may produce a relatively low CT index value even when its fracture energy or peak strength is high. Figure 4-14 presents representative load–displacement curves for Mix K and Mix U to illustrate this behavior. Mix K exhibited a relatively high peak strength of 209 psi and a fracture energy of 11,940 J/m², but its CT index was only 75. In contrast, Mix U exhibited a substantially lower peak strength of 131 psi and a similar fracture energy of 11,578 J/m², while its CT index reached 290. This difference is mainly attributed to the post-peak response. Mix K reached a higher peak load but showed a much steeper post-peak descending branch, indicating a more brittle cracking response after the peak load. Mix U, although having a lower peak load, exhibited a more gradual post-peak reduction and greater displacement tolerance, resulting in a higher CT index.

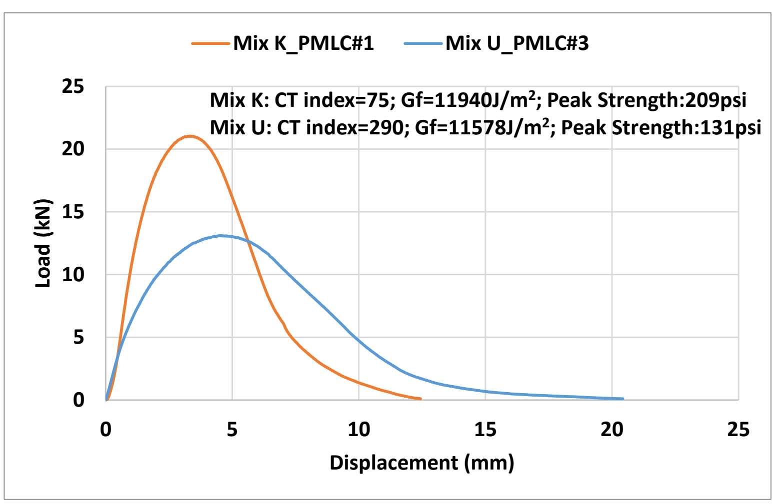

Figure 4-14 Load vs displacement curve of Mix K and Mix U.

To provide a more complete interpretation of the IDEAL-CT response, peak strength was further evaluated as an additional parameter. Figure 4-15(a) compares the peak strength of reheated PMLC specimens and LMLC STA4h specimens. In general, the LMLC STA4h specimens showed higher peak strength than the reheated PMLC specimens. As summarized in Figure 4-15(b), the average peak strength increased from 156 psi for reheated PMLC specimens to 188 psi for LMLC STA4h specimens. The 25th percentile also increased from 132 psi to 172 psi, and the average-minus-standard-deviation value increased from 129 psi to 158 psi. Figure 4-15(c) compares the peak strength of PMLC and LMLC specimens after LTA at 115°C for 20 h. After long-term aging, the peak strength values increased substantially for both PMLC and LMLC specimens. As shown in Figure 4-15(d), the average peak strength increased to 211 psi for PMLC specimens and 224 psi for LMLC specimens after LTA115°C20h. The 25th percentile values were 189 psi and 203 psi for aged PMLC and aged LMLC specimens, respectively. The average-minus-one-standard-deviation values were 184 psi for aged PMLC specimens and 196 psi for aged LMLC specimens. The increase in peak strength after long-term aging is consistent with oxidative binder hardening, which generally increases mixture stiffness and peak tensile resistance.

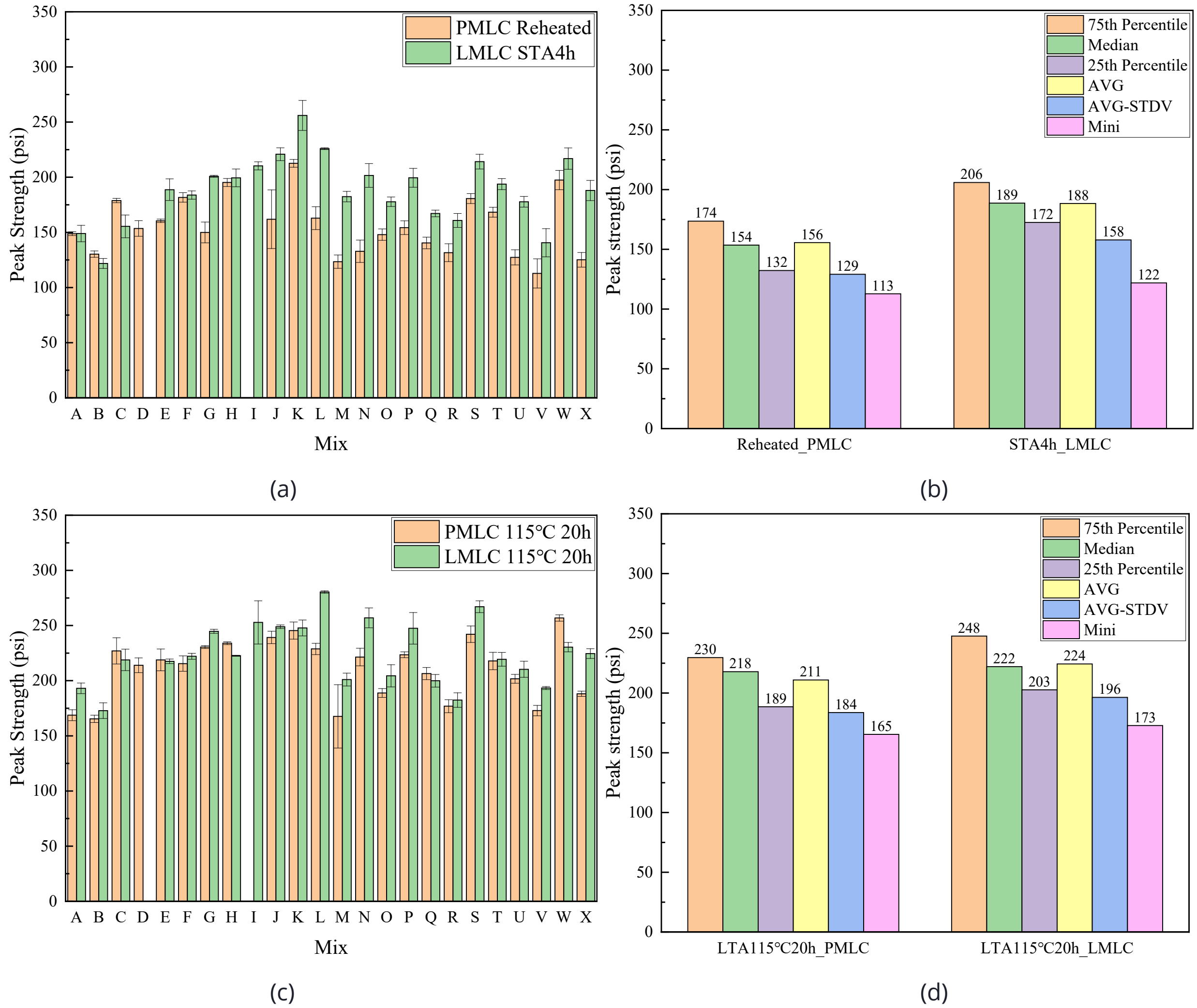

Figure 4-15 Peak strength comparison and threshold analysis: (a) peak strength of reheated PMLC and STA4h LMLC specimens; (b) peak strength thresholds for reheated PMLC and STA4h LMLC specimens; (c) peak strength of PMLC and LMLC specimens after LTA115°C20h; and (d) peak strength thresholds after LTA115°C20h.

These results indicate that the CT index and peak strength characterize different portions of the IDEAL-CT load–displacement response. The CT index primarily reflects post-peak cracking tolerance, whereas peak strength characterizes pre-peak tensile resistance. A mixture with relatively high peak strength but a low CT index may exhibit a stiff and brittle response, whereas a mixture with a high CT index but relatively low peak strength may exhibit favorable post-peak deformation tolerance but limited pre-peak tensile resistance. Therefore, peak strength should be interpreted together with the CT index. A preliminary combined threshold framework is recommended for cracking evaluation, in which the CT index remains the primary cracking-tolerance parameter and peak strength serves as a supplementary parameter for identifying combinations of pre-peak and post-peak response.

4.3.2 RT index of PMLC and LMLC

Figure 4-16 presents the IDEAL-RT index results of reheated PMLC specimens and LMLC specimens subjected to 2 hours of short-term aging at 135°C. The RT index values ranged from approximately 50 to 137 for PMLC specimens and from approximately 50 to 173 for LMLC specimens, indicating substantial variability in rutting resistance among the evaluated mixtures. Overall, the LMLC specimens generally exhibited higher RT index values than the corresponding PMLC specimens. This trend was reflected in the bar chart, threshold summary, and cumulative frequency distribution curves. The higher RT index values of LMLC specimens may likely be attributed to aging conditioning applied during specimen preparation. The LMLC mixtures were subjected to 2 hours of STA at 135°C, whereas the PMLC mixtures were only reheated to the compaction temperature. The additional laboratory aging likely increased binder stiffness, which improved resistance to shear deformation at high temperature.

The RT index results also suggest that separate preliminary rutting thresholds should be developed for PMLC and LMLC specimens. Because LMLC specimens subjected to 2 hours of STA generally exhibited higher RT index values than reheated PMLC specimens, applying a single RT index threshold to both specimen preparation conditions may lead to inconsistent or biased mixture evaluation. Therefore, if the RT index threshold is used for production verification, it should be developed based on reheated plant mixture behavior. In contrast, if a threshold is used during mix design, a separate threshold should be established to account for the effect of 2-hour STA on rutting resistance of LMLC specimens.

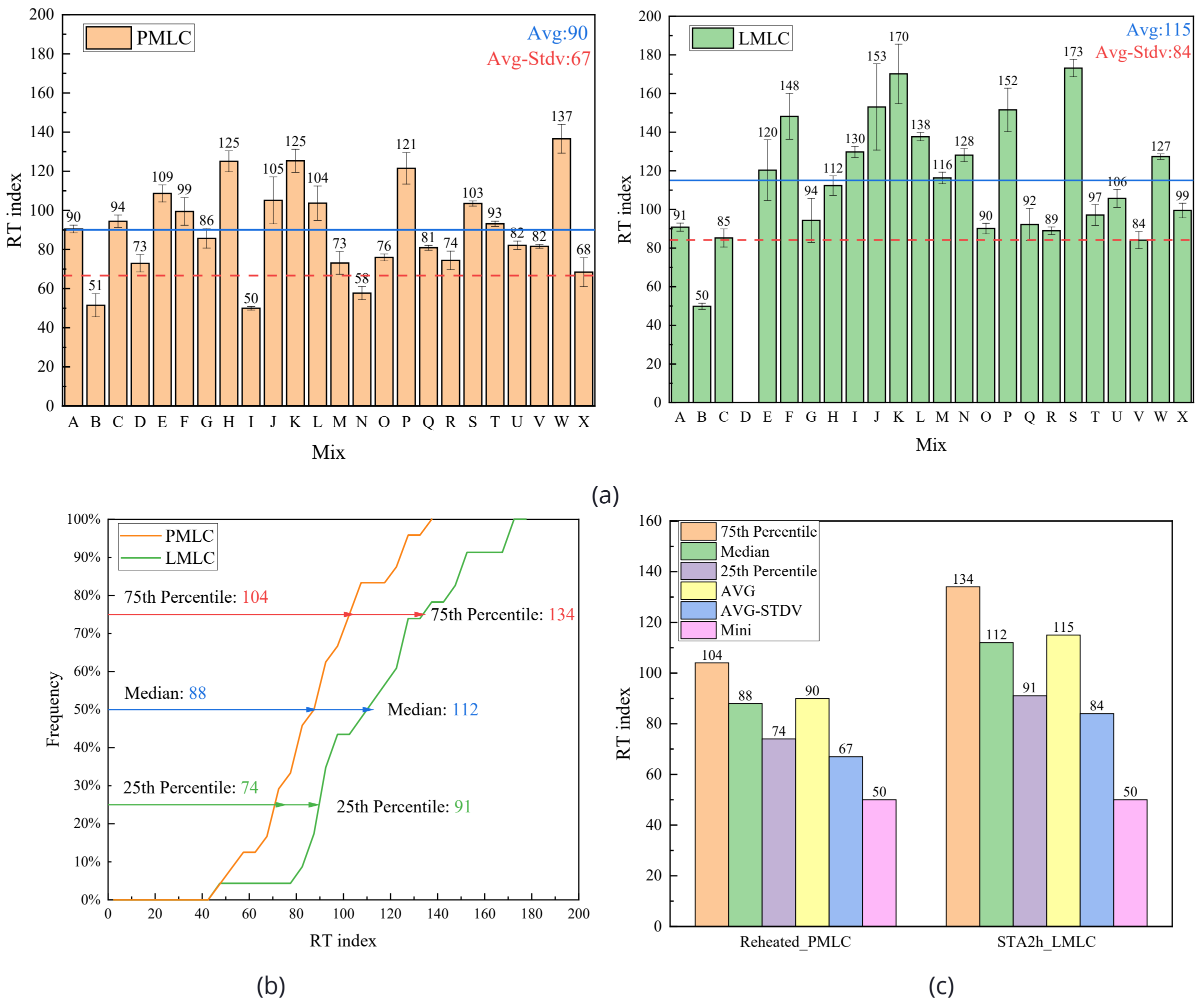

Figure 4-16 PMLC vs LMLC (a) RT index; (b) RT index cumulative distribution;(c) RT index thresholds

4.3.3 TN-CT Index of PMLC and LMLC

4.3.3.1 TN-CT index of reheated PMLC and STA4h LMLC

Figure 4-17 presents the TN-CT index results for reheated PMLC specimens and LMLC specimens subjected to 4 hours of STA. Similar to the IDEAL-CT results, the TN-CT index values of LMLC specimens were generally lower than those of the corresponding reheated PMLC specimens. This confirms that the lower cracking resistance observed in LMLC specimens was not limited to the 6-inch SGC IDEAL-CT test but was also reflected in the 4-inch Marshall TN-CT test.

Under the short-term condition, the cumulative distribution curves showed that the 25th, 50th, and 75th percentiles of the TN-CT index for LMLC specimens were approximately 39, 54, and 78, respectively. The corresponding percentile values for PMLC specimens were higher, approximately 48, 66, and 150, respectively.

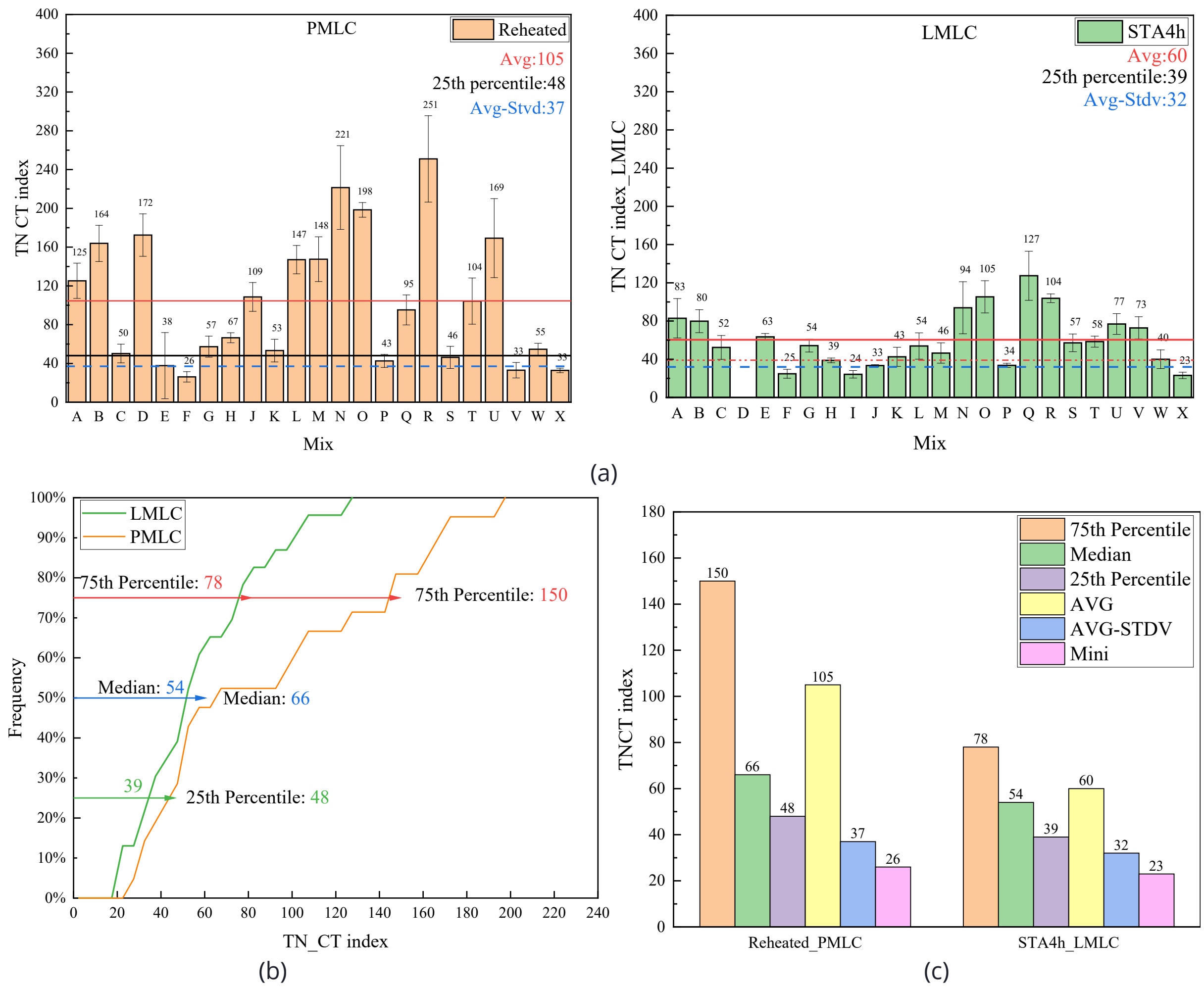

Figure 4-17 PMLC VS LMLC (a)TN CT index; (b) TN CT index cumulative distribution;(c) TNCT index thresholds

4.3.3.2 TN-CT index of PMLC and LMLC under LTA115 ℃ for 20h

Figure 4-18 shows the TN-CT index results of PMLC and LMLC under LTA115℃ for 20h. After loose-mixture aging at 115°C for 20 hours, TN-CT index values decreased significantly for both PMLC and LMLC specimens. The cumulative frequency distribution curves shifted leftward, demonstrating a clear reduction in cracking tolerance due to long-term aging. For PMLC specimens after LTA115, the 25th, 50th, and 75th percentiles decreased to 20, 29, and 59, respectively. For LMLC specimens after LTA115, the 25th, 50th, and 75th percentiles decreased to 18, 24, and 44, respectively. Consistent with the CT index results, LMLC specimens maintained lower TN-CT index values than PMLC specimens after LTA. This is likely because the LMLC specimens already had lower cracking resistance after 4-hour STA; therefore, after the same long-term aging protocol, their TN-CT values remained lower. These results suggest that the TN-CT index is sensitive to aging and can capture the reduction in cracking resistance after LTA.

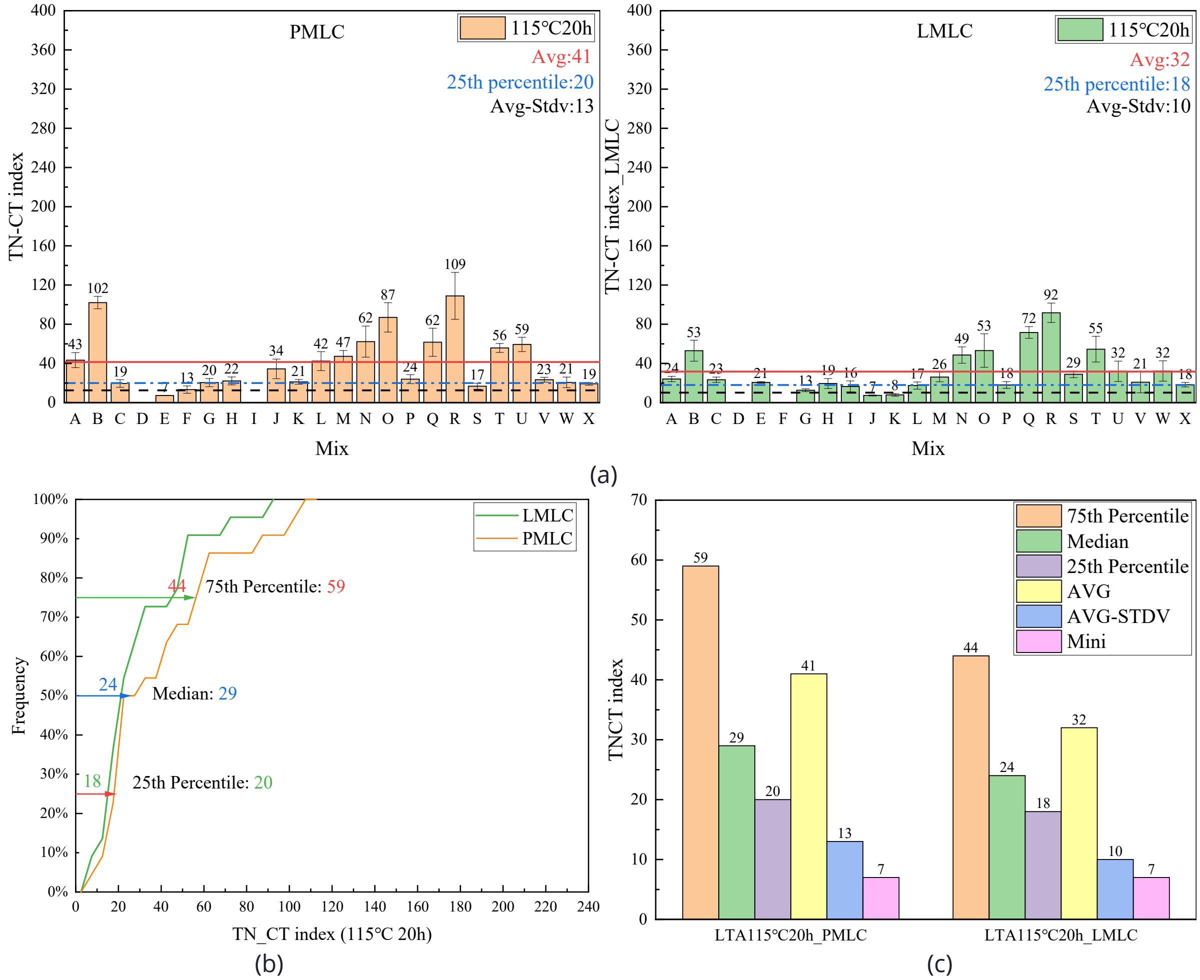

Figure 4-18 PMLC VS LMLC under LTA115℃ 20h (a) TN CT index; (b) cumulative distribution;(c) TNCT index thresholds

4.3.3.3 Peak strength in TN-CT test results

Figure 4-19 summarizes the TN-CT peak-strength distributions under the evaluated conditioning conditions. Overall, the LMLC specimens exhibited higher peak strengths than the corresponding PMLC specimens, and specimens subjected to LTA at 115°C for 20 h generally exhibited higher peak strengths than those under reheated or STA conditions. This trend was consistent with the IDEAL-CT peak-strength results and reflects the increased stiffness and tensile resistance associated with binder aging. However, aging increased peak strength while reducing the TN-CT index, indicating that peak strength alone should not be interpreted as improved cracking resistance. The TN-CT index primarily characterizes post-peak cracking tolerance, whereas peak strength represents pre-peak tensile resistance. Therefore, peak strength should be interpreted together with the TN-CT index.

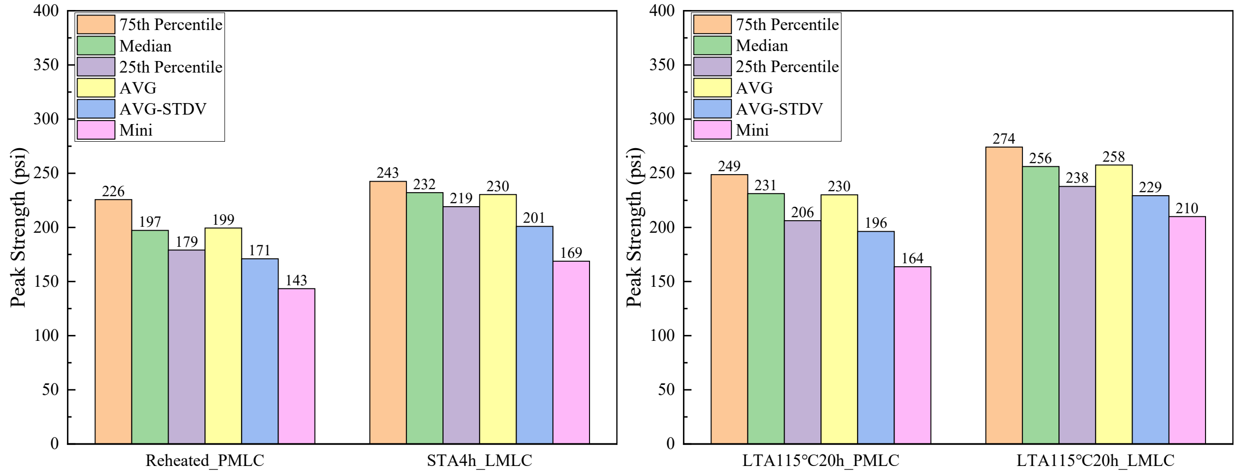

(a) (b)

Figure 4-19 Peak strength comparison and threshold analysis: (a) peak strength thresholds for reheated PMLC and STA4h LMLC specimens; (b) peak strength thresholds after LTA115°C20h.

4.3.4 HT-IDT Strength of PMLC and LMLC

Figure 4-20 presents the HT-IDT strength results for reheated PMLC specimens and LMLC specimens subjected to 2 hours of STA. For PMLC specimens, the HT-IDT strength ranged from 142 to 466 kPa. The overall mean value was approximately 283 kPa, the mean minus one standard deviation was approximately 210 kPa, and the 25th, 50th, and 75th percentiles were approximately 241, 278, and 316 kPa, respectively. The LMLC specimens generally exhibited higher HT-IDT strength values than the corresponding reheated PMLC specimens. This trend is consistent with the IDEAL-RT results, where LMLC specimens also showed higher RT index values. The higher HT-IDT strength of LMLC specimens can be attributed to the 2-hour STA conditioning, which likely increased binder stiffness and improved high-temperature strength. Therefore, both the 6-inch IDEAL-RT and 4-inch HT-IDT tests indicated that LMLC specimens tended to show greater rutting resistance than reheated PMLC specimens.

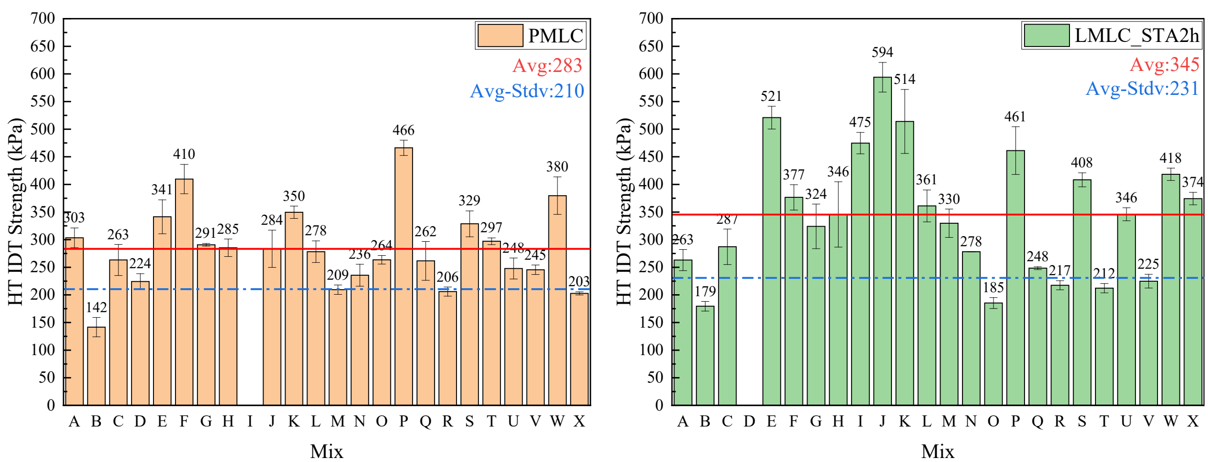

(a)

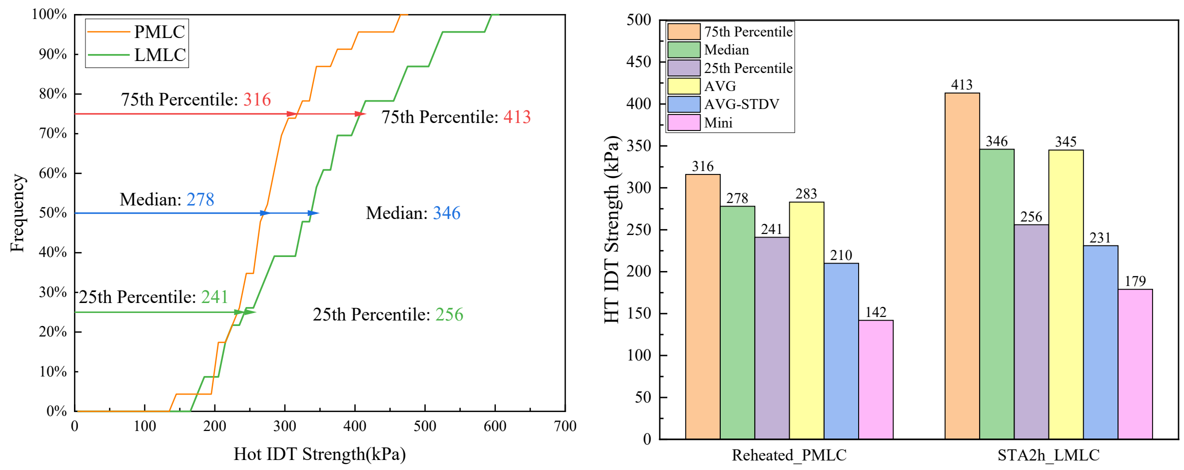

(b) (c)

Figure 4-20 PMLC VS LMLC(a) HT-IDT strength; (b) cumulative distribution; (c)HT-IDT thresholds

4.3.5 HWTT rut depth of PMLC and LMLC

Figure 4-21 presents the corrected rut depth at 20,000 passes (CRD20K) for PMLC and LMLC specimens. In this analysis, the HWTT rut depth was corrected when the rutting curve exhibited a stripping inflection point (SIP). The original plots of the HWTT results are provided in Appendix B Figure A-1 and Figure A-2 . For the majority of the mixtures tested, no obvious SIP was observed in the rut depth versus load cycle curves. For these mixtures, the final rut depth was determined as the average total rut depth at 20,000 passes (TRD20k) of the two-wheel tracking paths. The values highlighted in red in Appendix B Table A-2 indicate that a stripping point was identified in the corresponding wheel path. For these cases, the rutting curve before the SIP was fitted using the previously described method, and the corrected rut depth at 20,000 passes was extrapolated from the pre-stripping rutting trend. Therefore, the red values represent corrected CRD20K values rather than the raw rut depth directly measured after stripping occurred. This correction was used to reduce the influence of moisture-induced stripping and to better isolate the rutting component of the HWTT response. As shown in Figure 4-21, the fitted linear regression line had a slope of approximately 0.50. This suggests that, on average, the LMLC CRD20K values were lower than the corresponding PMLC CRD20K values. In other words, the LMLC specimens generally exhibited less rutting in HWTT than PMLC specimens. This may be attributed to the 2-hour short-term aging applied to LMLC mixtures, which increased mixture stiffness and improved rutting resistance.

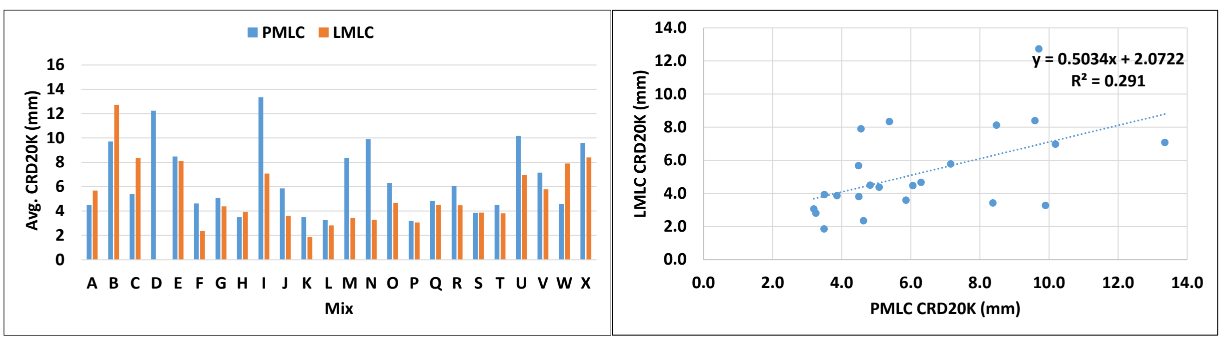

Figure 4-21 Corrected rut depth at 20k pass of PMLC and LMLC

4.3.6 Preliminary threshold recommendations

Based on the benchmarking results, both the 25th percentile and the average minus one standard deviation were considered as practical statistical approaches for preliminary threshold development. To facilitate implementation, the recommended threshold values were rounded to the nearest 5 or 10. Since the performance distributions differ between PMLC and LMLC specimens and between reheated/STA and LTA conditions, separate preliminary thresholds are recommended for each specimen preparation and aging condition, as listed in Table 4-2. These preliminary threshold values are intended to identify mixtures with relatively poor cracking or rutting resistance among currently approved TDOT 411-D mixtures without imposing overly restrictive requirements at the initial stage of BMD implementation.

Table 4-2 Preliminary threshold

Specimen Type	*Aging Condition*	*CT Index (with Peak strength)*	*RT Index*	*TN-CT Index (with Peak strength)*	*HT-IDT Strength*
PMLC	Reheated	75 (130psi)	70	45 (175psi)	210 kPa
PMLC	LTA115℃ 20hours	25(185psi)	—	15 (200psi)	—
LMLC	STA135℃ 4hours	50(160psi)	85	30 (200psi)	230kPa
LMLC	LTA115℃ 20hours	15(200psi)	—	10 (230psi)	—

4.4 Correlation between performance tests

One of the major objectives of this study was to evaluate whether the performance results obtained from 4-inch Marshall specimens could be correlated with those obtained from 6-inch SGC specimens. This comparison is important for TDOT because the current TDOT asphalt mix design practice is based on Marshall-compacted specimens, while many nationally developed BMD performance tests were originally developed using SGC specimens. Therefore, establishing reliable relationships between Marshall-based and SGC-based test results can support TDOT's transition toward BMD implementation while maintaining compatibility with existing Marshall-based practice. This section evaluates the relationships between cracking-related and rutting-related performance indices. The cracking correlation focused on the relationship between the 6-inch IDEAL-CT index and the 4-inch TN-CT index. The rutting correlations included the relationships between IDEAL-RT index and Hot-IDT strength, IDEAL-RT index and HWTT corrected rut depth, and Hot-IDT strength and HWTT corrected rut depth.

4.4.1 Correlation between CT_{index} and $TN\text{-}CT_{index}$

Figure 4-22 presents the relationship between the IDEAL-CT index obtained from 6-inch SGC specimens and the TN-CT index obtained from 4-inch Marshall specimens. Overall, a positive linear relationship was observed between the two cracking indices. Mixtures with higher CT index values generally also showed higher TN-CT index values, indicating that both tests captured similar trends in cracking resistance.

For PMLC specimens, the correlation between CT index and TN-CT index was strong. The fitted regression line had a coefficient of determination, R^2, of approximately 0.86, indicating that the TN-CT index was strongly related to the IDEAL-CT index for plant-produced mixtures. The fitted slope was approximately 0.60, suggesting that the TN-CT index was generally about 60% of the corresponding IDEAL-CT index. In addition, the similarity of slopes across reheated, LTA, and combined datasets indicates that long-term aging does not significantly alter the proportional relationship between the two indices.

For LMLC specimens, the relationship between CT index and TN-CT index was weaker than that observed for PMLC specimens, with an R^2 of approximately 0.75. The fitted slope was approximately 0.60, indicating that the TN-CT values were approximately 60% of the corresponding CT index values for LMLC specimens. The weaker correlation may be associated with the inherent variability of laboratory-produced mixtures. Compared with plant-produced mixtures, LMLC mixtures may have less uniform aggregate coating and homogeneity, which can increase variability in cracking test results.

When all PMLC and LMLC data under both short-term and long-term aging conditions were combined, a reasonably strong overall relationship was still observed, with an R^2 of approximately 0.85. The combined fitted slope was approximately 0.60, indicating that the 4-inch TN-CT index is about 60% of the corresponding 6-inch IDEAL-CT index. These results indicate that TN-CT can provide useful cracking performance information that is broadly consistent with IDEAL-CT. This may be attributed to specimen size effects.

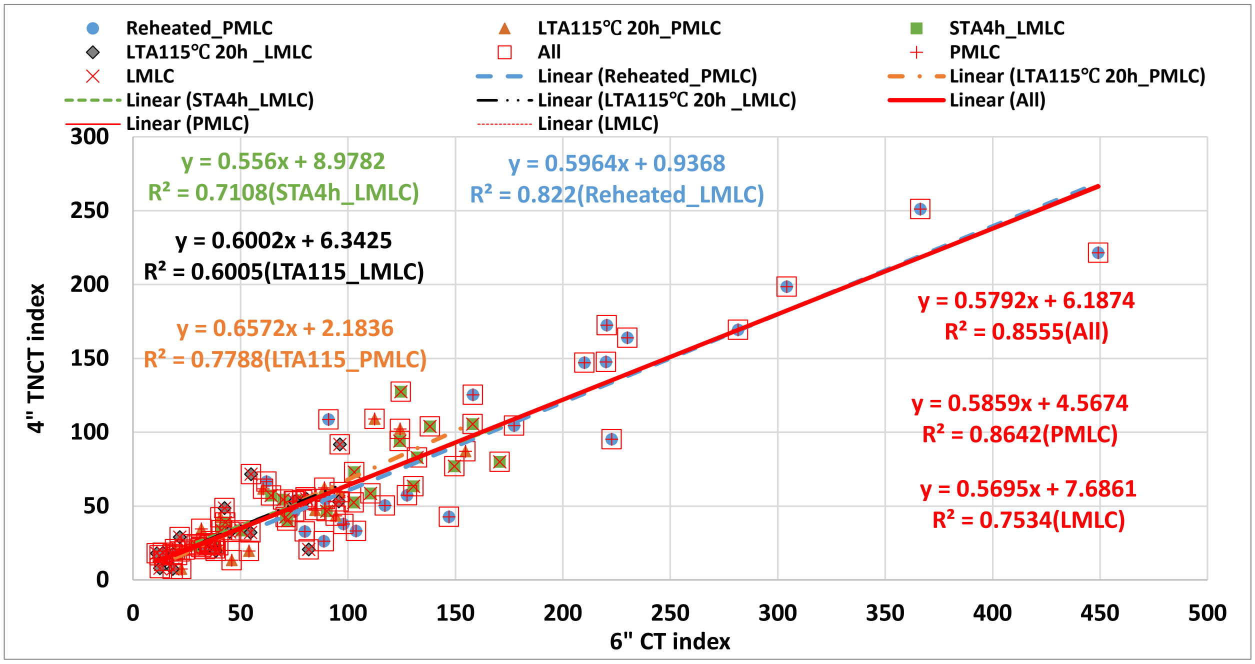

Figure 4-22 Correlation between CT $_{index}$ and TNCT $_{index}$

4.4.2 Correlation between RT $_{index}$ and HT-IDT strength

Figure 4-23 presents the relationship between the IDEAL-RT index obtained from 6-inch SGC specimens and the HT-IDT strength obtained from 4-inch Marshall specimens. A positive relationship was observed between RT index and Hot-IDT strength. Mixtures with higher RT index values generally exhibited higher Hot-IDT strength, suggesting that both indices characterize rutting-related performance of asphalt mixtures. For PMLC specimens, the coefficient of determination was approximately 0.64. For LMLC specimens, the R^2 value was approximately 0.61. When PMLC and LMLC data were combined, the R^2 value was approximately 0.65. These values indicate a moderate correlation between the two rutting-related indices.

The observed correlation between RT index and HT-IDT strength was weaker than the correlation observed between CT index and TN-CT index. This difference can be attributed to the fundamental distinctions between the two rutting-related test methods. The CT and TN-CT tests primarily differ in specimen size and compaction method, while sharing a similar indirect tensile loading mechanism and cracking index calculation framework. In contrast, RT index and Hot-IDT strength are obtained from tests with different loading modes and stress states. The Hot-IDT test involves indirect tensile loading at elevated temperature, whereas the IDEAL-RT test is dominated by shear deformation mechanisms. As a result, the two indices captured different aspects of mixture behavior at high temperature, which likely contributed to the increased scatter and reduced correlation.

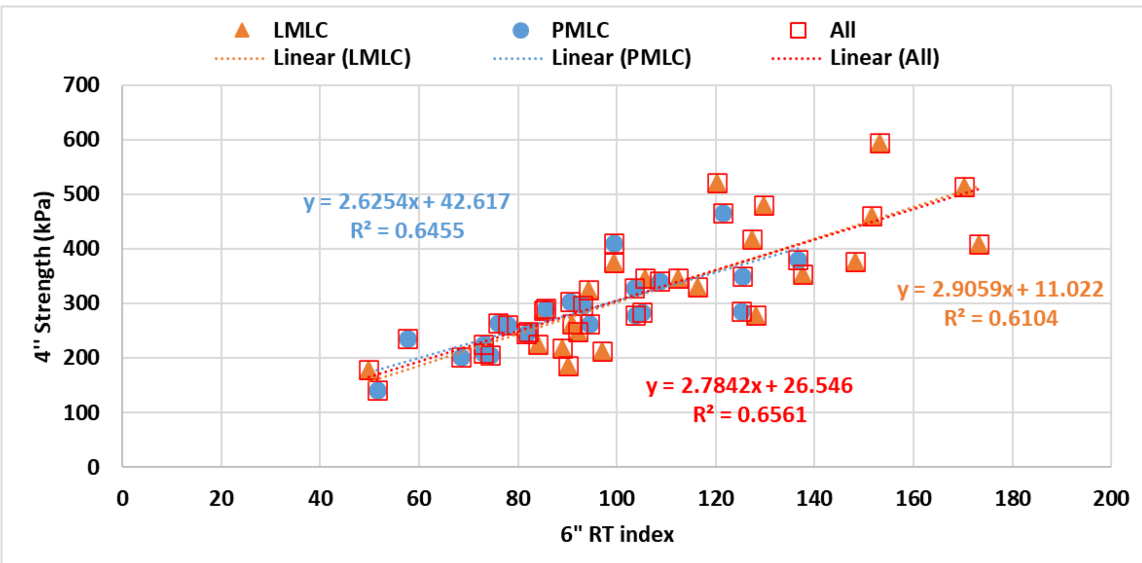

Figure 4-23 Correlation between RT $_{index}$ and HT-IDT strength

4.4.3 Correlation Between RT Index and HWTT

Figure 4-24 presents the relationship between the IDEAL-RT index and HWTT-derived rutting parameters. The HWTT results were evaluated using the corrected rut depth at 20,000 passes, CRD20k, and the rutting resistance index, RRI.

Overall, the RT index showed a reasonable relationship with HWTT-derived rutting performance. Mixtures with higher RT index values generally exhibited lower corrected rut depths and higher RRI values. This indicates that the IDEAL-RT test was able to capture the general trend of rutting resistance measured by HWTT. However, the linear regression results showed only moderate predictive capability, with R^2 of 0.39 and 0.56 for LMLC and PMLC, respectively. This is expected because the two tests evaluate rutting resistance using different loading configurations and boundary conditions. The IDEAL-RT is a rapid monotonic shear-dominated test, while HWTT measures accumulated rutting under repeated wheel loading in a submerged condition. Therefore, HWTT captures not only rutting deformation but also moisture susceptibility and potential stripping behavior, which are not directly captured by the RT index.

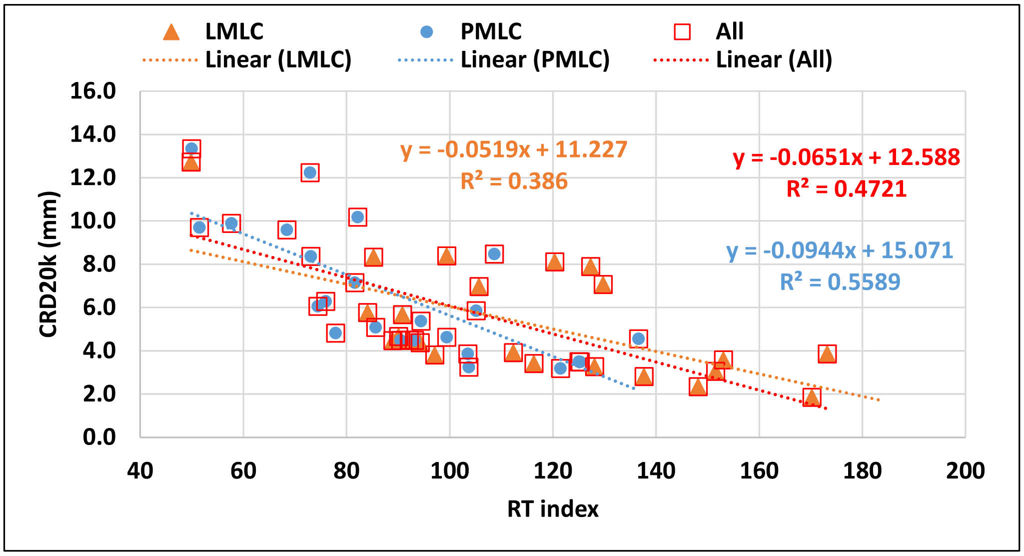

(a)

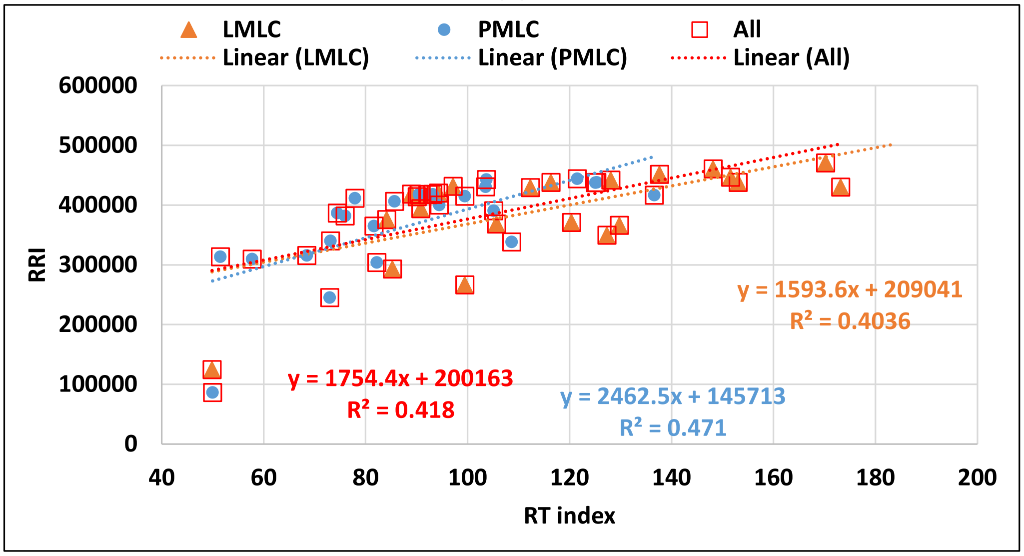

(b)

Figure 4-24 Correlation between RT $_{index}$ and HWTT results: (a) RT $_{index}$ vs CRD20k; (b) RT $_{index}$ vs RRI

In addition to linear regression analysis, Spearman correlation analysis was conducted to evaluate the ranking consistency between the RT index and HWTT-derived rutting parameters. Unlike linear regression, Spearman correlation evaluates whether two variables follow a consistent monotonic trend, regardless of the exact linear form of the relationship. Therefore, this analysis is particularly useful for assessing whether the RT index can reasonably rank mixtures in terms of rutting resistance relative to HWTT results.

For CRD20k, the Spearman correlation coefficients were -0.62, -0.77, and -0.71 for LMLC, PMLC, and all data, respectively. The negative coefficients are expected because higher RT index values indicate better rutting resistance, while lower CRD20k values indicate better rutting performance in HWTT. These results show that mixtures with higher RT index values generally had lower HWTT corrected rut depths. The ranking consistency was stronger for PMLC specimens than for LMLC specimens, suggesting that the RT–HWTT relationship was more stable for plant-mixed materials.

Similarly, the Spearman correlation coefficients between RT index and RRI were 0.63, 0.77, and 0.70 for LMLC, PMLC, and all data, respectively. The positive correlations are expected because both RT index and RRI increase with improved rutting resistance. These results further confirm that RT index can reasonably capture the relative ranking of mixture rutting resistance measured by HWTT.

Overall, the Spearman correlation results indicate a moderate-to-strong monotonic relationship between RT index and HWTT-derived rutting parameters. Although the linear regression R^2 values indicate only moderate capability for direct prediction of HWTT rut depth, the Spearman results suggest that RT index provides reasonable ranking consistency with HWTT. Therefore, IDEAL-RT has potential as a rapid surrogate for rutting resistance evaluation, particularly for identifying mixtures with relatively high or low rutting resistance.

4.4.4 Correlation Between HT-IDT strength and HWTT

Figure 4-25 presents the relationship between Hot-IDT strength and HWTT-derived rutting parameters, including corrected rut depth at 20,000 passes (CRD20k) and rutting resistance index (RRI). Overall, the linear regression results showed a weak relationship between HT-IDT strength and HWTT-derived rutting performance. Although mixtures with higher HT-IDT strength generally tended to show lower CRD20k and higher RRI, the scatter was relatively large. This indicates that HT-IDT strength alone cannot reliably predict HWTT rutting performance.

Spearman correlation analysis was also conducted to evaluate the ranking consistency between HT-IDT strength and HWTT-derived rutting parameters. For LMLC specimens, the Spearman correlation coefficients between HT-IDT strength and CRD20k and between HT-IDT strength and RRI were -0.22 and 0.25, respectively. In contrast, stronger monotonic relationships were observed for PMLC specimens. The Spearman correlation coefficients between HT-IDT strength and CRD20k and between HT-IDT strength and RRI were -0.72 and 0.72, respectively. When all data were combined, the Spearman correlation coefficients were -0.45 for CRD20k and 0.44 for RRI, indicating only moderate-to-weak overall ranking consistency.

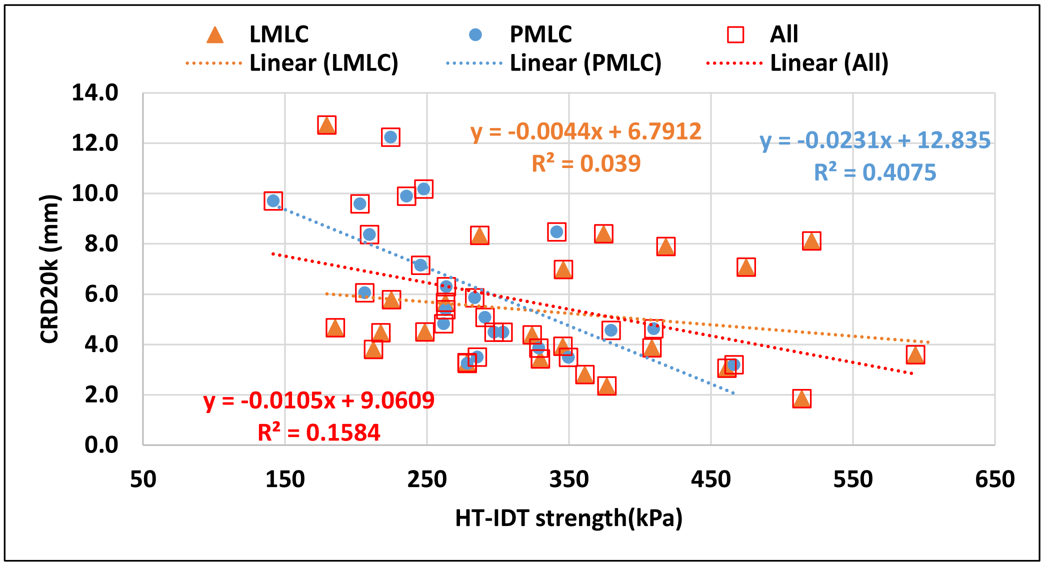

(a)

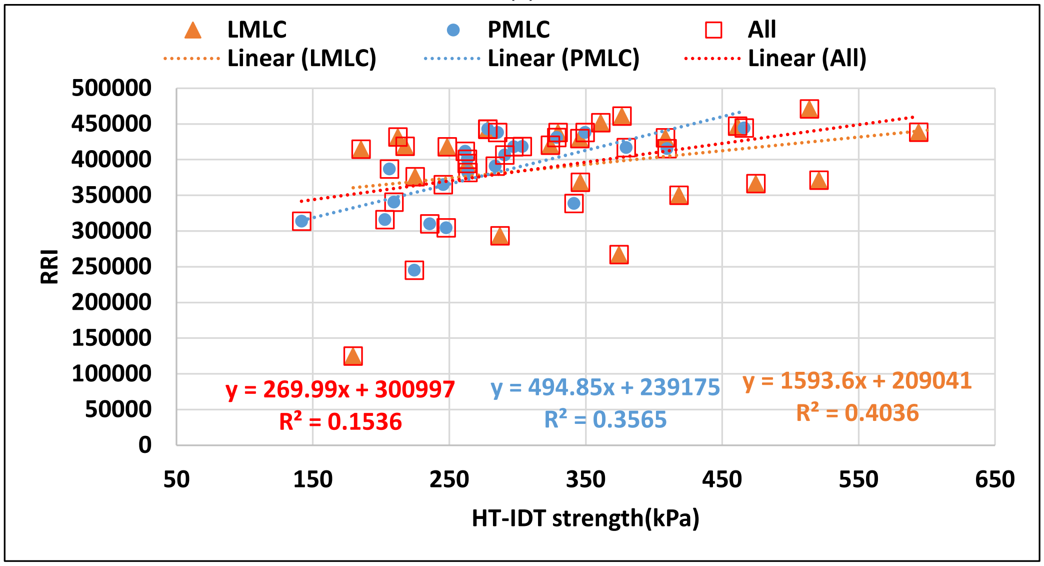

(b)

Figure 4-25 Correlation between HT-IDT strength and HWTT results: (a) HT-IDT strength vs CRD20k;(b) HT-IDT strength vs RRI

Overall, compared with HT-IDT strength, the RT index appears to be more suitable as a potential surrogate for HWTT rutting performance, based on its stronger ranking consistency with HWTT-derived rutting parameters. However, the IDEAL-RT test is currently conducted using 6-inch SGC specimens, and a comparable IDEAL-RT loading fixture is not available for 4-inch Marshall specimens. Therefore, HT-IDT remains useful because it provides practical Marshall-compatible rutting-related information. Nevertheless, HT-IDT should not be considered a standalone replacement for HWTT without additional validation. For TDOT BMD implementation, HWTT remains necessary when repeated-load rutting behavior, moisture susceptibility, and stripping potential need to be evaluated.

4.5 Performance Space Diagram Analysis

Performance space diagrams (PSD) were plotted to evaluate both cracking and rutting resistance for the collected mixtures. In each diagram, the vertical axis represents a cracking-related index, while the horizontal axis represents a rutting-related index. PSDs provide a visual framework to assess asphalt mixture performance by combining results from multiple performance tests, offering a comprehensive understanding of both cracking and rutting resistance.

4.5.1 Performance Space Diagram of PMLC

Figure 4-26 compares the performance distributions obtained from 6-inch SGC specimens and 4-inch Marshall specimens for reheated PMLC mixtures. Overall, the two performance space diagrams exhibited similar general trends, indicating that both specimen types captured comparable performance characteristics. For example, Mix B consistently demonstrated relatively poor rutting resistance in both PSDs. This consistency suggests that mixtures with clearly inferior rutting resistance can be identified regardless of whether 6-inch SGC or 4-inch Marshall specimens are used. A similar agreement was also observed for several mixtures with relatively strong balanced performance. For instance, Mix A, L, O, Q, U, T, W, etc., were generally located in the upper-right or acceptable-performance region of the PMLC performance space, indicating relatively better cracking and rutting resistance. Their positions in the 4-inch Marshall-based diagram were also generally consistent with the 6-inch SGC-based interpretation, further supporting the ability of the Marshall performance tests to reflect the overall performance ranking of PMLC mixtures.

However, discrepancies were observed for certain mixtures, particularly those located close to the preliminary threshold lines. For example, Mix E exhibited a 6-inch CT index that exceeded the CT threshold. The same mixture fell below the TN-CT threshold in the 4-inch Marshall-based diagram. Therefore, while the 4-inch Marshall-based performance space can identify mixtures with clearly poor or clearly acceptable performance, mixtures near the threshold region should be interpreted with caution.

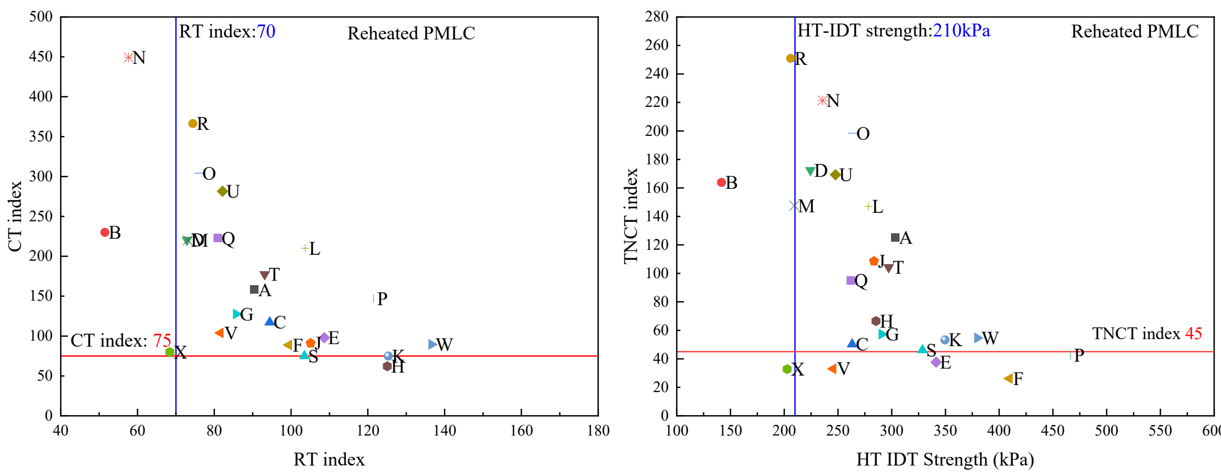

(a) (b)

Figure 4-26 Performance Space Diagram of PMLC: (a) SGC specimens;(b) Marshall specimens

4.5.2 Performance Space Diagram of LMLC

Figure 4-27 presents the performance space diagrams for LMLC specimens. Compared with PMLC specimens, the LMLC specimens generally showed lower cracking-related indices and higher rutting-related indices. This reflects the influence of laboratory short-term aging.

4-inch Marshall-based performance space showed trends similar to the 6-inch SGC-based performance space. This indicates that TN-CT and HT-IDT can help identify lower-performing mixtures that are generally consistent with the CT index and the RT index. Therefore, 4-inch Marshall performance testing appears feasible for TDOT BMD implementation. However, because the 4-inch and 6-inch tests have different specimen geometries, compaction methods, and loading mechanisms, separate performance thresholds should be developed for each test and specimen preparation condition.

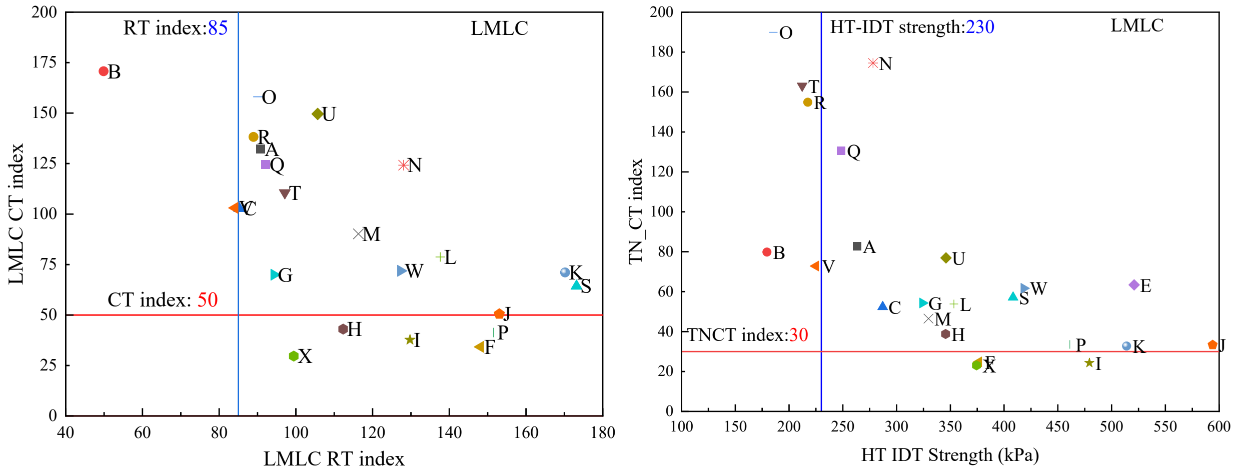

(a) (b)

Figure 4-27 Performance Space Diagram of LMLC: (a) SGC specimens;(b) Marshall specimens

4.5.3 Three-Dimensional Performance Space Considering Peak Strength

To evaluate the effect of incorporating peak strength into the conventional cracking–rutting performance space, three-dimensional performance space diagrams were developed using the cracking-related index, corresponding peak strength, and rutting-related index. The complete diagrams for the PMLC and LMLC specimens prepared using the SGC and Marshall compactors are provided in Appendix C. In each diagram, the shaded region represents the combinations satisfying all three preliminary performance thresholds, whereas points outside the shaded region fail at least one threshold.

The three-dimensional performance space provides an additional screening dimension beyond the conventional two-dimensional cracking–rutting framework. In particular, some mixtures satisfied both the cracking- and rutting-related thresholds but exhibited peak strengths below the corresponding preliminary reference level. For example, among the reheated PMLC SGC specimens, Mixes M, U, and V satisfied the CT index and RT index thresholds but did not satisfy the preliminary peak-strength threshold of 130 psi. These mixtures would have been classified as acceptable in the two-dimensional performance space but were flagged for additional review when peak strength was incorporated.

Chapter 5 Conclusion

This study was conducted to support TDOT's implementation of BMD for TDOT 411-D dense-graded surface mixtures. A total of twenty-four currently approved mixtures were collected from different regions across Tennessee. Both PMLC and LMLC specimens were prepared using the Superpave gyratory compactor (SGC) and Marshall hammer. The performance tests included IDEAL-CT, TN-CT, IDEAL-RT, high-temperature indirect tensile strength (HT-IDT), and Hamburg Wheel Tracking Test (HWTT). The study evaluated five long-term aging protocols, compared 6-inch SGC-based and 4-inch Marshall-based performance test results, developed a generalized aging method, and recommended preliminary performance thresholds to support future TDOT BMD implementation.

The major conclusions are summarized as follows:

- Long-term aging substantially reduced the cracking resistance of TDOT 411-D mixtures. For plant-produced mixtures, the reheated PMLC specimens showed the highest CT index values, while long-term aged specimens showed clear reductions. The aging severity generally followed the order: reheated condition < 85°C for 5 days compacted aging < 115°C for 20 hours loose aging < 95°C for 3 days loose aging < 135°C for 8 hours loose aging < 85°C for 5 days loose aging. Loose-mixture aging at 115°C for 20 hours was identified as the most practical LTA protocol for the current stage of TDOT BMD implementation because it produced CT index results comparable to the 95°C for 3 days loose-aging protocol, required less conditioning time, and avoided potential high-temperature concerns associated with 135°C aging. Additional field validation is still needed before formal specification adoption.
- The generalized aging method framework provides a practical tool for interpreting and comparing cracking resistance under different aging conditions. By converting oven aging time to equivalent aging time, this method integrates the effects of aging temperature and duration into a unified aging severity parameter. It can be used to evaluate mixture cracking resistance, quantify aging sensitivity, compare different laboratory aging protocols, and provide a potential bridge between field aging and laboratory aging once field-aged mixture data become available.
- PMLC and LMLC specimens exhibited different performance distributions. For cracking-related tests, LMLC specimens subjected to 4 hours of STA generally showed lower CT index and TN-CT index values than reheated PMLC specimens. In contrast, for rutting-related tests, LMLC specimens subjected to 2 hours of STA generally showed higher RT index and HT-IDT strength values than reheated PMLC specimens. Therefore, separate thresholds should be developed for LMLC specimens used in mix design and PMLC specimens used in QA/QC or production verification, respectively.
- The 4-inch Marshall-based performance tests demonstrated reasonable feasibility for TDOT BMD practice. The TN-CT index correlated reasonably well with the 6-inch IDEAL-CT index, particularly for PMLC specimens, while the combined PMLC and LMLC dataset also exhibited a meaningful relationship between the two indices. Rutting-related correlations were weaker than the cracking-test relationship because IDEAL-RT, HT-IDT, and HWTT involve different loading modes, specimen configurations, and stress states. Therefore, HT-IDT may be considered as a Marshall-compatible rutting test but is not

recommended to replace HWTT at this stage. Performance space diagrams also showed similar overall performance distribution trends between 6-inch SGC-based and 4-inch Marshall-based tests, indicating that Marshall specimens and associated performance tests can reasonably support TDOT BMD practice. The CT index and TN-CT index primarily characterize post-peak cracking tolerance, whereas peak strength provides complementary information on pre-peak tensile resistance. The peak strength can be therefore considered as an additional parameter to be interpreted together with the applicable cracking index.

- The 25th percentile and average minus one standard deviation of overall performance test results are reasonable preliminary statistical approaches for TDOT BMD threshold development. These methods can identify mixtures with relatively poor performance among currently approved TDOT mixtures without imposing overly restrictive criteria during the initial implementation stage. Preliminary recommended thresholds were developed separately by specimen type and conditioning condition.
  - For reheated PMLC specimens, the recommended thresholds are CT index ≥ 75, RT index ≥ 70, TN-CT index ≥ 45, and HT-IDT strength ≥ 210 kPa.
  - For PMLC specimens after LTA115, the recommended thresholds are CT index ≥ 25 and TN-CT index ≥ 15.
  - For LMLC specimens under STA conditions, the recommended thresholds are CT index ≥ 50 (STA for 4h at 135°C), RT index ≥ 85 (STA for 2h at 135°C), TN-CT index ≥ 30 (STA for 4h at 135°C), and HT-IDT strength ≥ 230 kPa (STA for 2h at 135°C).
  - For LMLC specimens after LTA115, the recommended thresholds are CT index ≥ 15 and TN-CT index ≥ 10.

  These values should be considered preliminary and should be further validated using field performance data before formal specification adoption.

Based on these findings, the following implementation recommendations are provided for TDOT:

- Loose-mixture aging at 115°C for 20 hours is recommended as the primary LTA protocol for continued BMD research and preliminary implementation.
- Performance thresholds should be established separately for PMLC and LMLC specimens, and separate criteria should also be maintained for 6-inch SGC-based and 4-inch Marshall-based tests.
- TN-CT can be used as a practical Marshall-compatible cracking test to support TDOT's transition toward BMD, while HT-IDT may be used as a Marshall-compatible rutting test candidate. However, the weak correlations between HT-IDT and IDEAL-RT with HWTT indicated that they can not replace HWTT.
- The preliminary thresholds recommended in this report should be treated as initial implementation values and refined using additional production data, field performance monitoring, and TDOT's future QA/QC experience.

Overall, this study provides a technical basis for TDOT's stepwise implementation of BMD for dense-graded surface mixtures. The results support the use of practical long-term aging, Marshall-compatible performance testing, and distribution-based preliminary thresholds as initial tools and a solid foundation for developing performance-informed asphalt mixture specifications in Tennessee.

References

[1] F. Yin and R. West, "Balanced Mix Design Resource Guide," National Center for Asphalt Technology, 2021.

[2] R. West, C. Rodezno, F. Leiva, and F. Yin, "Development of a Framework for Balanced Mix Design," National Center for Asphalt Technology, Auburn University, Alabama, NCHRP 20-07/Task 406, Aug. 2018. [Online]. Available: https://onlinepubs.trb.org/onlinepubs/nchrp/docs/NCHRP20-07(406)_Revised_final_report.pdf

[3] "Glossary of Terms for Balanced Design of Asphalt Mixtures," Transportation Research Board, Washington, D.C. USA, Oct. 2022. [Online]. Available: https://onlinepubs.trb.org/onlinepubs/circulars/ec280.pdf

[4] AASHTO R132-25, *Standard Practice for Balanced Design of Asphalt Mixtures*, Washington, D.C. USA., 2025. [Online]. Available: https://store.transportation.org/Item/PublicationDetail?ID=5466

[5] NAPA, "BMD Implementation Efforts," BMD Implementation Efforts. Accessed: Jul. 20, 2025. [Online]. Available: https://www.asphaltpavement.org/expertise/engineering/resources/bmd-resource-guide/implementation-efforts

[6] "Guide for Implementing Balanced Mix Design Specifications," National Center for Asphalt Technology, NCHRP 10-107, Apr. 2023.

[7] S. D. Diefenderfer and B. F. Bowers, "Initial Approach to Performance (Balanced) Mix Design: The Virginia Experience," *Transportation Research Record*, vol. 2673, no. 2, pp. 335–345, Feb. 2019, doi: 10.1177/0361198118823732.

[8] B. F. Bowers, S. D. Diefenderfer, N. Moore, and T. Lynn, "Balanced Mix Design and Benchmarking: A Case Study in Establishing Performance Test Thresholds," *Transportation Research Record*, vol. 2676, no. 12, pp. 586–598, Dec. 2022, doi: 10.1177/03611981221096434.

[9] D. Vivanco Sala, N. Tran, F. Yin, and B. F. Bowers, "Evaluating Impact of Corrected Optimum Asphalt Content and Benchmarking Cracking Resistance of Georgia Mixtures for Balanced Mix Design Implementation," *Transportation Research Record*, vol. 2676, no. 5, pp. 13–29, May 2022, doi: 10.1177/03611981221082547.

[10] S. Pant, M. Akentuna, L. N. Mohammad, S. B. Cooper, and S. B. Cooper, "Field performance validation of the Louisiana balanced asphalt mix design framework," *Construction and Building Materials*, vol. 428, p. 136251, May 2024, doi: 10.1016/j.conbuildmat.2024.136251.

[11] L. Mohammad, J. Liu, W. Cao, P. Barghabany, and Louisiana Transportation Research Center, "Implementation of Semi-Circular Bend (SCB) Test for QC/QA of Asphalt Mixtures," FHWA/LA.24/685, Jun. 2024. Accessed: May 20, 2025. [Online]. Available: https://rosap.ntl.bts.gov/view/dot/75660

[12] V. Chitnis, Sukhija ,Mayank, and E. and Coleri, "Benchmarking the performance of asphalt mixtures for the implementation of Balanced Mix Design (BMD) in Oregon," *International Journal of Pavement Engineering*, vol. 26, no. 1, p. 2489760, Dec. 2025, doi: 10.1080/10298436.2025.2489760.

[13] V. Chitnis, M. Sukhija, and E. Coleri, “Exploring the implementation of balanced mix design (BMD) in Oregon, United States: a case study,” *International Journal of Pavement Engineering*, vol. 27, no. 1, p. 2612226, Jan. 2026, doi: 10.1080/10298436.2025.2612226.
[14] G. M. Nsengiyumva, Y.-R. Kim, J. Hu, University of Nebraska--Lincoln. Dept. of Civil Engineering, and Texas A&M University. Zachry Department of Civil Engineering, “Feasibility and Implementation of Balanced Mix Design in Nebraska,” SPR-P1(19) M080, Sep. 2020. Accessed: May 19, 2025. [Online]. Available: https://rosap.ntl.bts.gov/view/dot/54749
[15] F. Yazdipanah, M. Khedmati, H. F. Haghshenas, University of Nebraska--Lincoln. Nebraska Transportation Center, and University of Nebraska--Lincoln. Dept. of Civil Engineering, “Nebraska Balanced Mix Design – Phase I,” SPR-FY22(002), May 2023. Accessed: May 19, 2025. [Online]. Available: https://rosap.ntl.bts.gov/view/dot/67907
[16] R. West, F. Yin, C. Rodezno, A. Taylor, and Auburn University. National Center for Asphalt Technology, “Balanced Mixture Design Implementation Support,” WHRP 0092-20-04, Mar. 2021. Accessed: Apr. 10, 2024. [Online]. Available: https://rosap.ntl.bts.gov/view/dot/62612
[17] F. Zhou, S. Hu, and D. Newcomb, “Development of a performance-related framework for production quality control with ideal cracking and rutting tests,” *Construction and Building Materials*, vol. 261, p. 120549, Nov. 2020, doi: 10.1016/j.conbuildmat.2020.120549.
[18] J. Liu, F. Liu, Z. Wang, S. Yang, E. O. Fanijo, and L. Wang, “Transitioning from Lab-Based to AI-Assisted Balanced Mix Design: Comprehensive Overview of Research, Development, and Future Perspectives,” *Transportation Research Record*, p. 03611981251322465, May 2025, doi: 10.1177/03611981251322465.
[19] K. Huang and B. Huang, “Balanced Mix Design—a 1-Year Reality Check on Quality Control Testing and State DOT Adoption,” Mar. 2026. Accessed: Jun. 03, 2026. [Online]. Available: https://rosap.ntl.bts.gov
[20] D. Newcomb *et al.*, *Short-Term Laboratory Conditioning of Asphalt Mixtures*. Washington, D.C.: Transportation Research Board, 2015, p. 22077. doi: 10.17226/22077.
[21] W. S. Mogawer, A. J. Austerman, K. D. Stuart, I. A. Abdalfattah, and F. Zhou, “Comprehensive Balanced Mixture Design Protocol: Design Phase through Production Quality Assurance,” *Transportation Research Record*, p. 03611981231186422, Jul. 2023, doi: 10.1177/03611981231186422.
[22] AASHTO R 30, *Standard Practice for Laboratory Conditioning of Asphalt Mixtures*, (AASHTO) R30, Washington, D.C. USA., 2022.
[23] D. Newcomb, E. Arámbula-Mercado, A. E. Martin, M. Yuan, N. Tran, and F. Yin, *Field Verification of Proposed Changes to the AASHTO R 30 Procedures for Laboratory Conditioning of Asphalt Mixtures*. Washington, D.C.: Transportation Research Board, 2019. doi: 10.17226/25608.
[24] C. Chen, F. Yin, P. Turner, R. C. West, and N. Tran, “Selecting a Laboratory Loose Mix Aging Protocol for the NCAT Top-Down Cracking Experiment,” *Transportation Research Record*, vol. 2672, no. 28, pp. 359–371, Dec. 2018, doi: 10.1177/0361198118790639.
[25] Y. R. Kim *et al.*, *Long-Term Aging of Asphalt Mixtures for Performance Testing and Prediction*. Washington, D.C.: Transportation Research Board, 2017, p. 24959. doi: 10.17226/24959.
[26] A. F. Braham, W. G. Buttlar, T. R. Clyne, M. Marasteanu, and M. I. Turos, “The effect of long-term laboratory aging on asphalt concrete fracture energy: Asphalt Paving Technology

2009, AAPT," *Asphalt Paving Technology: Association of Asphalt Paving Technologists-Proceedings of the Technical Sessions*, vol. 78, pp. 417–445, 2009.
[27] Y. R. Kim *et al.*, *Long-Term Aging of Asphalt Mixtures for Performance Testing and Prediction: Phase III Results*. Washington, D.C.: Transportation Research Board, 2021, p. 26133. doi: 10.17226/26133.
[28] F. Zhou, W. S. Mogawer, M. Elwardany, D. J. Mensching, and E. Mahmoud, "Development of a Laboratory Operations-Friendly Long-Term Loose Mix Aging Protocol for New Asphalt Pavements," *Transportation Research Record*, p. 03611981221137595, Dec. 2022, doi: 10.1177/03611981221137595.
[29] A. E. Martin *et al.*, "Evaluation of the Moisture Susceptibility of WMA Technologies," 2014. Accessed: Apr. 24, 2026. [Online]. Available: https://www.nationalacademies.org/publications/22429
[30] AASHTO R 30, *Standard Practice for Laboratory Conditioning of Asphalt Mixtures*, Washington, D.C. USA., 2002.
[31] I. Boz, E. Y. Hajj, J. Habbouche, S. D. Diefenderfer, I. Alam, and H. El Hajj, "A Practical Oven-Aging Method for Evaluating Long-Term Cracking Performance of Asphalt Mixtures in Virginia," Aug. 2025. Accessed: Oct. 29, 2025. [Online]. Available: https://rosap.ntl.bts.gov/view/dot/85678
[32] E. Y. Hajj, I. Alam, H. El Hajj, I. Boz, J. Habbouche, and S. D. Diefenderfer, "Practical Laboratory Aging Protocol for Cracking Evaluation of Asphalt Surface Mixtures in Virginia," *Transportation Research Record*, p. 03611981251366269, Oct. 2025, doi: 10.1177/03611981251366269.
[33] AASHTO R121-24, *Standard Practice for Long-Term Laboratory Conditioning of Asphalt Mixtures*, Washington, D.C. USA., 2024. [Online]. Available: https://store.transportation.org/Item/PublicationDetail?ID=5318
[34] F. Yin, C. Chen, R. West, A. E. Martin, and E. Arambula-Mercado, "Determining the Relationship Among Hamburg Wheel-Tracking Test Parameters and Correlation to Field Performance of Asphalt Pavements," *Transportation Research Record*, vol. 2674, no. 4, pp. 281–291, Apr. 2020, doi: 10.1177/0361198120912430.
[35] "Does IDEAL-RT Correlate with HWTT for Rutting Evaluation of Asphalt Mixtures?" Accessed: Apr. 11, 2026. [Online]. Available: http://eng.auburn.edu//research/centers/ncat/newsroom/2025-fall/ideal-rt-hwtt-rutting
[36] F. Zhou, S. Im, L. Sun, and T. Scullion, "Development of an IDEAL cracking test for asphalt mix design and QC/QA," *Road Materials and Pavement Design*, vol. 18, no. sup4, pp. 405–427, Nov. 2017, doi: 10.1080/14680629.2017.1389082.
[37] A. Leavitt, A. E. Martin, and E. Arámbula-Mercado, "Mitigation Strategy Selection for Asphalt Mixtures with High Reclaimed Asphalt Pavement Content," *Transportation Research Record*, vol. 2677, no. 11, pp. 602–614, Nov. 2023, doi: 10.1177/03611981231166392.
[38] M. D. Elwardany, F. Yousefi Rad, C. Castorena, and Y. R. Kim, "Evaluation of asphalt mixture laboratory long-term ageing methods for performance testing and prediction," *Road Materials and Pavement Design*, vol. 18, no. sup1, pp. 28–61, Jan. 2017, doi: 10.1080/14680629.2016.1266740.
[39] J. Reed, "Evaluation of the Effects of Aging on Asphalt Rubber Pavements," M.S., Arizona State University, 2010. [Online]. Available: https://keep.lib.asu.edu/items/149502

[40] F. Yin *et al.*, "Validation of Loose Mix Aging Procedures for Cracking Resistance Evaluation in Balanced Mix Design," NRRA202308, Nov. 2023. Accessed: Oct. 13, 2024. [Online]. Available: https://rosap.ntl.bts.gov/view/dot/73129

[41] Y. Sun, J. Chen, and B. Huang, "Characterization of asphalt concrete linear viscoelastic behavior utilizing Havriliak–Negami complex modulus model," *Construction and Building Materials*, vol. 99, pp. 226–234, Nov. 2015, doi: 10.1016/j.conbuildmat.2015.09.016.

[42] M. Elwardany, V. Veginati, A. Andriescu, and D. Mensching, "Understanding the Sensitivity of Mixture Cracking Performance Tests to Binder Properties and Long-Term Aging," *Transportation Research Record*, vol. 2678, no. 1, pp. 335–349, Jan. 2024, doi: 10.1177/03611981231170629.

[43] A. Leavitt, A. Epps Martin, and E. Arámbula, "Model for Evaluating Cracking Performance of Asphalt Pavements with Field Aging Based on IDEAL-CT Parameters," *Transportation Research Record*, p. 03611981241231806, Mar. 2024, doi: 10.1177/03611981241231806.

Appendices

Appendix A: Mixture information

Table A-1 Summary of collected TDOT 411-D asphalt mixtures and JMF properties

Mix ID	*Region*	*JMF No.*	*Binder PG*	*Optimum AC*	*Coarse Aggregate*	*RAP content*	*NMAS*	*Mix type*
A	1	1230712	70-22	5.70%	Limestone	1/2"-10%	1/2"	Plant & Lab
B	2	2230234	64-22/67-22	5.70%	Limestone	1/2"-10%	1/2"	Plant & Lab
C	2	2230309	64-22/67-22	5.80%	Granite	1/2"-15%	3/8"	Plant & Lab
D	3	3230064	64-22/67-22	5.70%	Limestone	1/2"-10%	1/2"	Only Plant
E	3	3232042	76-22	5.70%	Limestone	3/8"-10%	1/2"	Plant & Lab
F	4	4230130	70-22	5.70%	Gravel	1/2" - 8% 3/8" - 7%	1/2"	Plant & Lab
G	4	4240011	70-22	6.00%	Gravel	1/2"-10%	3/8"	Plant & Lab
H	1	1240632	70-22	5.70%	Gravel/Granite	1/2"-10%	3/8"	Plant & Lab
I	1	1240622	64-22/67-22	5.70%	Gravel	1/2"-10%	3/8"	Plant & Lab
J	2	2240260	70-22	5.70%	Sandstone	1/2"-10%	1/2"	Plant & Lab
K	2	2240040	76-22	5.90%	Granite	1/2"-10%	3/8"	Plant & Lab
L	3	3248001	76-22	6.58%	Gravel	1/2"-10% 5/16"-5%	1/2"	Plant & Lab
M	2	2250033	70-22	5.70%	Limestone	1/2"-10%	1/2"	Plant & Lab
N	3	3252068	76-22	5.70%	Limestone	1/2"-10%	1/2"	Plant & Lab
O	4	4250084	76-22	5.90%	Gravel	1/2"-10%	1/2"	Plant & Lab
P	4	4250319	76-22	6.10%	Gravel	1/2"-10%	1/2"	Plant & Lab
Q	1	1250629	76-22	5.70%	Quartzite	1/2"-10%	3/8"	Plant & Lab
R	1	1250316	76-22	6.00%	Quartzite	5/16"-10%	3/8"	Plant & Lab
S	1	1250341	76-22	6.00%	Gravel	3/8"-10%	3/8"	Plant & Lab
T	2	2250353	76-22	5.70%	Limestone	1/2"-10%	1/2"	Plant & Lab
U	2	2250269	76-22	6.40%	Limestone	1/2"- 7.3%RAP 3/8"- 2.7%RAS	1/2"	Plant & Lab
V	1	1250649	64-22/67-22	5.70%	Gravel	0	3/8"	Plant & Lab
W	3	3252006	76-22	5.70%	Limestone	1/2"-15%	1/2"	Plant & Lab
X	4	4250324	64-22/67-22	6.00%	Gravel	3/8"-15%	3/8"	Plant & Lab

Mix ID	*Region*	*JMF No.*	*G_{mm}*	*VMA*	*VFA*	*Eff. Gravity of Agg.*	*Marshall stability (lb)*	*Flow (0.01")*
A	1	1230712	2.547	17.4	77.9	2.796	4167	10.7
B	2	2230234	2.475	17.1	77.1	2.704	3373	13.8
C	2	2230309	2.437	17	77.4	2.661	3717	13.3
D	3	3230064	2.420	16.8	76.5	2.635	2510	12.2
E	3	3232042	2.431	17	75.7	2.649	3500	13.2
F	4	4230130	2.379	16.7	75.8	2.583	3768	14.3
G	4	4240011	2.314	16.9	76.4	2.514	3403	16.8
H	1	1240632	2.468	17	77.4	2.696	3483	11.7
I	1	1240622	2.440	17	76.3	2.660	4585	14.2
J	2	2240260	2.410	16.8	76.3	2.622	3155	12.5
K	2	2240040	2.448	17.3	77.7	2.679	3233	33.2
L	3	3248001	2.225	17.7	77	2.423	2926	16.5
M	2	2250033	2.481	17.3	75.9	2.712	3125	11.0
N	3	3252068	2.420	16.7	76.9	2.635	2178	11.0
O	4	4250084	2.390	17.3	75.6	2.605	NA	NA
P	4	4250319	2.292	17	76.5	2.490	4358	12.8
Q	1	1250629	2.448	16.9	76.8	2.670	4669	11.3
R	1	1250316	2.420	17.7	76.6	2.649	3533	14.0
S	1	1250341	2.417	17.4	77.9	2.644	4242	13.7
T	2	2250353	2.494	17.2	77.2	2.729	3398	11.9
U	2	2250269	2.367	18.2	77.7	2.597	3050	10.7
V	1	1250649	2.472	17.1	76.7	2.699	4153	15.1
W	3	3252006	2.418	16.8	76.4	2.632	2858	11.6
X	4	4250324	2.340	17.1	76.4	2.547	3392	11.5

Appendix B: HWTT results and figures

Table A-2 HWTT results of PMLC and LMLC.

Mix ID	*JMF NO.*	*PMLC (reheated)*					*LMLC(STA2h)*				
		Avg. CRD20K (mm)	*Left CRD20k (mm)*	*Right CRD20k (mm)*	*Left SIP*	*Right SIP*	*Avg. CRD20K (mm)*	*Left CRD20k (mm)*	*Right CRD20k (mm)*	*Left SIP*	*Right SIP*
A	1230712	4.5	3.66	5.32	N	N	5.7	5.76	5.60	N	N
B	2230234	9.7	8.10	11.32	N	Y	12.7	12.39	13.07	N	N
C	2230309	5.4	4.76	6.00	N	N	8.3	8.75	7.92	Y	Y
D	3230064	12.2	11.30	13.18	N	N	NA	NA	NA	NA	NA
E	3232042	8.5	6.46	10.50	N	Y	8.1	6.84	9.40	N	Y
F	4230130	4.6	4.63	4.63	N	N	2.4	2.65	2.05	N	N
G	4240011	5.1	4.52	5.65	N	N	4.4	3.85	4.91	N	N
H	1240632	3.5	3.26	3.74	N	N	3.9	4.14	3.72	N	N
I	1240623	13.4	13.72	12.99	N	N	7.1	8.09	6.06	N	N
J	2240260	5.9	4.88	6.84	N	Y	3.6	3.48	3.71	N	N
K	2240040	3.5	3.63	3.35	N	N	1.9	2.02	1.68	N	N
L	3248001	3.3	3.24	3.26	N	N	2.8	3.06	2.56	N	N
M	2250033	8.4	7.65	9.10	N	Y	3.4	3.50	3.35	N	N
N	3252068	9.9	9.40	10.40	N	Y	3.3	4.21	2.35	N	N
O	4250084	6.3	6.05	6.54	N	N	4.7	5.04	4.30	N	N
P	4250319	3.2	3.11	3.28	N	N	3.1	3.05	3.07	N	N
Q	1250629	4.8	4.40	5.24	N	N	4.5	3.79	5.21	N	N
R	1250316	6.1	5.97	6.15	N	N	4.5	4.67	4.28	N	N
S	1250341	3.9	3.67	4.05	N	N	3.9	4.46	3.28	N	N
T	2250353	4.5	4.02	4.97	N	N	3.8	3.63	3.99	N	N
U	2250269	10.2	10.34	10.03	N	N	7.0	6.83	7.13	N	N
V	1250649	7.2	6.13	8.18	N	Y	5.8	6.70	4.86	Y	N
W	3252006	4.6	4.43	4.69	N	N	7.9	8.61	7.19	N	N
X	4250324	9.6	9.29	9.90	Y	Y	8.4	9.67	7.13	Y	Y

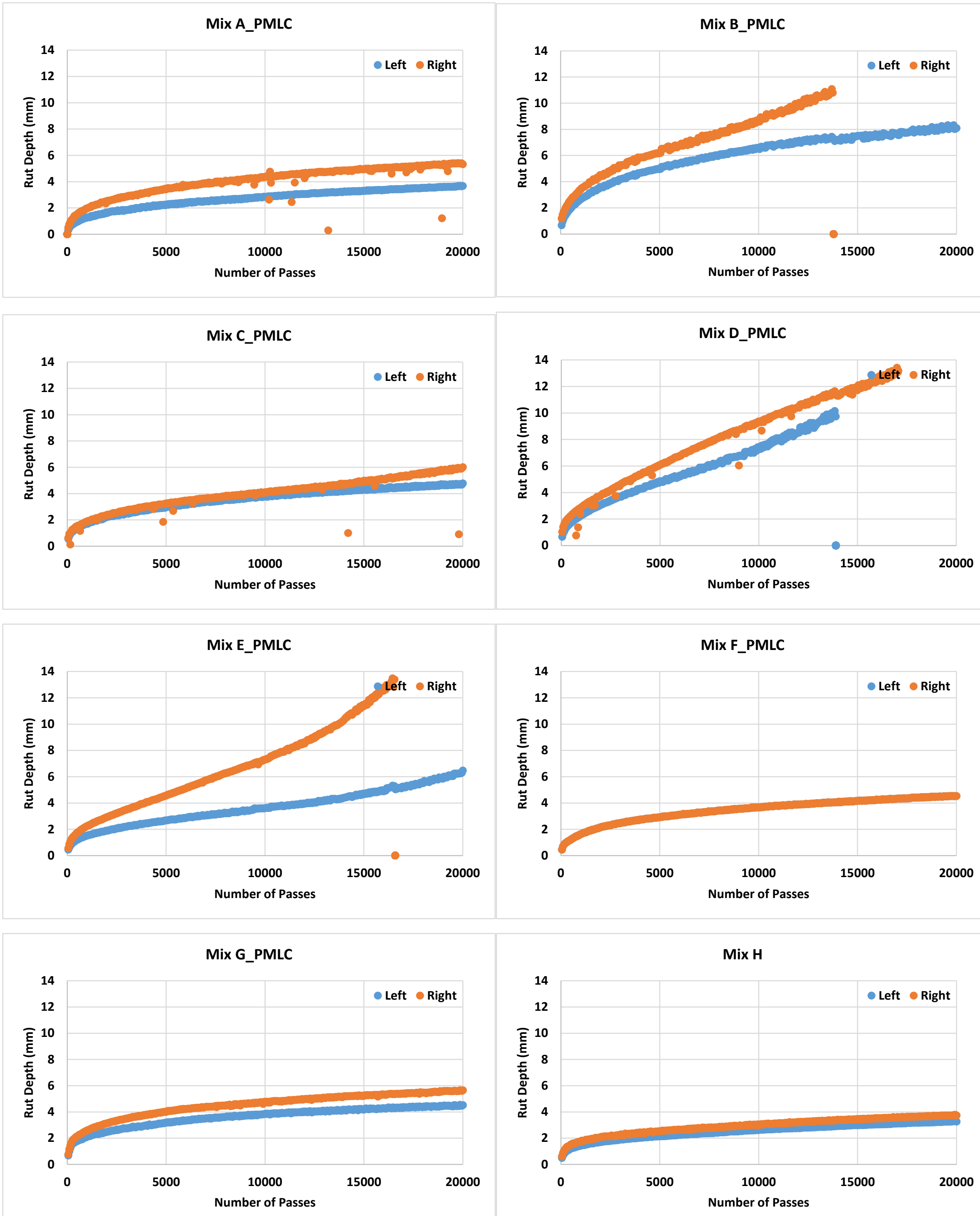
Mix A_PMLC
Mix B_PMLC
Mix C_PMLC
Mix D_PMLC
Mix E_PMLC
Mix F_PMLC
Mix G_PMLC
Mix H
Left
Right
Rut Depth (mm)
Number of Passes
0
2
4
6
8
10
12
14
0
5000
10000
15000
20000

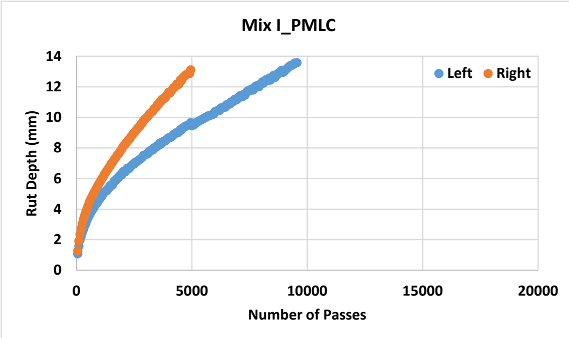
Mix I_PMLC
Left
Right
Rut Depth (mm)
0 2 4 6 8 10 12 14
0 5000 10000 15000 20000
Number of Passes

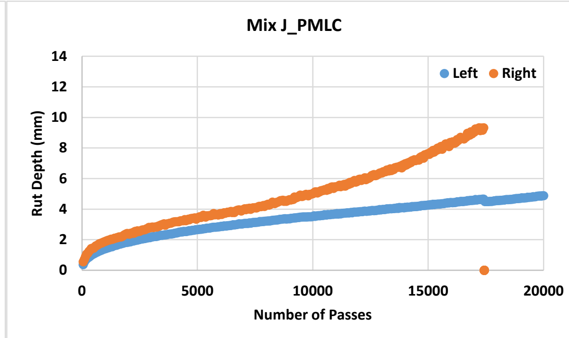
Mix J_PMLC
Left
Right
Rut Depth (mm)
0 2 4 6 8 10 12 14
0 5000 10000 15000 20000
Number of Passes

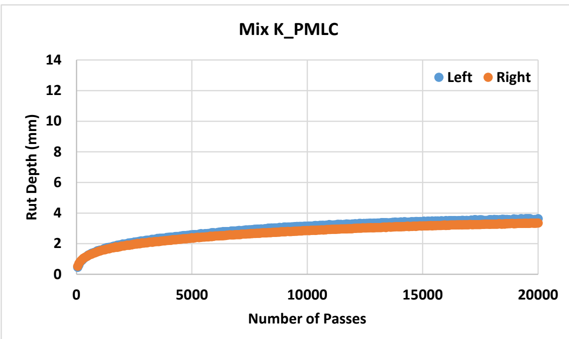
Mix K_PMLC
Left
Right
Rut Depth (mm)
0 2 4 6 8 10 12 14
0 5000 10000 15000 20000
Number of Passes

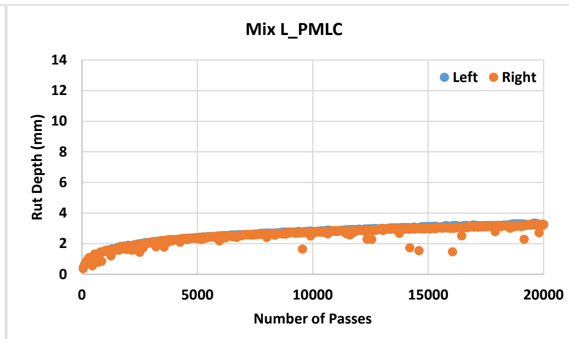
Mix L_PMLC
Left
Right
Rut Depth (mm)
0 2 4 6 8 10 12 14
0 5000 10000 15000 20000
Number of Passes

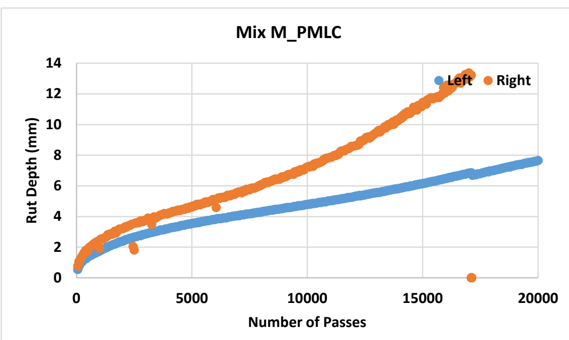
Mix M_PMLC
Left
Right
Rut Depth (mm)
0 2 4 6 8 10 12 14
0 5000 10000 15000 20000
Number of Passes

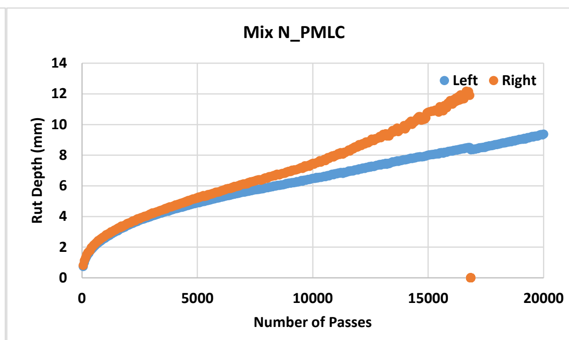
Mix N_PMLC
Left
Right
Rut Depth (mm)
0 2 4 6 8 10 12 14
0 5000 10000 15000 20000
Number of Passes

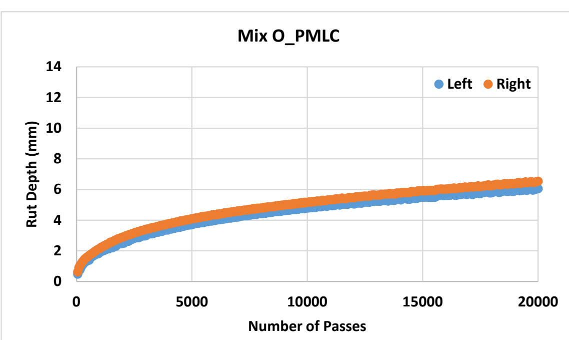
Mix O_PMLC
Left
Right
Rut Depth (mm)
0 2 4 6 8 10 12 14
0 5000 10000 15000 20000
Number of Passes

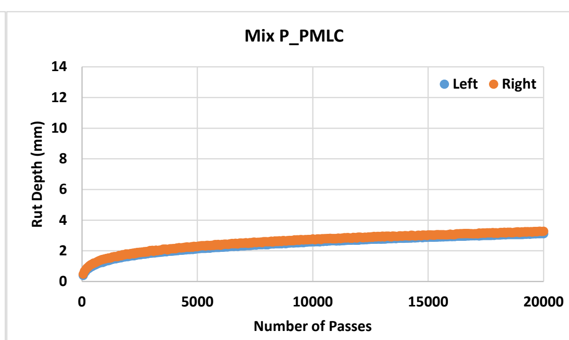
Mix P_PMLC
Left
Right
Rut Depth (mm)
0 2 4 6 8 10 12 14
0 5000 10000 15000 20000
Number of Passes

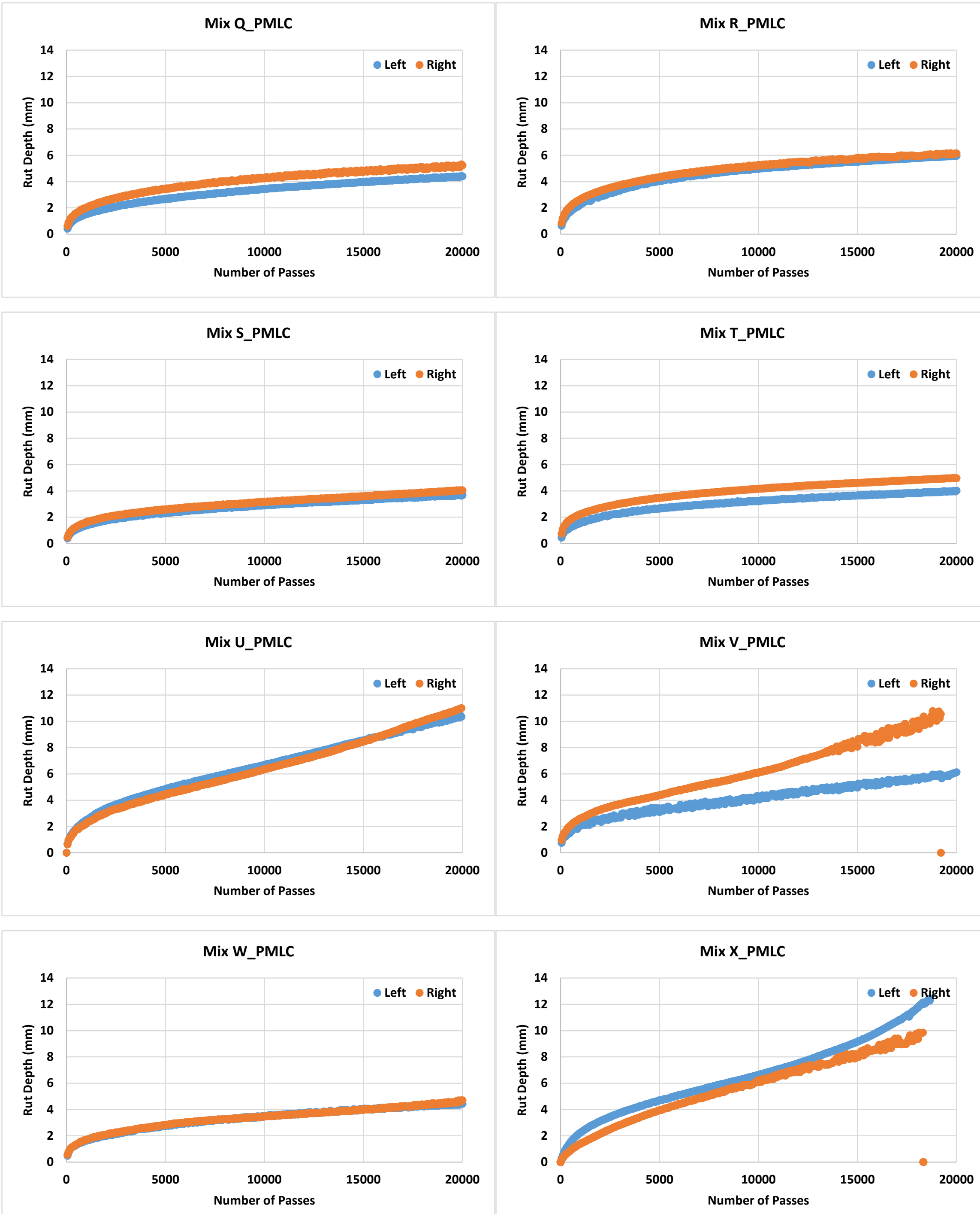

Figure A-1 HWTT results of PMLC

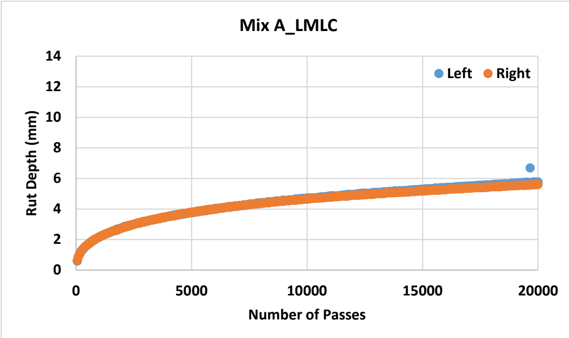
Mix A_LMLC
Left
Right
Rut Depth (mm)
Number of Passes
0
2
4
6
8
10
12
14
0
5000
10000
15000
20000

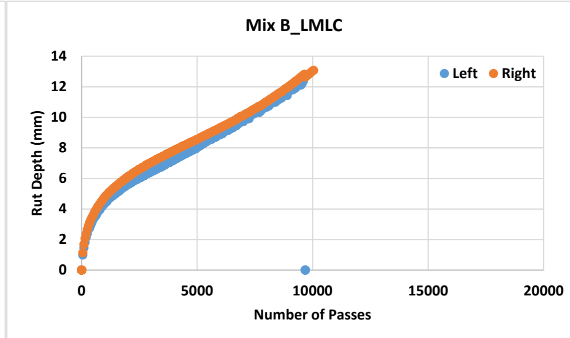
Mix B_LMLC
Left
Right
Rut Depth (mm)
Number of Passes
0
2
4
6
8
10
12
14
0
5000
10000
15000
20000

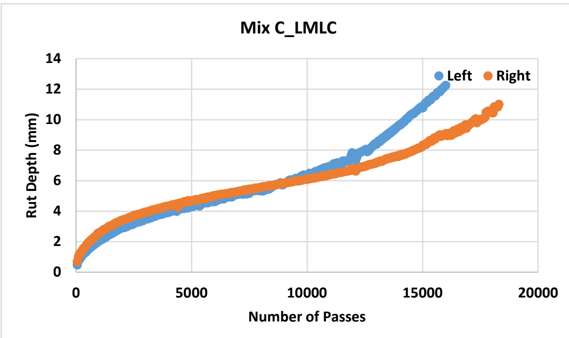
Mix C_LMLC
Left
Right
Rut Depth (mm)
Number of Passes
0
2
4
6
8
10
12
14
0
5000
10000
15000
20000

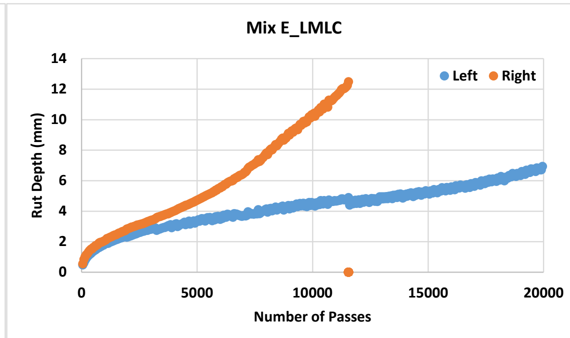
Mix E_LMLC
Left
Right
Rut Depth (mm)
Number of Passes
0
2
4
6
8
10
12
14
0
5000
10000
15000
20000

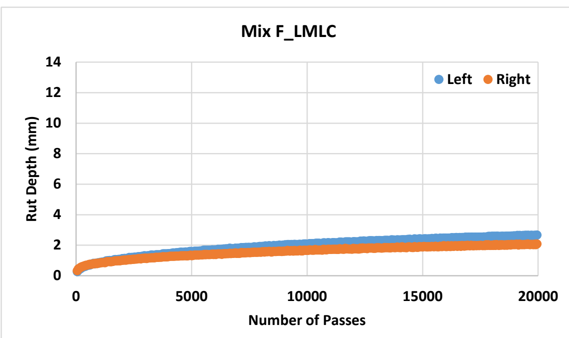
Mix F_LMLC
Left
Right
Rut Depth (mm)
Number of Passes
0
2
4
6
8
10
12
14
0
5000
10000
15000
20000

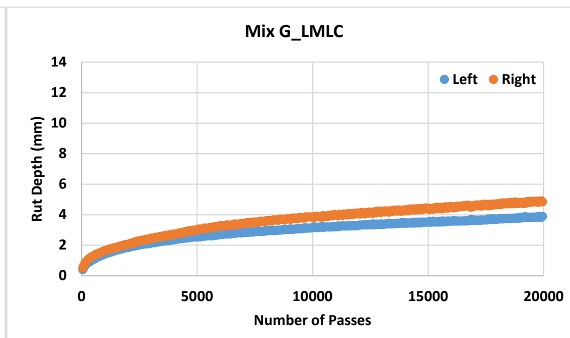
Mix G_LMLC
Left
Right
Rut Depth (mm)
Number of Passes
0
2
4
6
8
10
12
14
0
5000
10000
15000
20000

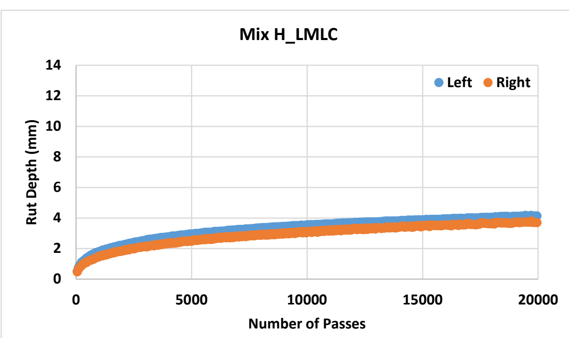
Mix H_LMLC
Left
Right
Rut Depth (mm)
Number of Passes
0
2
4
6
8
10
12
14
0
5000
10000
15000
20000

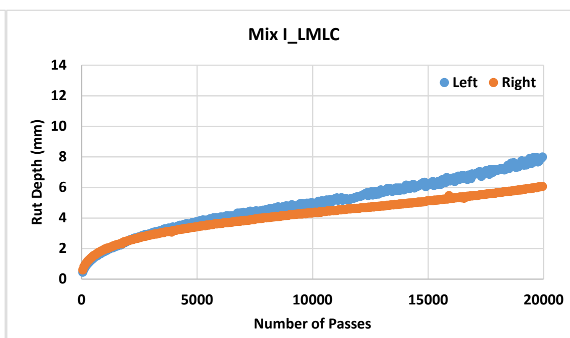
Mix I_LMLC
Left
Right
Rut Depth (mm)
Number of Passes
0
2
4
6
8
10
12
14
0
5000
10000
15000
20000

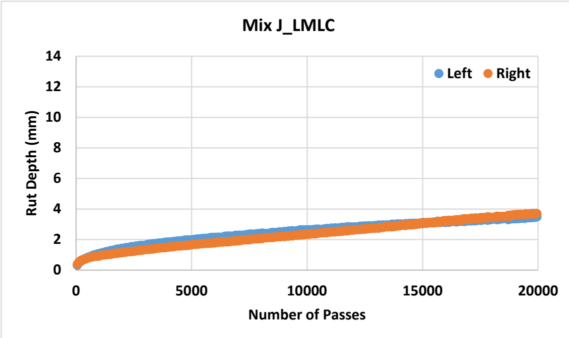
Mix J_LMLC
Left Right
Rut Depth (mm)
Number of Passes
0 2 4 6 8 10 12 14
0 5000 10000 15000 20000

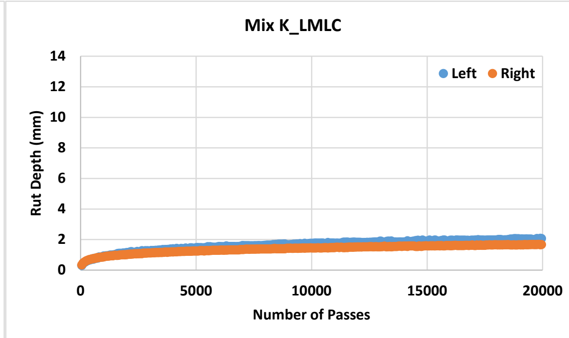
Mix K_LMLC
Left Right
Rut Depth (mm)
Number of Passes
0 2 4 6 8 10 12 14
0 5000 10000 15000 20000

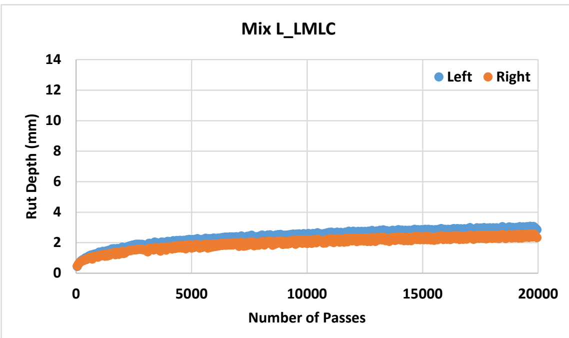
Mix L_LMLC
Left Right
Rut Depth (mm)
Number of Passes
0 2 4 6 8 10 12 14
0 5000 10000 15000 20000

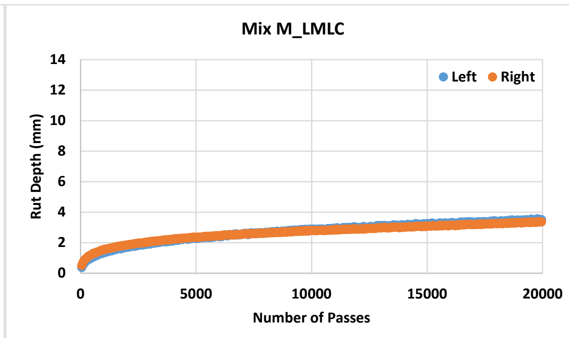
Mix M_LMLC
Left Right
Rut Depth (mm)
Number of Passes
0 2 4 6 8 10 12 14
0 5000 10000 15000 20000

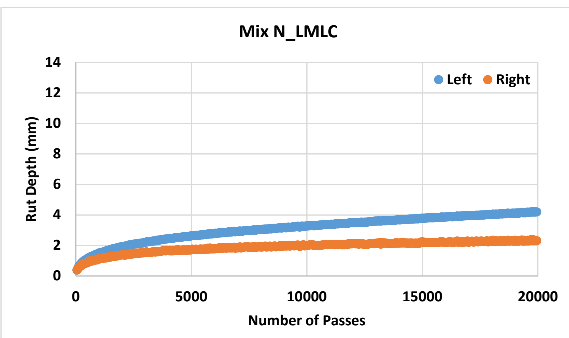
Mix N_LMLC
Left Right
Rut Depth (mm)
Number of Passes
0 2 4 6 8 10 12 14
0 5000 10000 15000 20000

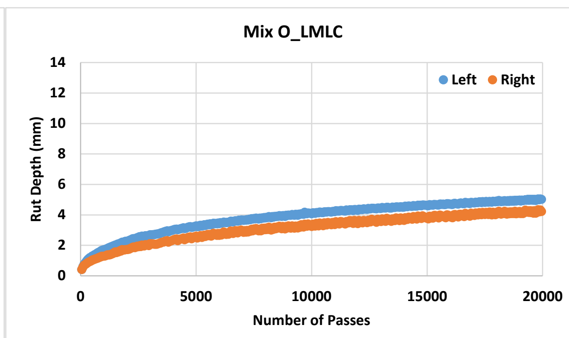
Mix O_LMLC
Left Right
Rut Depth (mm)
Number of Passes
0 2 4 6 8 10 12 14
0 5000 10000 15000 20000

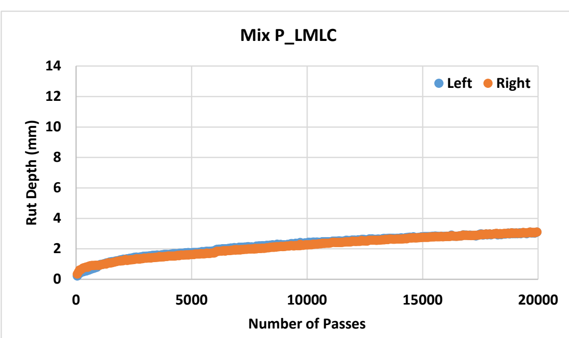
Mix P_LMLC
Left Right
Rut Depth (mm)
Number of Passes
0 2 4 6 8 10 12 14
0 5000 10000 15000 20000

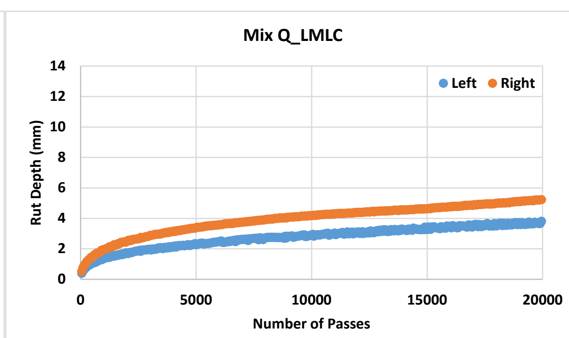
Mix Q_LMLC
Left Right
Rut Depth (mm)
Number of Passes
0 2 4 6 8 10 12 14
0 5000 10000 15000 20000

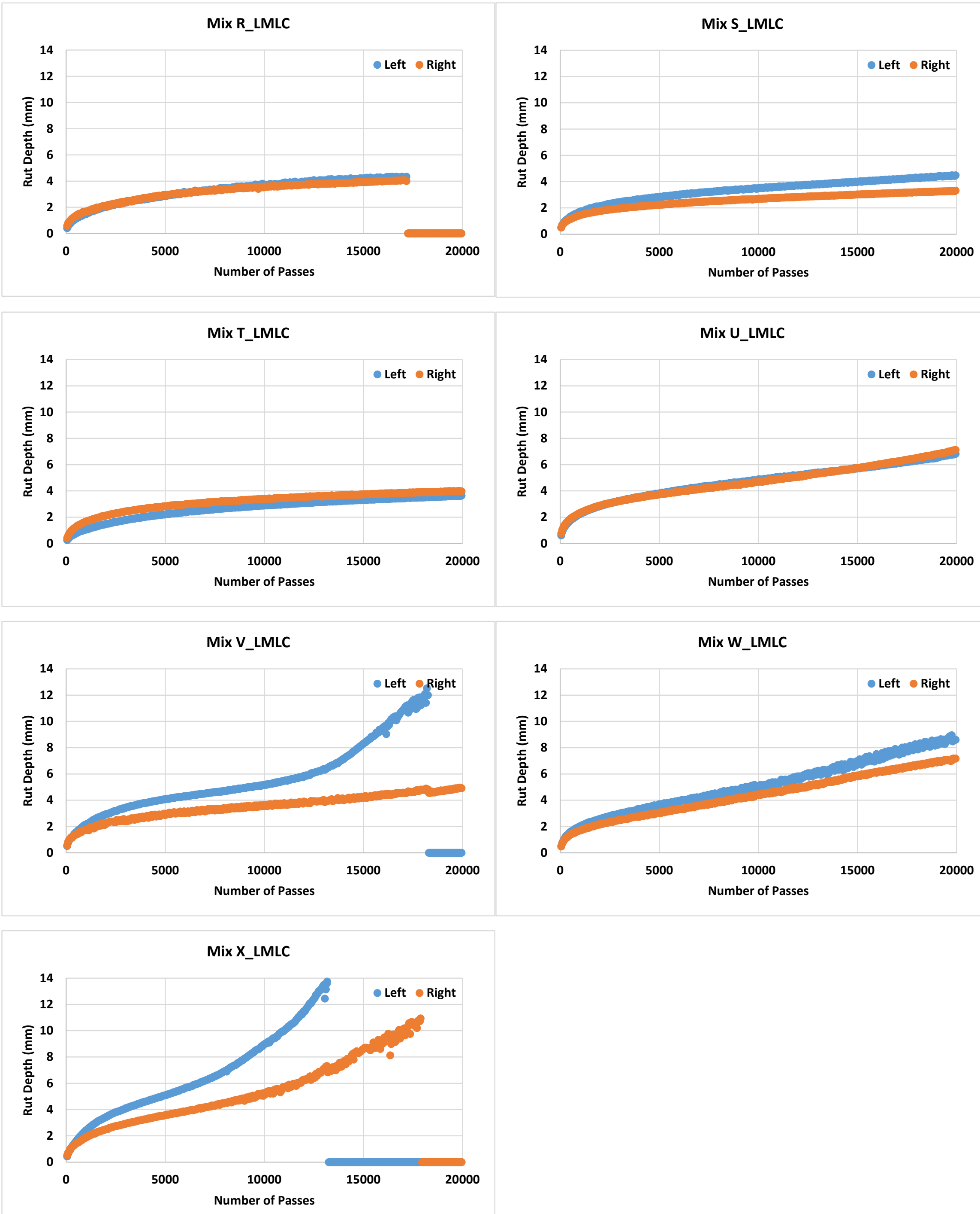

Figure A-2 HWTT results of LMLC

Appendix C: Three-Dimensional Performance Spaces Incorporating Peak-Strength Thresholds

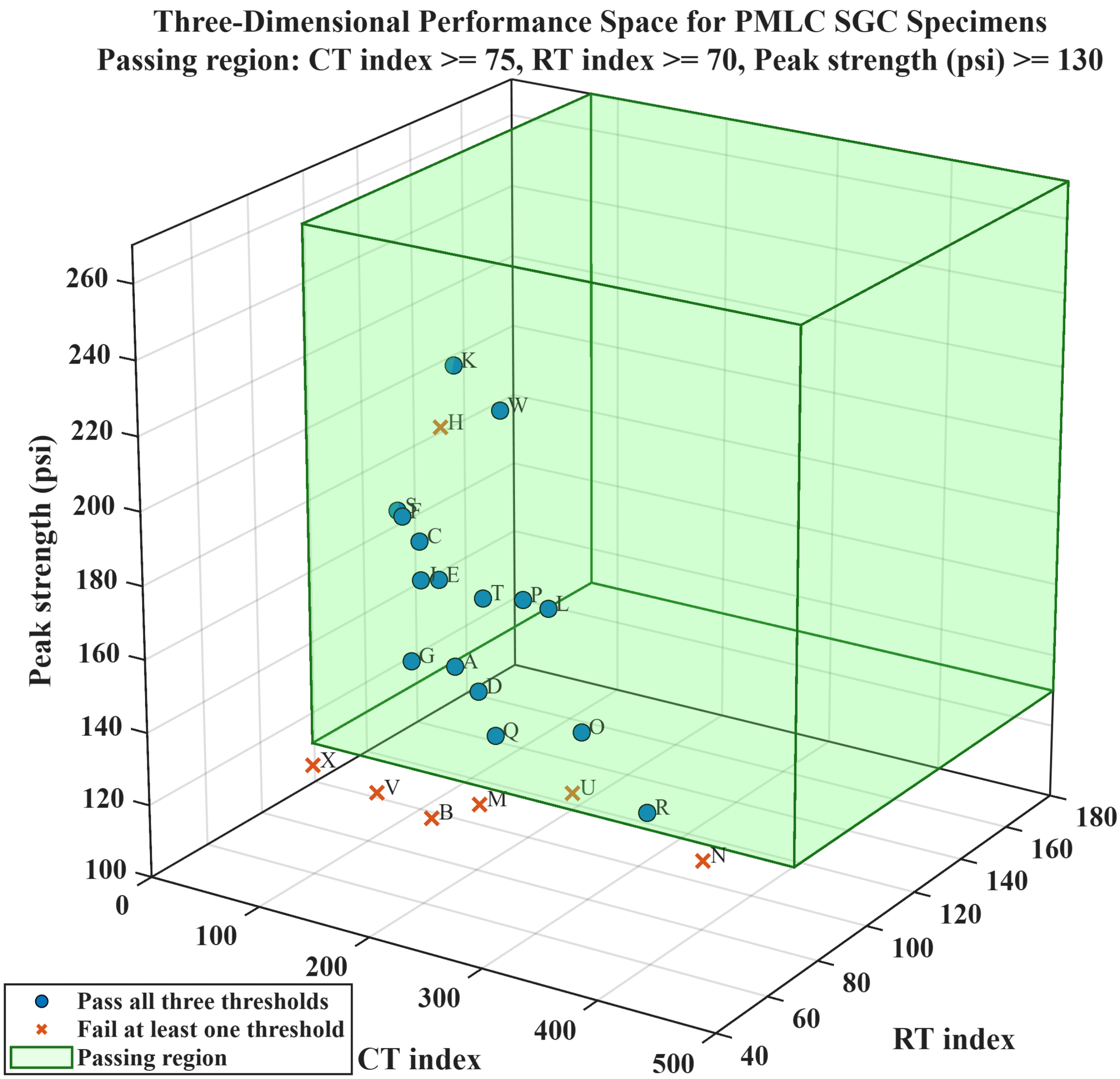

(a)

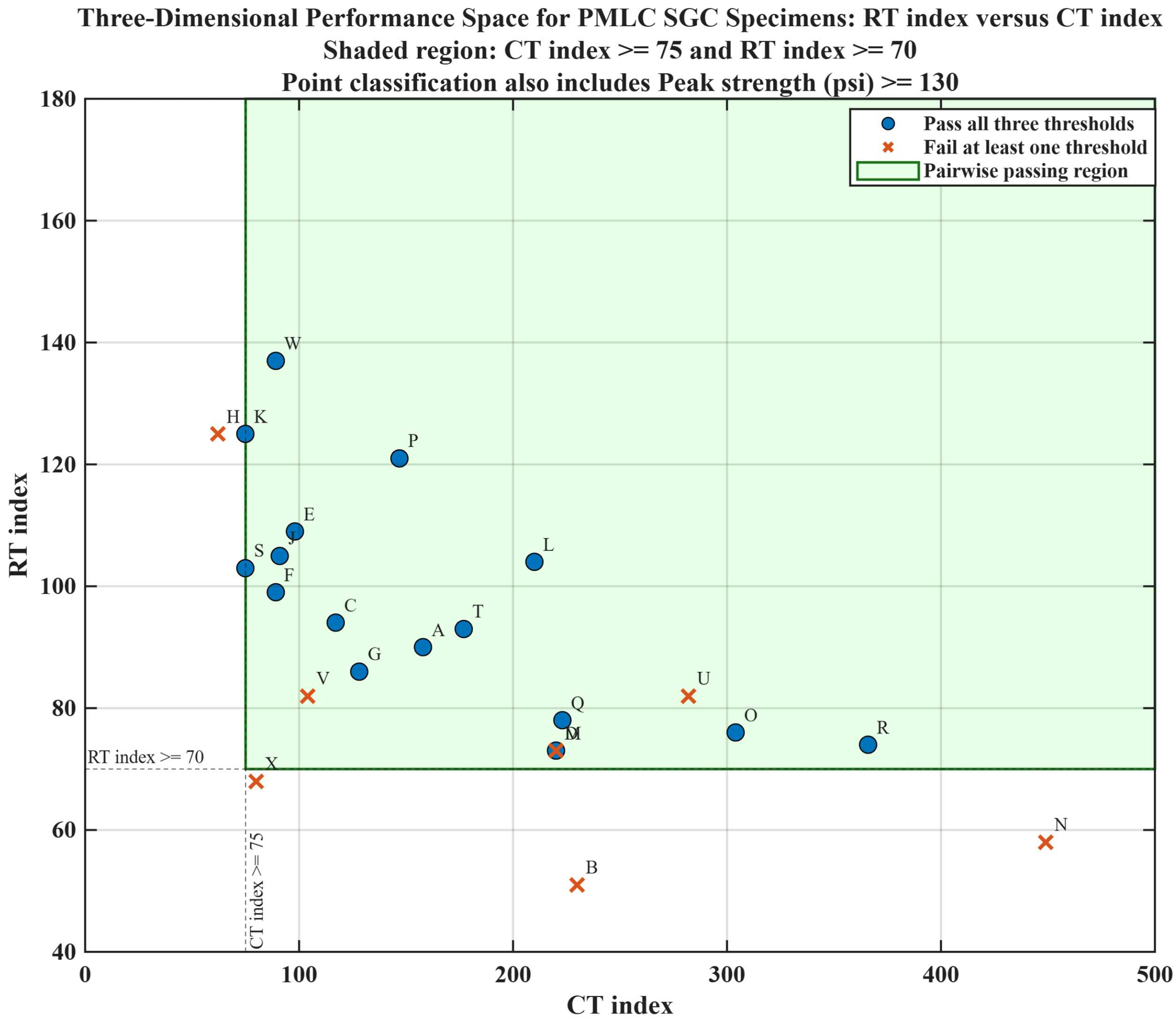

Three-Dimensional Performance Space for PMLC SGC Specimens: RT index versus CT index
Shaded region: CT index >= 75 and RT index >= 70
Point classification also includes Peak strength (psi) >= 130
Pass all three thresholds
Fail at least one threshold
Pairwise passing region
RT index
CT index
RT index >= 70
CT index >= 75

(b)

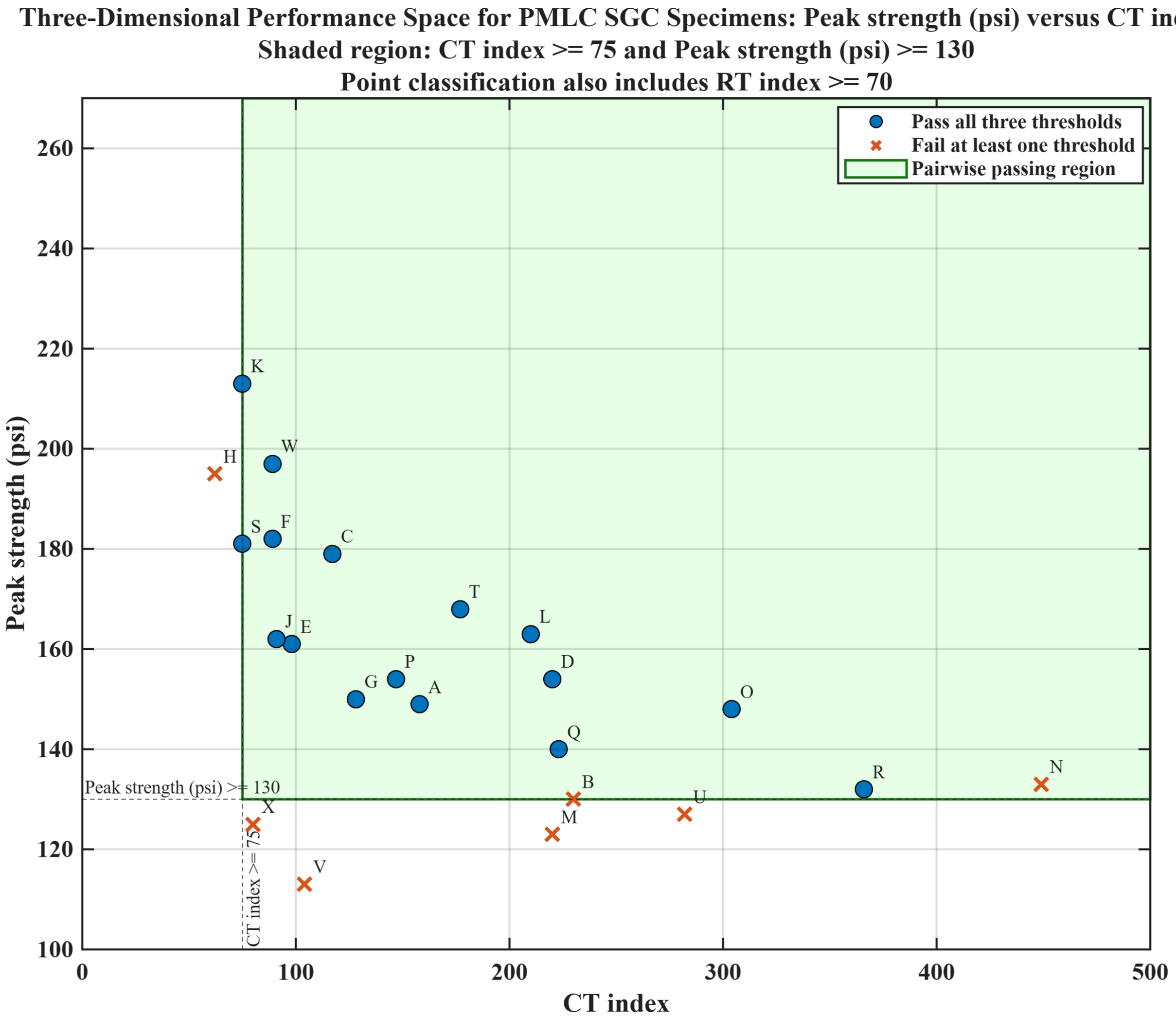
Three-Dimensional Performance Space for PMLC SGC Specimens: Peak strength (psi) versus CT index
Shaded region: CT index >= 75 and Peak strength (psi) >= 130
Point classification also includes RT index >= 70
Pass all three thresholds
Fail at least one threshold
Pairwise passing region
Peak strength (psi)
CT index
Peak strength (psi) >= 130
CT index >= 75
K
W
H
S
F
C
T
L
J
E
P
D
G
A
O
Q
R
N
B
X
M
U
V
260
240
220
200
180
160
140
120
100
0
100
200
300
400
500

(c)

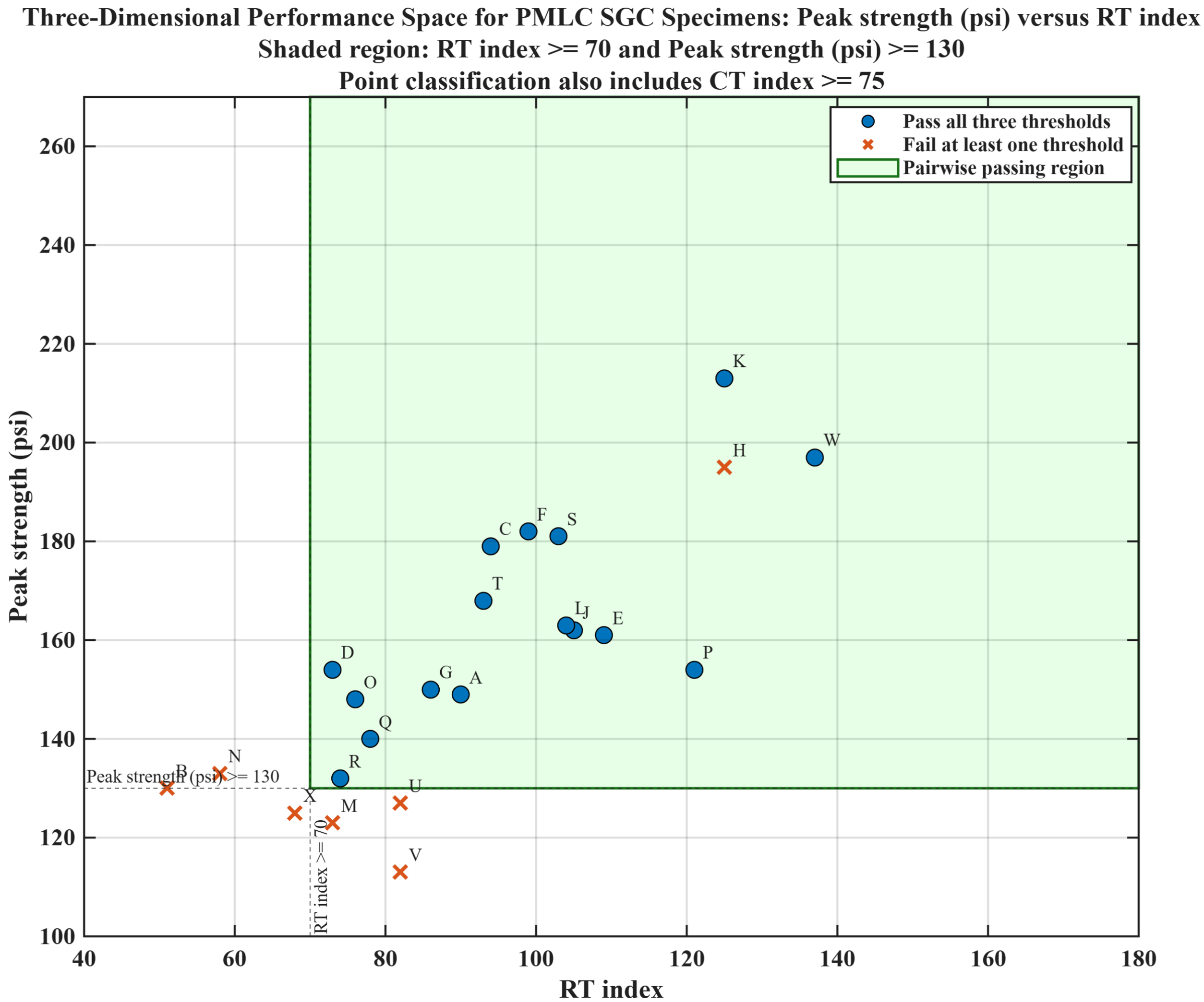

(d)

Figure A-3 Three-dimensional performance space for reheated PMLC SGC specimens based on CT index, RT index, and IDEAL-CT peak strength

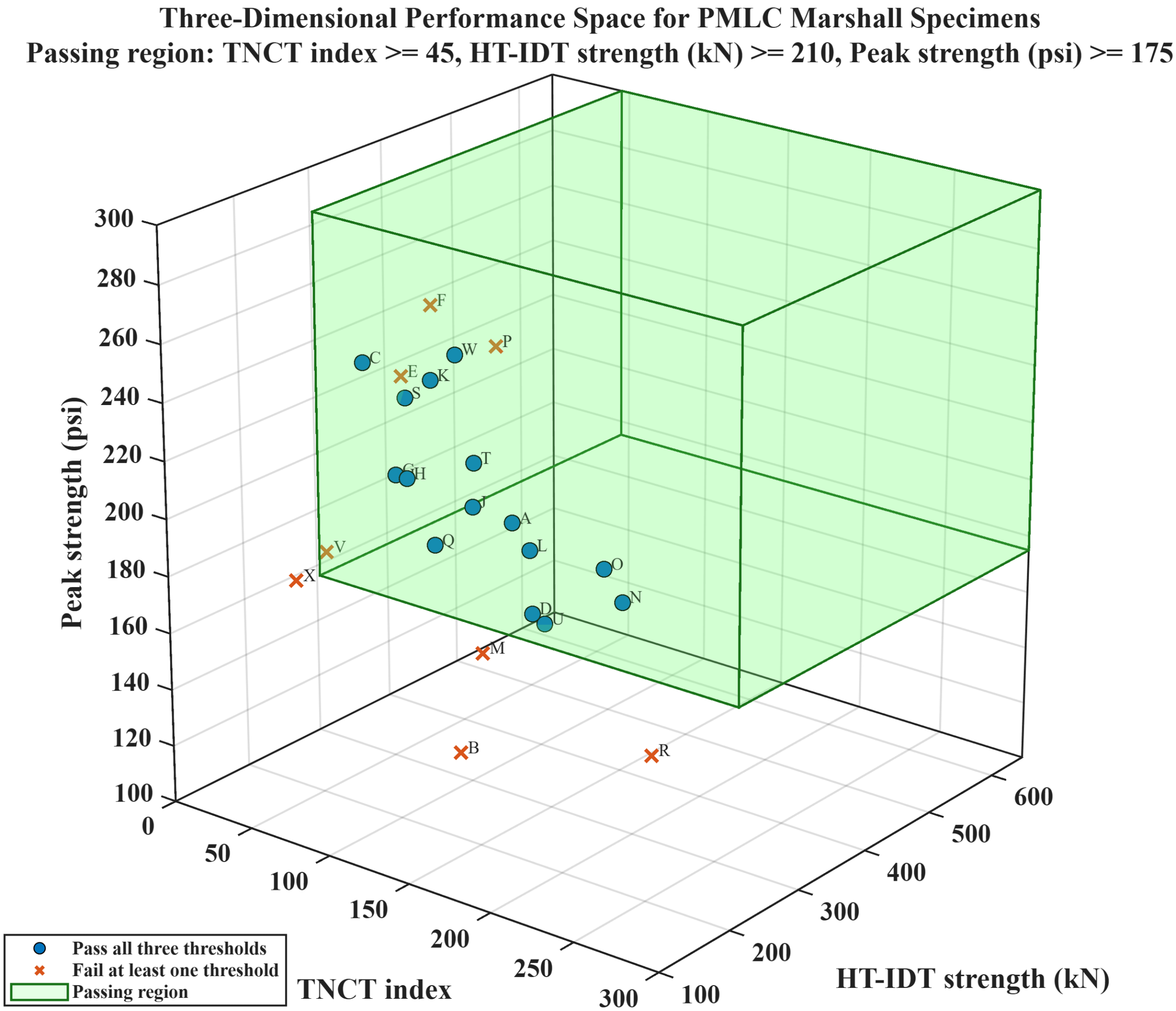
Three-Dimensional Performance Space for PMLC Marshall Specimens
Passing region: TNCT index >= 45, HT-IDT strength (kN) >= 210, Peak strength (psi) >= 175
Peak strength (psi)
TNCT index
HT-IDT strength (kN)
Pass all three thresholds
Fail at least one threshold
Passing region
A
B
C
D
E
F
G
H
J
K
L
M
N
O
P
Q
R
S
T
U
V
W
X

(a)

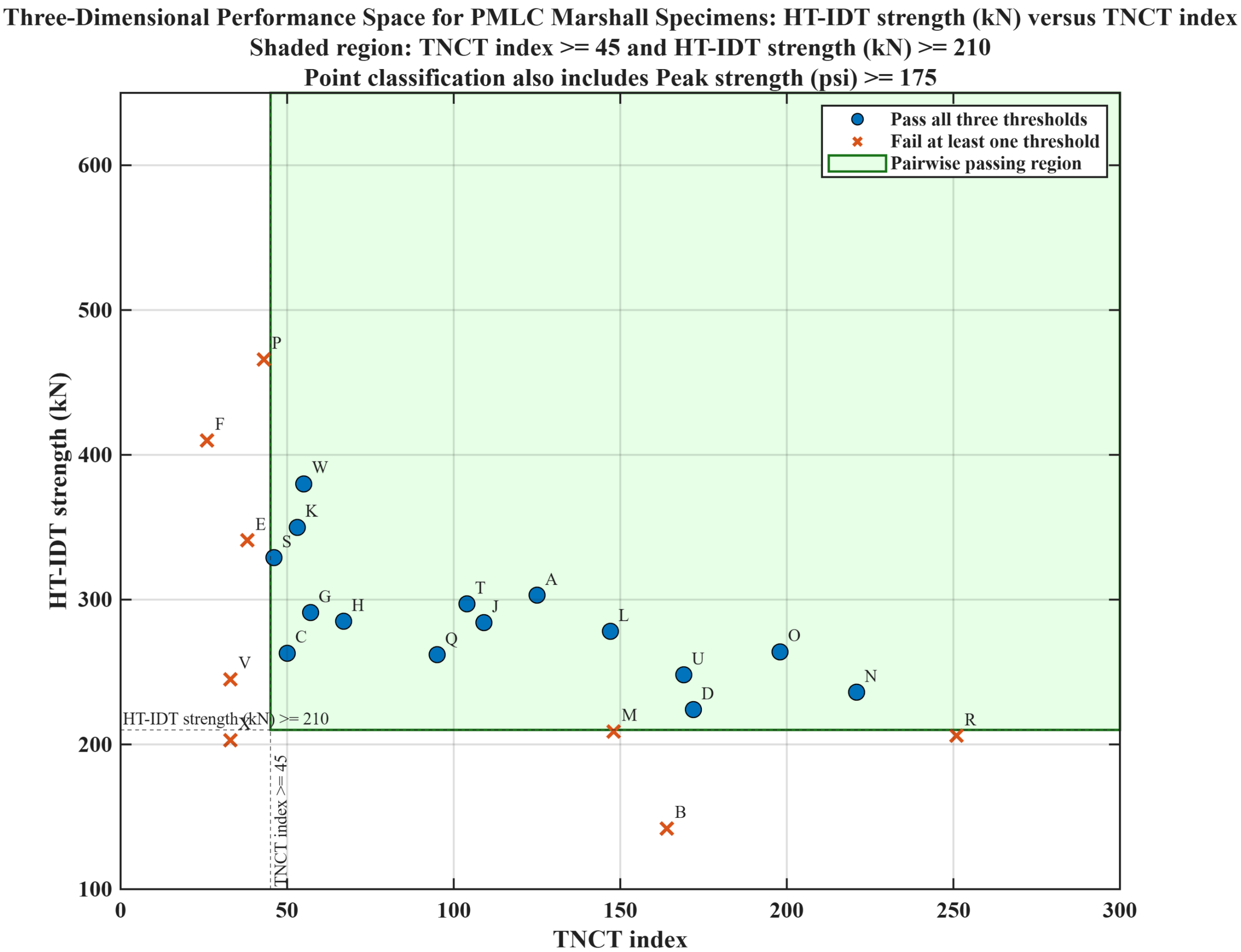
Three-Dimensional Performance Space for PMLC Marshall Specimens: HT-IDT strength (kN) versus TNCT index
Shaded region: TNCT index >= 45 and HT-IDT strength (kN) >= 210
Point classification also includes Peak strength (psi) >= 175
Pass all three thresholds
Fail at least one threshold
Pairwise passing region
HT-IDT strength (kN)
TNCT index
HT-IDT strength (kN) >= 210
TNCT index >= 45
600
500
400
300
200
100
0
50
100
150
200
250
300
P
F
W
K
E
S
G
H
T
J
A
L
C
Q
V
O
U
N
D
X
M
R
B

(b)

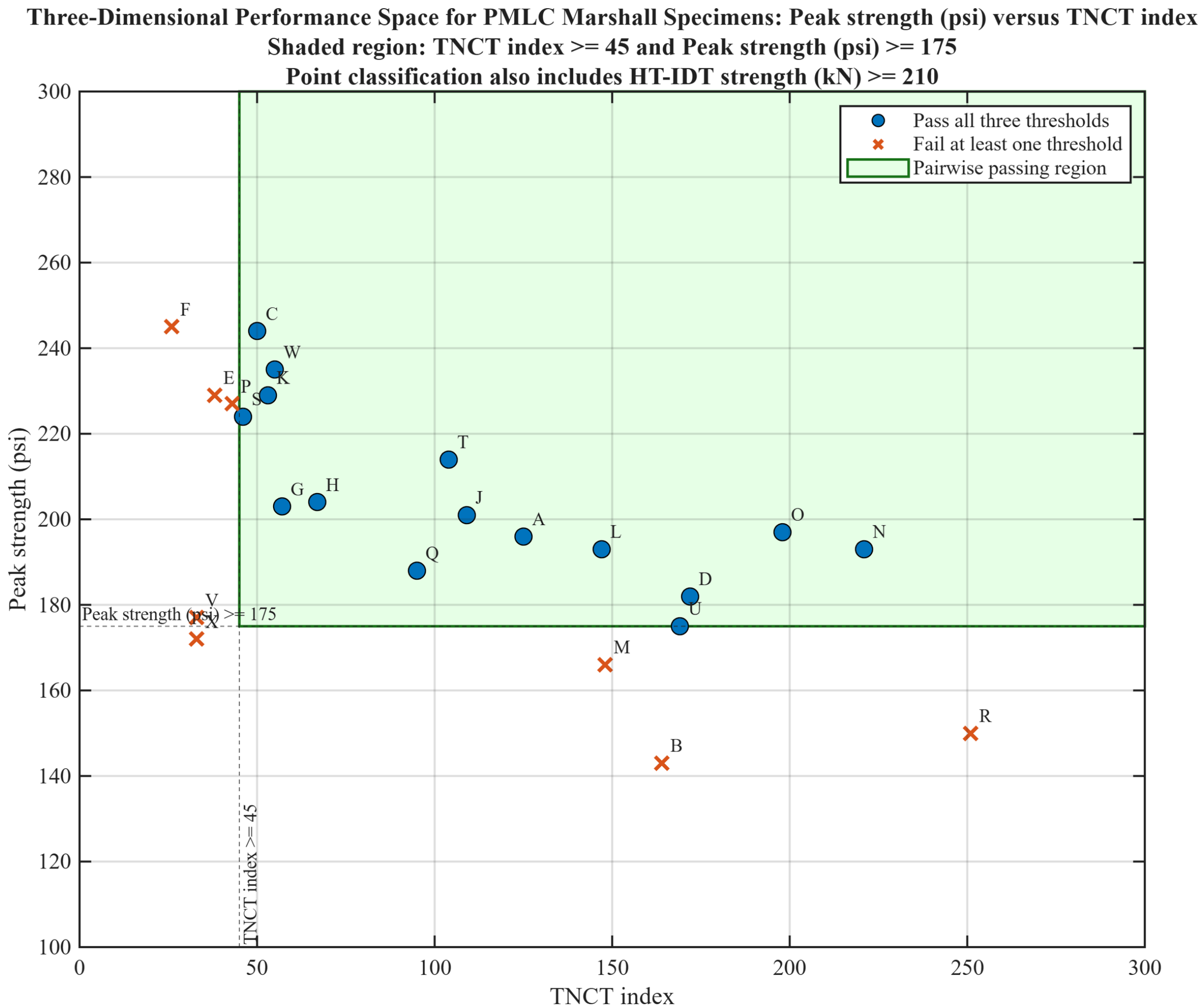
Three-Dimensional Performance Space for PMLC Marshall Specimens: Peak strength (psi) versus TNCT index
Shaded region: TNCT index >= 45 and Peak strength (psi) >= 175
Point classification also includes HT-IDT strength (kN) >= 210
Pass all three thresholds
Fail at least one threshold
Pairwise passing region
Peak strength (psi) >= 175
TNCT index >= 45
Peak strength (psi)
TNCT index
F
C
W
K
E
P
S
T
G
H
J
A
L
O
N
Q
D
U
V
X
M
B
R
300
280
260
240
220
200
180
160
140
120
100
0
50
100
150
200
250
300

(c)

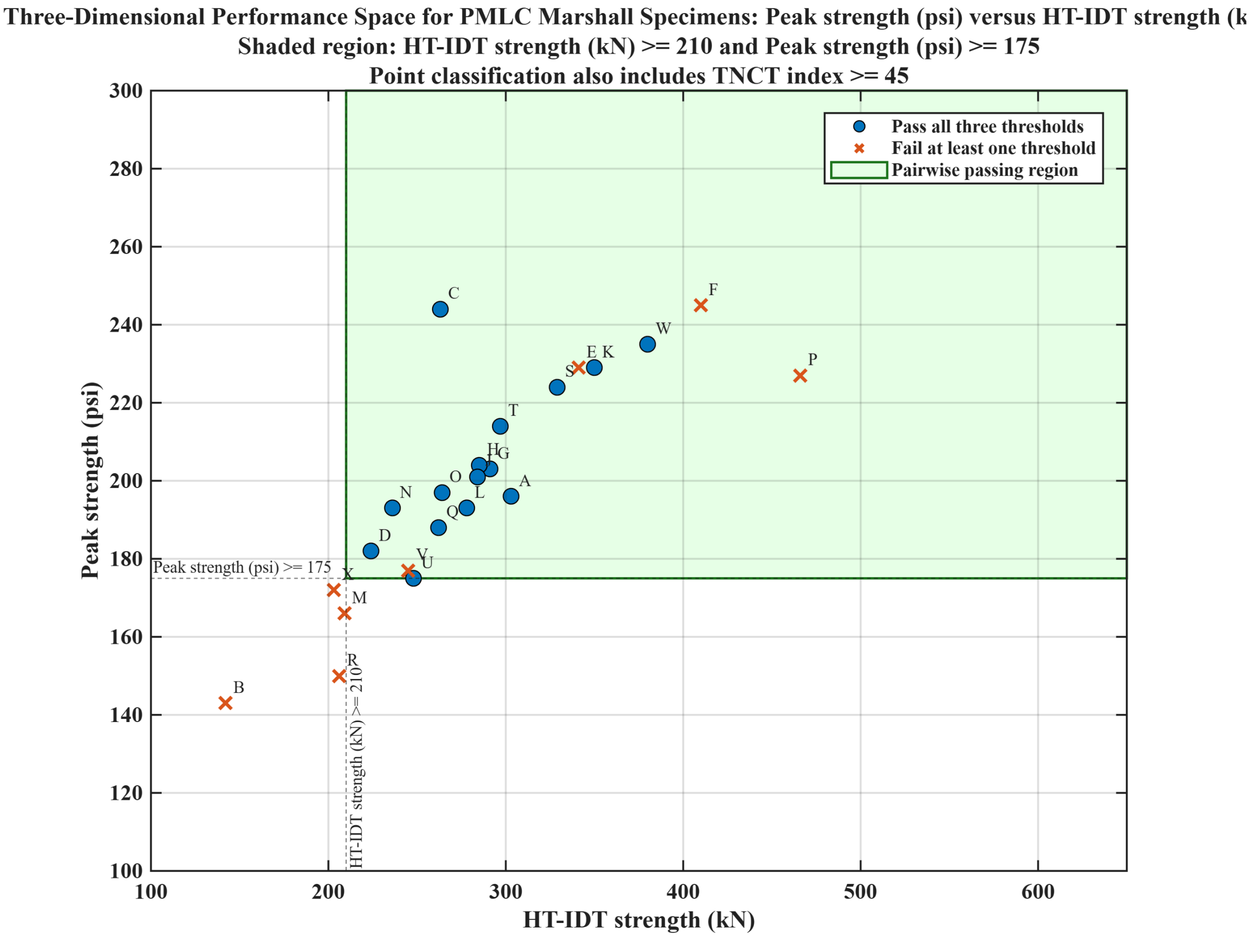

(d)

Figure A-4 Three-dimensional performance space for reheated PMLC Marshall specimens based on TN-CT index, HT-IDT strength, and TN-CT peak strength.

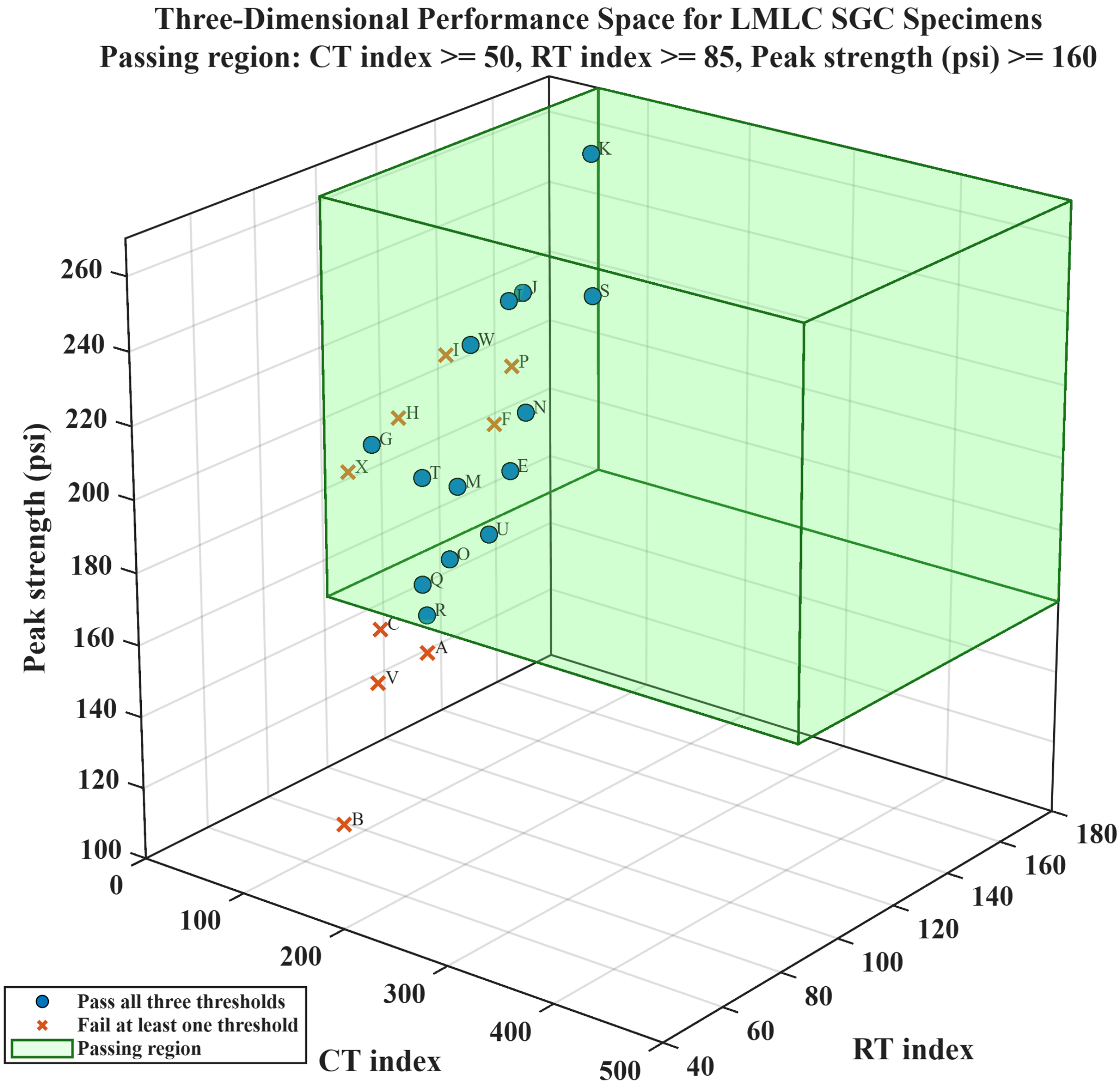
Three-Dimensional Performance Space for LMLC SGC Specimens
Passing region: CT index >= 50, RT index >= 85, Peak strength (psi) >= 160
Peak strength (psi)
CT index
RT index
Pass all three thresholds
Fail at least one threshold
Passing region

(a)

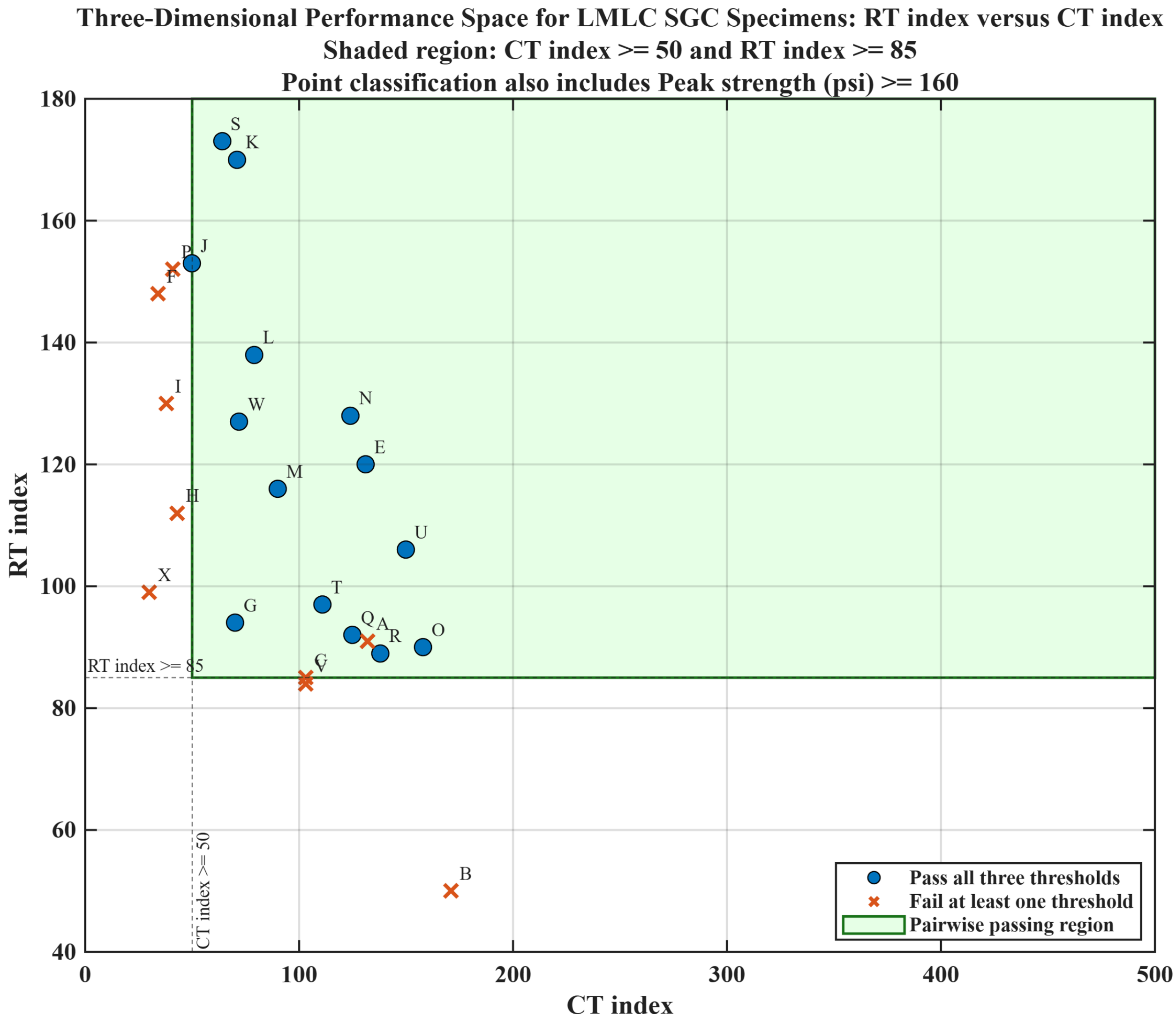
Three-Dimensional Performance Space for LMLC SGC Specimens: RT index versus CT index
Shaded region: CT index >= 50 and RT index >= 85
Point classification also includes Peak strength (psi) >= 160
RT index
CT index
RT index >= 85
CT index >= 50
180
160
140
120
100
80
60
40
0
100
200
300
400
500
S
K
P
J
F
L
I
W
N
E
M
H
U
X
T
G
Q
A
R
O
C
V
B
Pass all three thresholds
Fail at least one threshold
Pairwise passing region

(b)

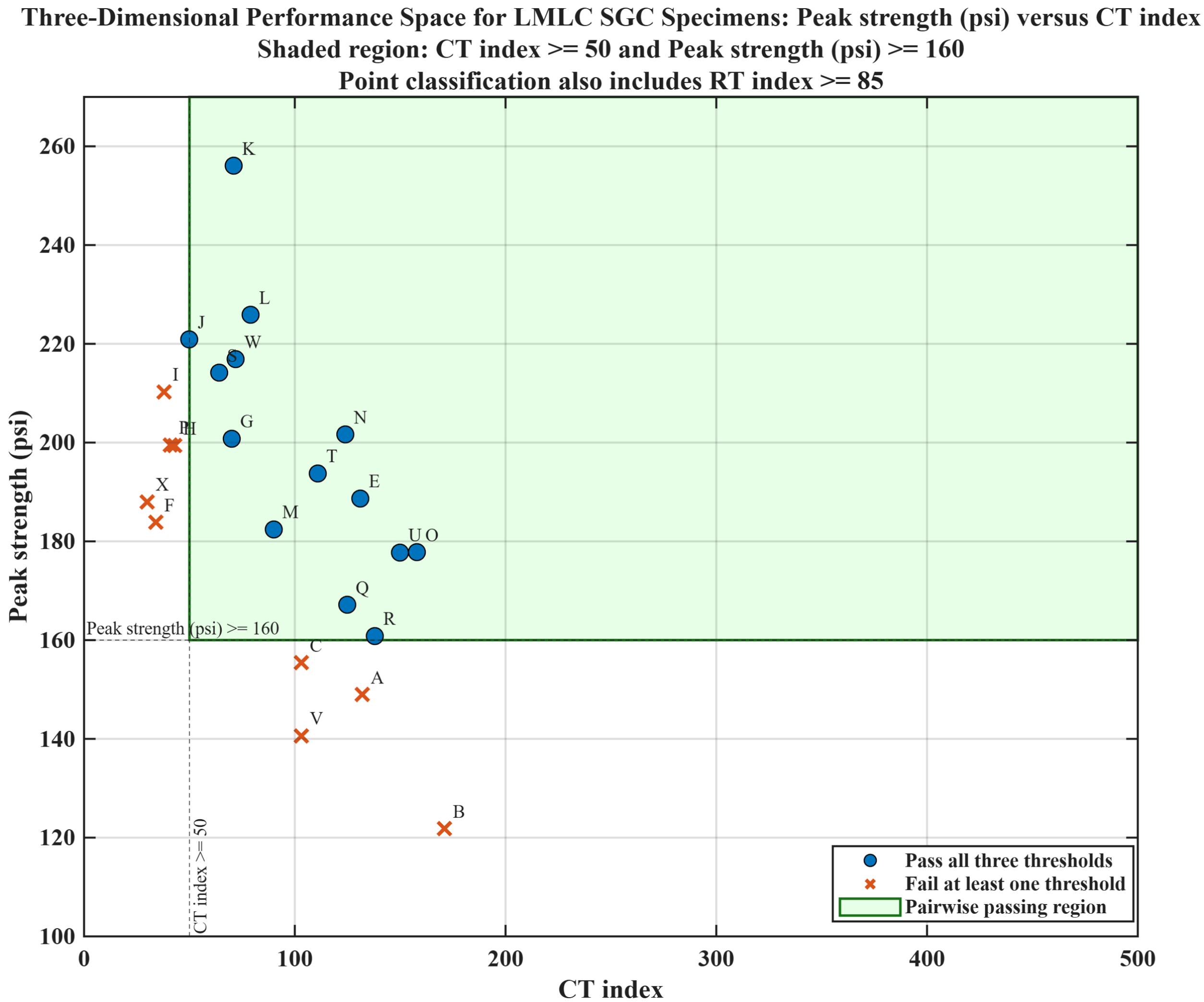
Three-Dimensional Performance Space for LMLC SGC Specimens: Peak strength (psi) versus CT index
Shaded region: CT index >= 50 and Peak strength (psi) >= 160
Point classification also includes RT index >= 85
Peak strength (psi)
CT index
Peak strength (psi) >= 160
CT index >= 50
K
L
J
W
S
I
N
G
T
E
X
F
M
U
O
Q
R
C
A
V
B
Pass all three thresholds
Fail at least one threshold
Pairwise passing region

(c)

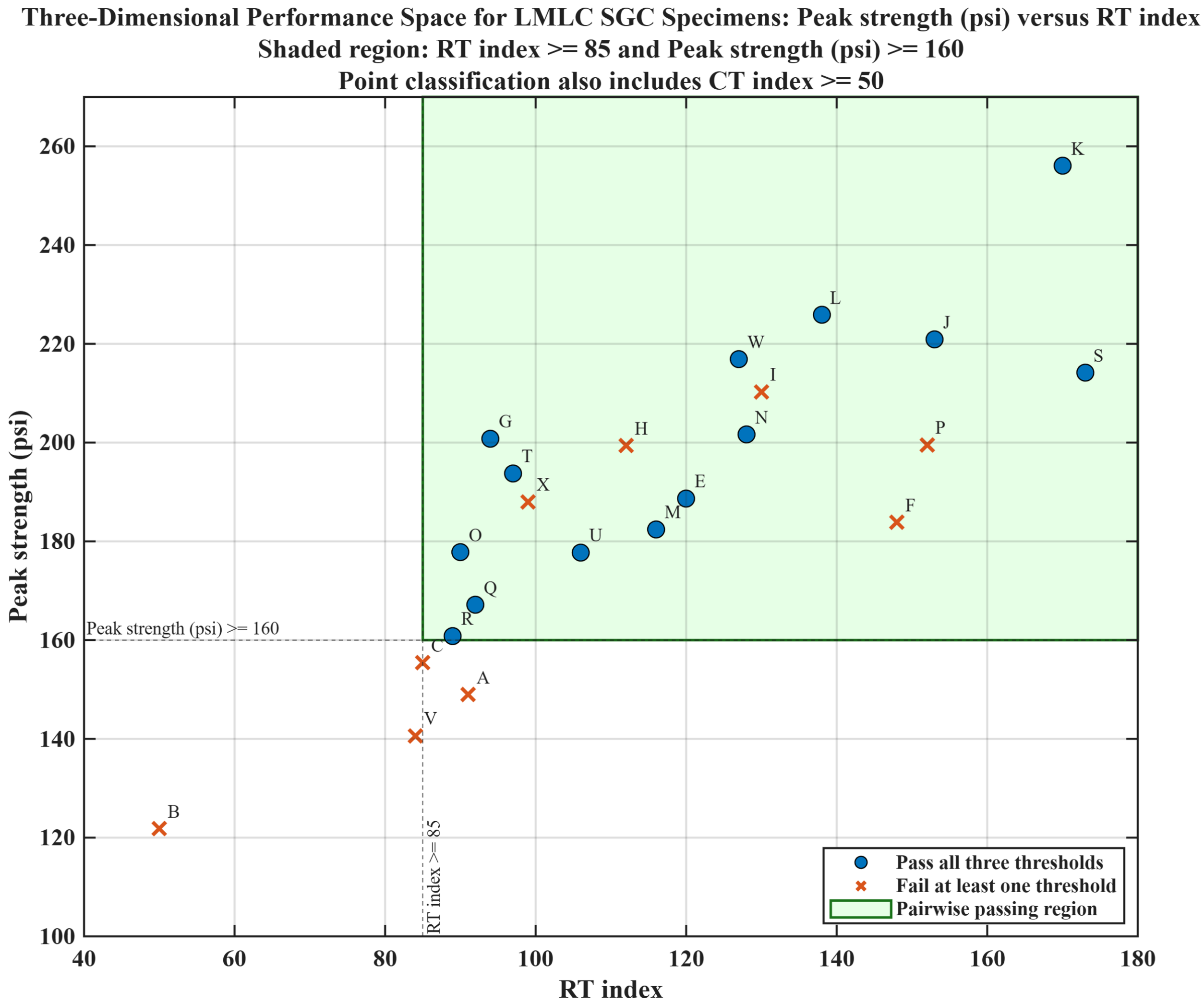

(d)

Figure A-5 Three-dimensional performance space for STA-conditioned LMLC SGC specimens based on CT index, RT index, and IDEAL-CT peak strength.

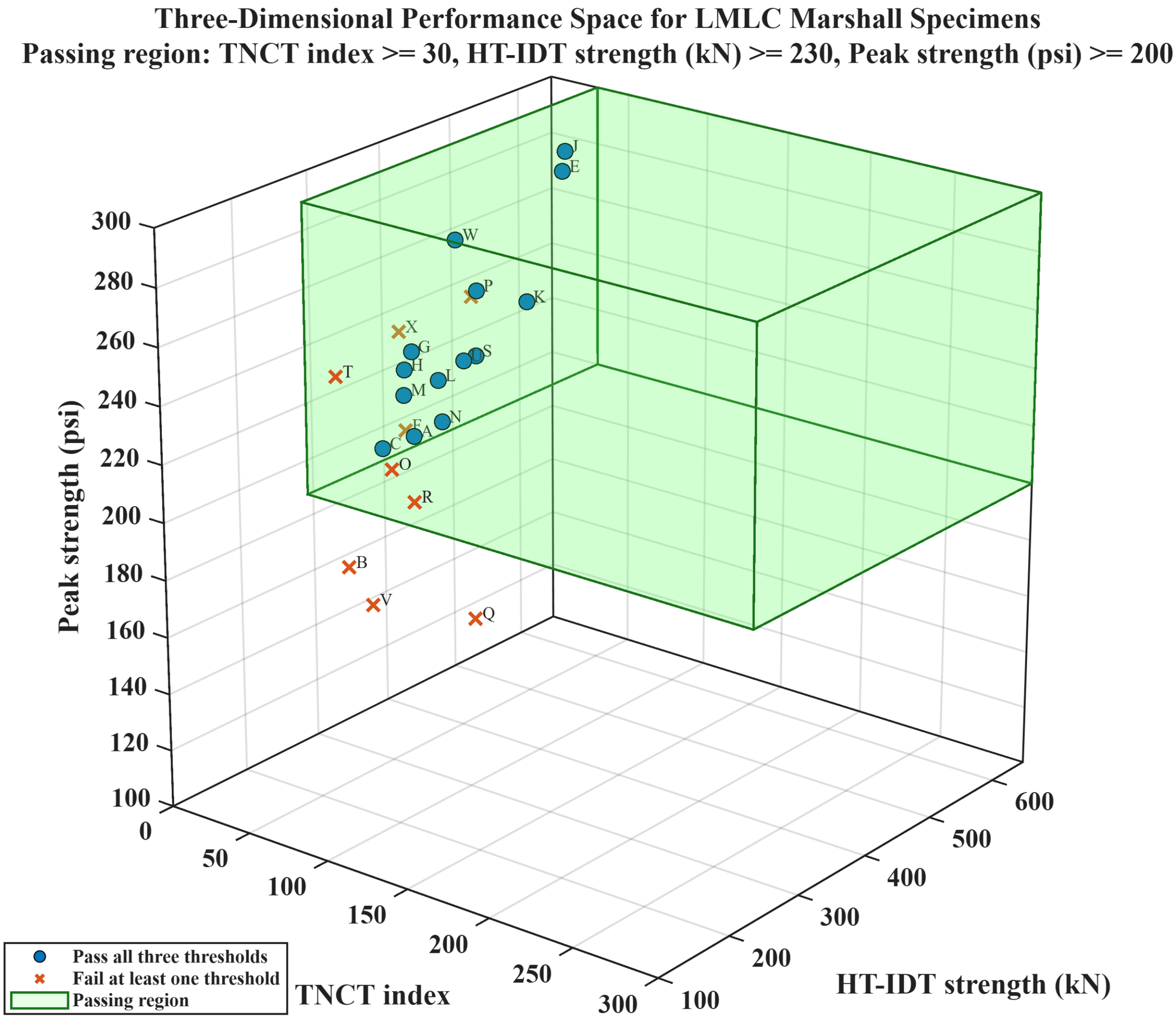
Three-Dimensional Performance Space for LMLC Marshall Specimens
Passing region: TNCT index >= 30, HT-IDT strength (kN) >= 230, Peak strength (psi) >= 200
Peak strength (psi)
TNCT index
HT-IDT strength (kN)
Pass all three thresholds
Fail at least one threshold
Passing region

(a)

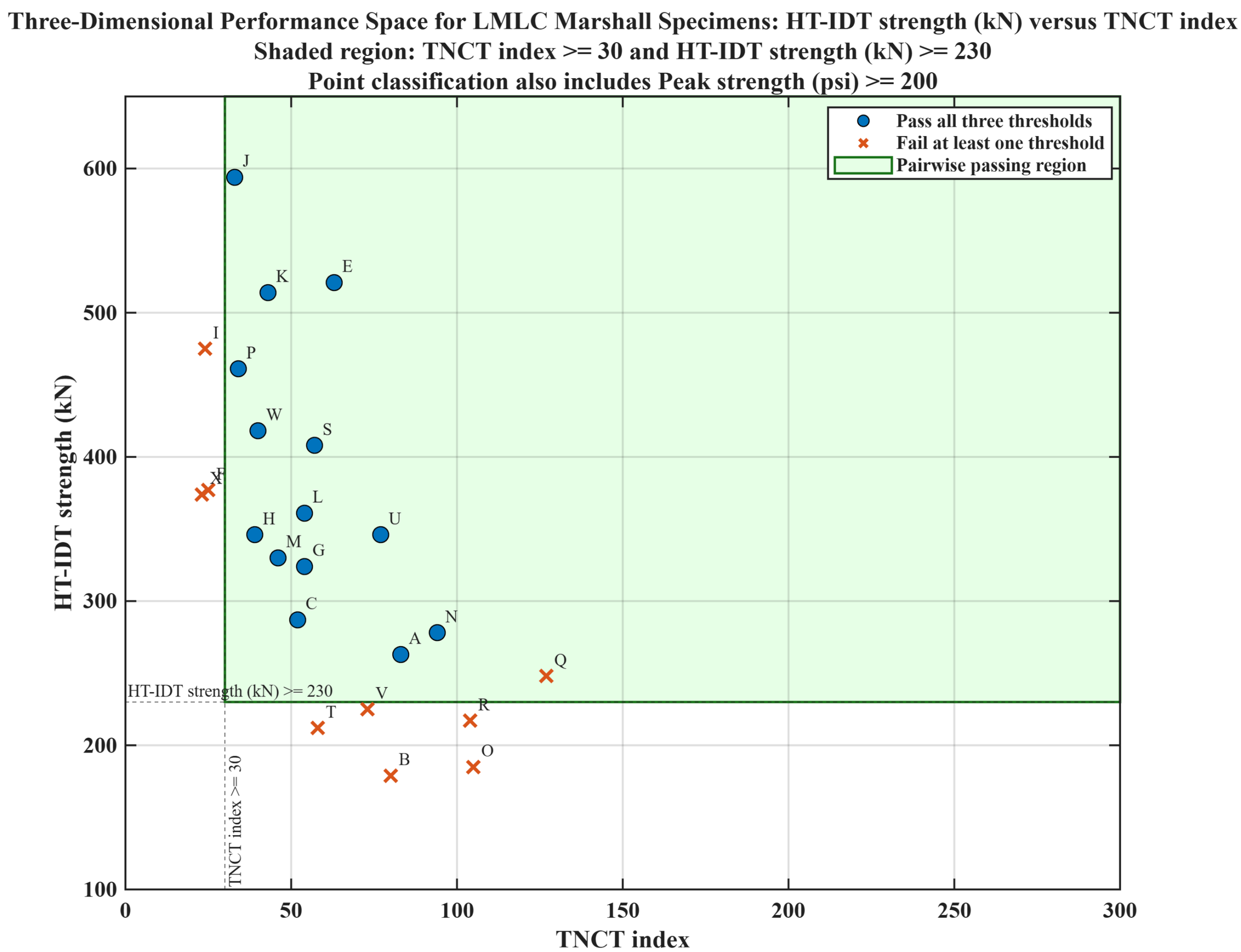
Three-Dimensional Performance Space for LMLC Marshall Specimens: HT-IDT strength (kN) versus TNCT index
Shaded region: TNCT index >= 30 and HT-IDT strength (kN) >= 230
Point classification also includes Peak strength (psi) >= 200
Pass all three thresholds
Fail at least one threshold
Pairwise passing region
HT-IDT strength (kN) >= 230
TNCT index >= 30
HT-IDT strength (kN)
TNCT index
J
K
E
I
P
W
S
X
F
L
H
U
M
G
C
N
A
Q
V
T
R
B
O
100
200
300
400
500
600
0
50
100
150
200
250
300

(b)

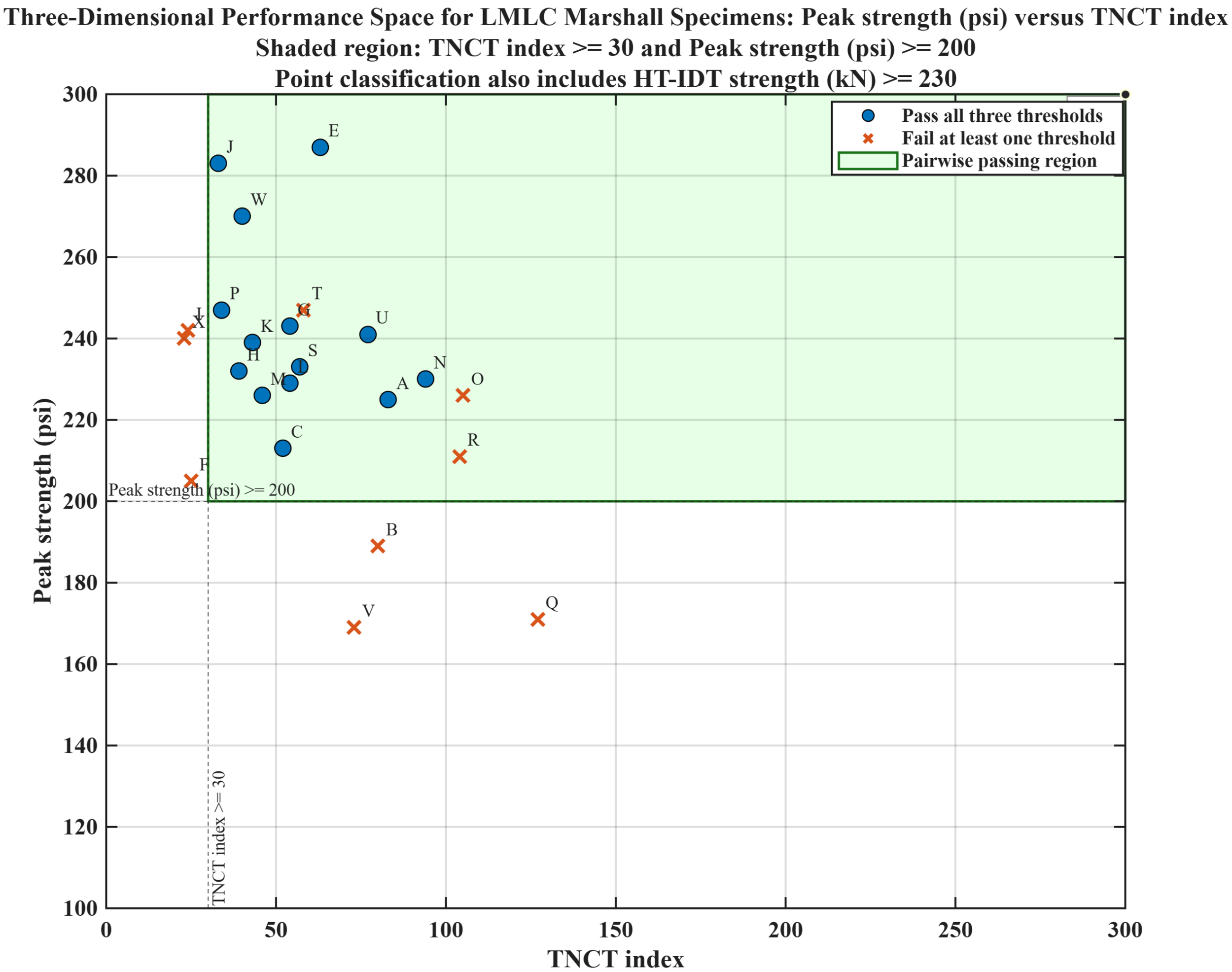
Three-Dimensional Performance Space for LMLC Marshall Specimens: Peak strength (psi) versus TNCT index
Shaded region: TNCT index >= 30 and Peak strength (psi) >= 200
Point classification also includes HT-IDT strength (kN) >= 230
Pass all three thresholds
Fail at least one threshold
Pairwise passing region
Peak strength (psi)
TNCT index
Peak strength (psi) >= 200
TNCT index >= 30
J
E
W
P
T
U
K
S
H
N
O
M
A
C
R
F
B
V
Q
X
I
300
280
260
240
220
200
180
160
140
120
100
0
50
100
150
200
250
300

(c)

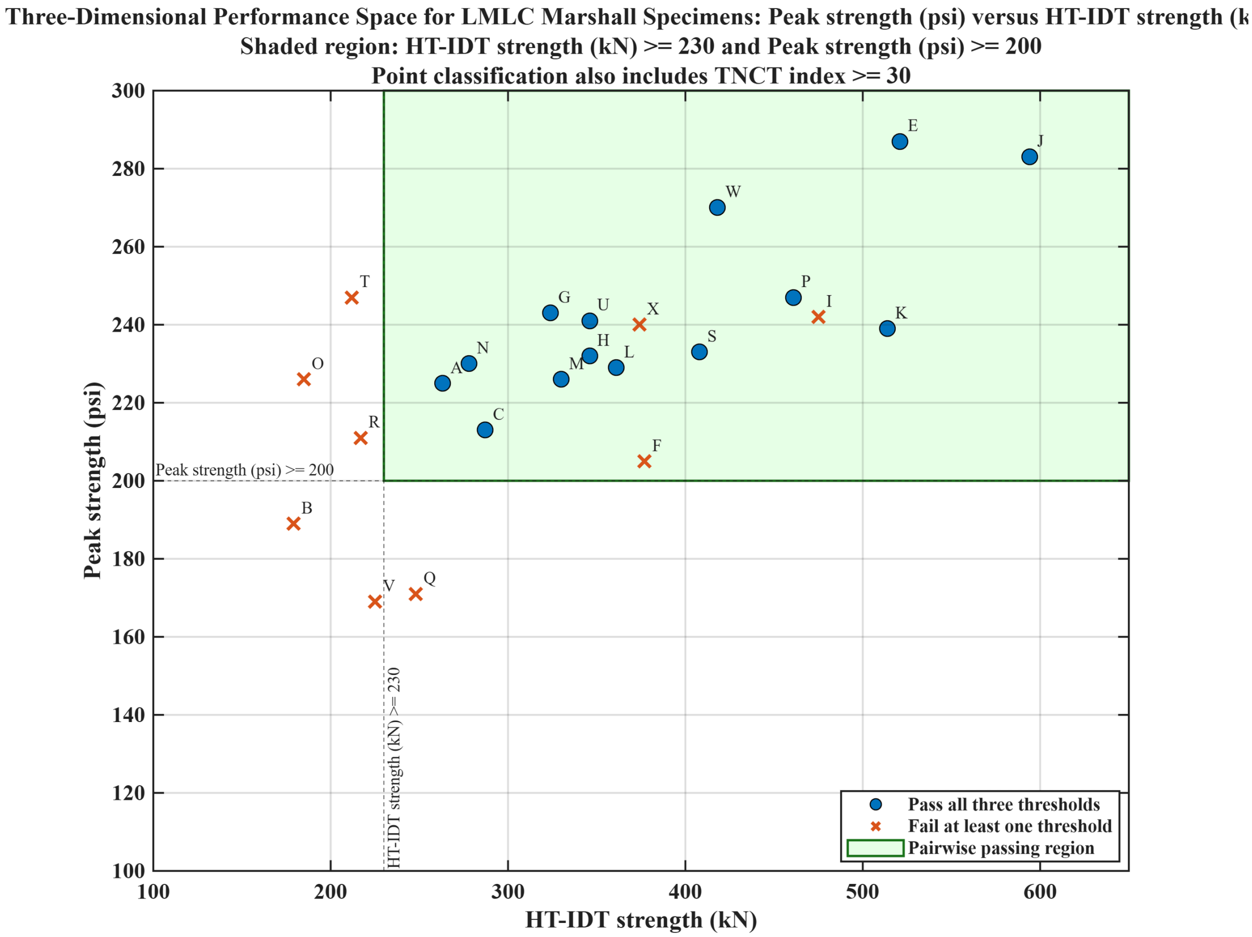

(d)

Figure A-6 Three-dimensional performance space for STA-conditioned LMLC Marshall specimens based on TN-CT index, HT-IDT strength, and TN-CT peak strength.